3-31-2016

Application of a Portable Hyperspectral Imaging System to Field Studies in Animal Camouflage and Coral Reef Symbiosis

Brandon J. Russell
University of Connecticut - Storrs, brandon.russell@uconn.edu

Application of a Portable Hyperspectral Imaging System to Field Studies in Animal Camouflage and Coral Reef Symbiosis

Brandon James Russell

University of Connecticut

2016

Abstract

Hyperspectral imaging (HSI) represents a powerful tool for measuring both the spatial and spectral components of a target. It has a wide variety of uses in marine science, but has previously been restricted to either large spatial scales or laboratory studies. Here, a portable imager is used in field research on biological camouflage and coral/dinoflagellate symbiosis.

Mats of the pelagic macroalgae *Sargassum* represent a complex environment for the study of marine camouflage at the air-sea interface, where endemic organisms have convergently evolved similar colors and patterns. Using HSI, spectral camouflage of two crab species (*Portunus sayi* and *Planes minutus*) was assessed. Crabs matched *Sargassum* reflectance across blue and green wavelengths (400-550 nm) and diverged at longer wavelengths, with maximum discrepancy in the far-red (i.e., 675 nm) due to Chlorophyll *a* absorption in *Sargassum.* Predator visual modeling showed that both species have effective color matching against blue/green sensitive dichromat fish, but are discernible to red sensitive, tetrachromat birds. The two species showed opposing trends in background matching with relation to body size. Held in a naturalistic light regime, *P. sayi* displayed a distinct diel cycle of dark/pale color change not observed under constant illumination. Individuals changed color in response to monochromatic black, grey, and white backgrounds, as integrated reflectance (ΣR) of crabs generally followed background

albedo. Dynamic color change in this species may play a photoprotective role, with possible use in enhancing cryptic color matching.

The imaging technology and methodology utilized in studying camouflage in the *Sargassum* environment was then applied to a different area of optical marine science. For stony corals, reflectance is driven by the pigments of photosynthetic endosymbionts. The warm inshore bays and cooler offshore reefs of Palau share a variety of coral species with differing symbiotic dinoflagellates (genus: *Symbiodinium*). Hyperspectral imagery revealed that coral integrated reflectance (ΣR 400 – 700 nm) had an inverse correlation to symbiont cell density. As hypothesized, coral colonies from offshore (Clade C symbionts) showed greater bleaching response to experimental heating than inshore counterparts with thermally resistant *S. trenchii*. Although no unique reflectance features were found to distinguish symbiont species, differences related to symbiont density could prove useful in field and remote sensing studies.

This dissertation demonstrates the suitability of portable hyperspectral imaging for a variety of field studies in marine science. This includes a unique at-sea use of HSI to study animal camouflage.

Application of a Portable Hyperspectral Imaging System to Field Studies in Animal Camouflage and Coral Reef Symbiosis

Brandon James Russell

B.S. Boston College 2007

A Dissertation

Submitted in Partial Fulfillment of the Requirements for the

Degree of Doctor of Philosophy

at the

University of Connecticut

2016

APPROVAL PAGE

Doctor of Philosophy Dissertation

Application of a Portable Hyperspectral Imaging System to Field Studies in Animal Camouflage and Coral Reef Symbiosis

Presented by

Brandon James Russell, B.S.

Major Advisor:_____
Heidi Dierssen

Associate Advisor:_____
Peter Auster

Associate Advisor:_____
Molly Cummings

University of Connecticut

2016

Acknowledgements

First and foremost, I would like to express my deepest gratitude to my advisor and mentor, Dr. Heidi Dierssen. In the past six years she has shown unflagging support of this work and my independent development of the questions, methods, and hypotheses which became this dissertation. Heidi made certain that I was not only producing quality science, but that I became an active and known member of the ocean optics community. She has an amazing ability to generate personal connections and recognize potential collaborations. For me personally, this has resulted in several important opportunities during my time in her lab, one of which became a chapter of this dissertation. When doing research, Heidi has always encouraged me to keep an open, observing mind and to be ready to ask new questions beyond what I have originally planned. The first two chapters of this dissertation were the result of just such flexibility.

I am also grateful to the other members of my advisory committee, Dr. Peter Auster and Dr. Molly Cummings of UT Austin. Both provided important insight, as did former committee member Dr. Robert Whitlatch. The faculty of the Department of Marine Sciences provided me with an excellent oceanographic education.

For his assistance in the field I would like to thank Eric Heupel, as well as the crew and researchers of the SSV Corwith Cramer, SV Sea Dragon, and the staff of Keys Marine Lab who helped sort through massive quantities of algae chasing small crabs on multiple occasions. I would also like to acknowledge the support and administrative staff of UConn Marine Sciences, who made it possible to conduct the research presented. During the past 6 years, my fellow lab members Kelley Bostrom and Kate Randolph have provided technical assistance and moral support.

This work was supported primarily through a grant to my advisor from the Office of Naval Research. I also received direct funding from the UConn Department of Marine Sciences, and educational support from NASA and UNIS. Valuable ship-time was donated by the Sea Education Alliance, as well as the Bermuda Alliance for the Sargasso Sea and Bermuda Aquarium, Museum, and Zoo.

Personally, I am deeply grateful for the love and support of my parents and family. My mother, herself trained in biology, provided unending support and a sounding board for my research. After spending many years working with optical electronics, my father has helped me to understand the technology of my instruments and to develop my own research equipment.

Table of Contents

1. Introduction

1.1. Reflectance in Marine Science

In marine sciences, remote sensing may be used to study an immense range of biological, geological, and physical subjects at scales ranging from individual phytoplankton to the global ocean. This involves measuring the light, or electromagnetic radiation, from a target without being in contact with the object or surface in question in order to gain information [1]. One of the basic quantities in optical remote sensing is spectral reflectance, a powerful tool that can be utilized in a diverse array of marine studies including benthic mapping [2–4], estimation and modeling of water column properties [5–8], primary productivity estimation [9,10], identification of plants, macroalgae, and phytoplankton [2,3,11,12], coral reef composition and health [13–16], and visual modeling [17–19]. In its simplest form, reflectance is the ratio of photons scattered backwards from a target to those incident on it, at every wavelength measured [6,17]. The resultant spectrum can be used to infer properties of the target based on the manner in which photons are absorbed or scattered. Reflectance is therefore an intrinsic property of the target, largely independent of the local light field.

1.2. Measurement Techniques

For close-range, small spatial-scale studies, the primary method of measuring reflectance has historically been fiber optic spectrometry [17,20]. Photons reflected by the target are collected in a fiber optic probe, diffracted, and channeled to a detector where the intensity and spectral distribution of the incoming light can be measured. This signal is then compared to the incoming light, either by using the same fiber optic to measure the signal from a standard of known reflectance, or by comparison to an intercalibrated reference sensor. This technique has

been successfully applied to a wide variety of subjects, including measuring benthic reflectance for sediments, coral reefs and seagrasses [2,5,21,22], animal coloration [19,23], and validation for airborne and satellite sensors [3,11]. The technique is relatively simple with a wide variety of affordable and customizable units commercially available, and can be employed in the lab or in the field. Fiber optic spectrometers are capable of providing high-resolution spectral data (e.g. 2 nm) over wide ranges of wavelengths (e.g. 350 – 2500 nm), depending on manufacturer configuration. While spectrally robust, fiber optic techniques are spatially poor, producing a single spectrum that is the result of light integrated from the probe's field of view, which may be 25° for a typical flat-faced probe.

For small or spatially complex targets such as individual coral polyps or animals with complex color patterns, adequately characterizing a sample with a fiber optic probe can be extremely difficult, requiring equipment modification and rigorous, time consuming techniques [19,24]. Spectra derived from fiber optics may not be statistically representative of the entire subject. Further, signal contamination by glare or saturation, often present for smooth or curved surfaces, can occur when using a fiber probe [25] (see chapters 2 and 3 of this dissertation). By contrast, photography provides data that is spatially robust but spectrally poor. A typical color photograph captures data in only 3 wide spectral bands. Modification of the lenses and sensor, as well as calibration against known light sources [26–29] can be utilized to expand the spectral range and utility of photographic cameras, but all data is necessarily of low spectral resolution.

Hyperspectral imagery (HSI) represents a combination of these traditional techniques, and is a powerful technology in marine science that is being used in an increasing number of applications. An imager provides a data cube, a virtually synoptic image with full spectral or "hyperspectral" information for every pixel. The cube is a 3-dimensional image, with spatial

information in the X and Y axes, and spectral information stored in the Z axis [17,30]. Both imagery and spectral analysis techniques can be applied to HSI data cubes, including manually or automatically selecting data by object identity or reflectance properties as described in this dissertation. The imager used here is a spatial-scanning style system. Light from a viewing area enters through a focusing and collection lens and is passed through a narrow slit such that only a small fraction of the visible scene is sampled at a given time. This light is dispersed by a diffraction grating onto a detector, which reads the relative amount of light at each wavelength [31,32]. In this way, the light from a single line of the image, one pixel wide, is spread across the detector at a given moment and spectrally measured. This data is saved to a computer, and a scanning mirror pans through the entire visual scene, building the data cube line by line. An entire cube is collected in a matter of seconds using this system. The user can set the spatial area and resolution through the selection of lens and distance to target.

Hyper or multi- spectral imaging technology has been utilized extensively for remote sensing of large spatial areas for over 30 years [1,11,33], and has more recently been used in laboratory-based studies of smaller subjects [13,14,30,34]. Developments in highly portable imagers allow the use of hyperspectral imagery in the field and onboard small vessels, as presented here.

1.3. Dissertation Organization and Objectives

While HSI has historically been utilized for regional or even global remote sensing, there has been relatively limited application to spatial scales at the level of individual marine animals. The overall goal of the dissertation was to use portable hyperspectral imaging to investigate phenomena in marine biota and showcase the utility of this tool in different field-based

applications. Two areas of study are presented: animal camouflage and coral/dinoflagellate symbiosis.

The first component of the animal camouflage investigation (Chapter 2) was published in PLoS ONE on September 9, 2015. The Appendix appeared as supplementary material at publication. The second component, Chapter 3, is prepared for submission to PLoS ONE. An investigation on coral symbiosis (Chapter 4) was published in the journal Remote Sensing on February 23, 2016 to a special issue: "Remote Sensing for Coral Reef Monitoring." The chapters are presented as intact, independent research articles written in the style of their respective journals. A brief introduction and summary of each chapter is provided below.

1.3.2. Animal Camouflage

One of the most common camouflage strategies in the marine environment is background matching, in which an animal's appearance generally matches the color, shade, or pattern of one or more background types [35]. The degree to which this matching is effective depends largely on the visual system of the predator or prey that the cryptic animal is hiding from. Additionally, the ambient light field and optical properties of the water will play a role in underwater color discrimination [17,30].

The main body of this dissertation is a study of spectral camouflage in fauna associated with floating mats of the pelagic algae *Sargassum*, a unique and complex environment at the air-sea interface. Due to patchy habitat distribution and lack of physical cover, *Sargassum* fauna must rely on camouflage to remain hidden from both water- and air-borne predators that may view them from many directions simultaneously. Endemic organisms have convergently evolved similar colors and patterns, but quantitative assessments of camouflage strategies are lacking.

The first objective of this dissertation was to evaluate the ability of *Sargassum* endemics to match the color of the algae in the view of the multiple predator types present in this habitat. In Chapter 2, a field study detailing the ability of two crab species, *Portunus sayi* and *Planes minutus*, to match the spectral reflectance of the floating macroalgae on which they live and hide is presented. In a unique at-sea study, I quantified the degree of general color matching for both species in the view of two known predator types: fish, which have two cone cell types sensitive to blue and green light, and seabirds, which possess four cone types and are sensitive to wavelengths in the far red. Further, I used optical modeling to investigate the impact of water column properties, distance, and the light field on camouflage effectiveness.

Chapter 3 presents an experiment building on these results, by examining the ability of *P. sayi* to change its coloration. Rapid color change can serve a variety of ecological functions [36]. For *Sargassum* fauna, which lack hard cover from predation and must rely on crypsis, dramatic color shifts can potentially have important consequences for camouflage. I describe the presence of a diel color cycle, in which crabs are dark during daylight hours and have a paler body color at night. I demonstrate that this cycle is not an endogenous circadian rhythm, but is at least largely regulated by ambient light, as crabs exposed to constant illumination displayed no such cycle. Crabs placed on backgrounds representing a range in albedo (0.04 – 0.73) were imaged at multiple time points to investigate the ability of *P. sayi* to change color in order to improve background matching.

1.3.3. Coral Symbiosis

In Chapter 4, I apply the measurement and processing techniques developed in the previous chapters to approach a very different subject matter, which may also be studied using

marine optics: coral reefs. The objective of this study was to use hyperspectral imagery to investigate potential reflectance differences in specific lineages of the photosynthetic endosymbionts that are critical in maintaining coral reef health.

Reef building corals represent a symbiosis between colonial cnidarians and endosymbiotic dinoflagellates (genus: *Symbiodinium*). Globally, coral reefs are threatened by frequent episodes of coral bleaching and mortality [37,38]. Coral bleaching or whitening occurs when symbiotic algae are expelled from the host in response to environmental stressors like warming sea surface temperature. The diversity of endosymbiotic dinoflagellates is tremendous, with significant differences in assemblages between ocean basins [39,40]. The same coral species from habitats less than several kilometers may even host different symbionts [39–41]. Thermal tolerance varies among *Symbiodinium* lineages, and corals with heat-tolerant symbionts may resist thermally induced bleaching [42–44]. In particular, *Symbiodinium trenchii* is known for being a generalist inhabiting corals in marginal conditions, and coral colonies with this symbiont can often tolerate higher temperatures than conspecifics with other endosymbionts [40,42,45]. This species is native to the western Pacific but has successfully invaded reef communities in the Caribbean, where it may offer corals increased resistance to thermal bleaching but at reduced calcification rates [43,46].

The interaction of white calcium carbonate skeleton, photoprotective and fluorescent host pigments, and the photosynthetic pigments of the endosymbiotic algae determine the spectral reflectance of the coral colony [16,47]. Reflectance has been used to differentiate between coral and other benthic objects [21] and may allow discrimination between different coral/dinoflagellate systems [48,49]. We are aware of no published research on whether communities of corals hosting different symbionts can be distinguished from colony-level

reflectance. Therefore, I investigated the reflectance of corals with different symbiont lineages from Palau, Micronesia. As part of a larger collaborative study, multiple colonies of two coral species were collected from sites with distinct temperature regimes that hosted different lineages of endosymbiotic algae.

Here, fragments from each colony were imaged in an attempt to identify reflectance features or markers of the thermally resistant *S. trenchii* not found in corals with other symbiont species. The density of endosymbiotic dinoflagellates within the host tissue, a physiological metric of coral health [50,51], is routinely measured through destructive sampling [52,53]. I present an initial method for estimating symbiont cell density from reflectance, which can be measured *in situ* or in the laboratory without damaging the coral. In a manipulative experiment, colony replicate fragments were exposed to control and elevated temperatures. I measured the change in symbiont density and spectral reflectance in response to heating and compared the response of the same coral species containing *S. trenchii* and symbionts from a different lineage (Clade C types).

References

1. Martin, S. *An Introduction to Ocean Remote Sensing*; Cambridge University Press: New York, **2004**.

2. Hedley, J.; Russell, B.; Randolph, K.; Dierssen, H. A physics-based method for the remote sensing of seagrasses. *Remote Sens. Environ.* **2016**, *174*, 134–147.

3. Dierssen, H. M. Overview of hyperspectral remote sensing for mapping marine benthic habitats from airborne and underwater sensors. In; Mouroulis, P.; Pagano, T. S., Eds.; **2013**; p. 88700L.

4. Johnsen, G.; Volent, Z.; Dierssen, H.; Pettersen, R.; Ardelan, M. V.; Søreide, F.; Fearns, P.; Ludvigsen, M.; Moline, M. Underwater hyperspectral imagery to create biogeochemical maps of seafloor properties. In *Subsea Optics and Imaging*; Elsevier, **2013**; pp. 508–540e.

5. Gilerson, A. A.; Stepinski, J.; Ibrahim, A. I.; You, Y.; Sullivan, J. M.; Twardowski, M. S.; Dierssen, H. M.; Russell, B.; Cummings, M. E.; Brady, P.; Ahmed, S. A.; Kattawar, G. W. Benthic effects on the polarization of light in shallow waters. *Appl. Opt.* **2013**, *52*, 8685.

6. Mobley, C. D. *Light and Water: Radiative Transfer in Natural Waters*; Academic Press: San Diego, **1994**.

7. Roesler, C. S.; Perry, M. J. In situ phytoplankton absorption, fluorescence emission, and particulate backscattering spectra determined from reflectance. *J. Geophys. Res.* **1995**, *100*, 13,279 – 13,294.

8. Garaba, S.; Voß, D.; Zielinski, O. Physical, Bio-Optical State and Correlations in North–Western European Shelf Seas. *Remote Sens.* **2014**, *6*, 5042–5066.

9. Hill, V. J.; Zimmerman, R. C.; Bissett, W. P.; Dierssen, H.; Kohler, D. D. R. Evaluating Light Availability, Seagrass Biomass, and Productivity Using Hyperspectral Airborne Remote Sensing in Saint Joseph's Bay, Florida. *Estuaries Coasts* **2014**, *37*, 1467–1489.

10. Chennu, A.; Färber, P.; Volkenborn, N.; Al-Najjar, M. A. A.; Janssen, F.; de Beer, D.; Polerecky, L. Hyperspectral imaging of the microscale distribution and dynamics of microphytobenthos in intertidal sediments: Hyperspectral imaging of MPB biofilms. *Limnol. Oceanogr. Methods* **2013**, *11*, 511–528.

11. Dierssen, H. M.; Chlus, A.; Russell, B. Hyperspectral discrimination of floating mats of seagrass wrack and the macroalgae Sargassum in coastal waters of Greater Florida Bay using airborne remote sensing. *Remote Sens. Environ.* **2015**, *167*, 247–258.

12. Dierssen, H.; McManus, G. B.; Chlus, A.; Qiu, D.; Gao, B.-C.; Lin, S. Space station image captures a red tide ciliate bloom at high spectral and spatial resolution. *Proc. Natl. Acad. Sci.* **2015**, *112*, 14783–14787.

13. Caras, T.; Karnieli, A. Ground-level spectroscopy analyses and classification of coral reefs using a hyperspectral camera. *Coral Reefs* **2013**, *32*, 825–834.

14. Mehrubeoglu, M.; Smith, D. K.; Smith, S. W.; Strychar, K. B.; McLauchlan, L. Investigating coral hyperspectral properties across coral species and coral state using hyperspectral imaging. In; Mouroulis, P.; Pagano, T. S., Eds.; **2013**; p. 88700M.

15. Anderson, D. A.; Armstrong, R. A.; Weil, E. Hyperspectral Sensing of Disease Stress in the Caribbean Reef-Building Coral, Orbicella faveolata - Perspectives for the Field of Coral Disease Monitoring. *PLoS ONE* **2013**, *8*, e81478.

16. Hedley, J. D.; Mumby, P. J. Biological and remote sensing perspectives of pigmentation in coral reef organisms. *Adv. Mar. Biol.* **2002**, *43*, 277–317.

17. Russell, B. J.; Dierssen, H. M. Use of Hyperspectral Imagery to Assess Cryptic Color Matching in Sargassum Associated Crabs. *PloS One* **2015**, *10*, e0136260.

18. Vorobyev, M.; Osorio, D. Receptor noise as a determinant of colour thresholds. *Proc. R. Soc. Lond. B Biol. Sci.* **1998**, *265*, 351–358.

19. Cummings, M. E.; Jordão, J. M.; Cronin, T. W.; Oliveira, R. F. Visual ecology of the fiddler crab, Uca tangeri: effects of sex, viewer and background on conspicuousness. *Anim. Behav.* **2008**, *75*, 175–188.

20. Johnsen, S. *The Optics of Life: A Biologist's Guide to Light in Nature*; Princeton U. Press: Princeton, **2012**.

21. Hochberg, E. J.; Atkinson, M. J. Spectral discrimination of coral reef benthic communities. *Coral Reefs* **2000**, *19*, 164–171.

22. Mazel, C. H.; Fuchs, E. Contribution of fluorescence to the spectral signature and perceived color of corals. *Limnol. Oceanogr.* **2003**, *48*, 390–401.

23. Akkaynak, D. Use of spectroscopy for assessment of color discrimination in animal vision. *J. Opt. Soc. Am. A* **2014**, *31*, A27.

24. Wangpraseurt, D.; Larkum, A. W. D.; Ralph, P. J.; Kühl, M. Light gradients and optical microniches in coral tissues. *Front. Microbiol.* **2012**, *3*.

25. Baldwin, J.; Johnsen, S. The male blue crab, *Callinectes sapidus*, uses both chromatic and achromatic cues during mate choice. *J. Exp. Biol.* **2012**, *215*, 1184–1191.

26. Troscianko, J.; Stevens, M. Image calibration and analysis toolbox - a free software suite for objectively measuring reflectance, colour and pattern. *Methods Ecol. Evol.* **2015**, *6*, 1320–1331.

27. Detto, T.; Hemmi, J. M.; Backwell, P. R. Y. Colouration and Colour Changes of the Fiddler Crab, Uca capricornis: A Descriptive Study. *PLoS ONE* **2008**, *3*, e1629.

28. Garcia, J. E.; Greentree, A. D.; Shrestha, M.; Dorin, A.; Dyer, A. G. Flower Colours through the Lens: Quantitative Measurement with Visible and Ultraviolet Digital Photography. *PLoS ONE* **2014**, *9*, e96646.

29. Leeuw, T. Crowdsourcing Water Quality Data Using the iPhone Camera. Master's, University of Maine, **2014**.

30. Chiao, C.-C.; Wickiser, J. K.; Allen, J. J.; Genter, B.; Hanlon, R. T. Hyperspectral imaging of cuttlefish camouflage indicates good color match in the eyes of fish predators. *Proc. Natl. Acad. Sci.* **2011**, *108*, 9148–9153.

31. Lerner, J. M. Imaging spectrometer fundamentals for researchers in the biosciences—A tutorial. *Cytometry A* **2006**, *69A*, 712–734.

32. Dell'Endice, F. Improving the performance of hyperspectral pushbroom imaging spectrometers for specific science applications. *Int. Arch. Photogramm. Remote Sens. Spat. Inf. Sci.* **2008**, *37*, B7.

33. Gordon, H. R.; Morel, A. Y. *Remote Assessment of Ocean Color for Interpretation of Satellite Visible Imagery*; Lecture Notes on Coastal and Estuarine Studies; Springer-Verlag: New York, **1983**; Vol. 4.

34. Caras, T.; Karnieli, A. Ground-Level Classification of a Coral Reef Using a Hyperspectral Camera. *Remote Sens.* **2015**, *7*, 7521–7544.

35. *Animal camouflage: mechanisms and function*; Stevens, M.; Merilaita, S., Eds.; Cambridge University Press: Cambridge, UK ; New York, **2011**.

36. Stuart-Fox, D.; Moussalli, A. Camouflage, communication and thermoregulation: lessons from colour changing organisms. *Philos. Trans. R. Soc. B Biol. Sci.* **2009**, *364*, 463–470.

37. Hoegh-Guldberg, O.; Mumby, P. J.; Hooten, A. J.; Steneck, R. S.; Greenfield, P.; Gomez, E.; Harvell, C. D.; Sale, P. F.; Edwards, A. J.; Caldeira, K.; others Coral reefs under rapid climate change and ocean acidification. *science* **2007**, *318*, 1737–1742.

38. Baker, A. C.; Glynn, P. W.; Riegl, B. Climate change and coral reef bleaching: An ecological assessment of long-term impacts, recovery trends and future outlook. *Estuar. Coast. Shelf Sci.* **2008**, *80*, 435–471.

39. LaJeunesse, T. C. Diversity and community structure of symbiotic dinoflagellates from Caribbean coral reefs. *Mar. Biol.* **2002**, *141*, 387–400.

40. LaJeunesse, T. C.; Pettay, D. T.; Sampayo, E. M.; Phongsuwan, N.; Brown, B.; Obura, D. O.; Hoegh-Guldberg, O.; Fitt, W. K. Long-standing environmental conditions, geographic isolation and host–symbiont specificity influence the relative ecological dominance and genetic diversification of coral endosymbionts in the genus *Symbiodinium*. *J. Biogeogr.* **2010**, *37*, 785–800.

41. Tonk, L.; Sampayo, E. M.; LaJeunesse, T. C.; Schrameyer, V.; Hoegh-Guldberg, O. *Symbiodinium* (Dinophyceae) diversity in reef-invertebrates along an offshore to inshore reef gradient near Lizard Island, Great Barrier Reef. *J. Phycol.* **2014**, *50*, 552–563.

42. Kemp, D. W.; Hernandez-Pech, X.; Iglesias-Prieto, R.; Fitt, W. K.; Schmidt, G. W. Community dynamics and physiology of *Symbiodinium* spp. before, during, and after a coral bleaching event. *Limnol. Oceanogr.* **2014**, *59*, 788–797.

43. LaJeunesse, T. C.; Smith, R. T.; Finney, J.; Oxenford, H. Outbreak and persistence of opportunistic symbiotic dinoflagellates during the 2005 Caribbean mass coral "bleaching"event. *Proc. R. Soc. B Biol. Sci.* **2009**, RSPB20091405.

44. LaJeunesse, T. C.; Wham, D. C.; Pettay, D. T.; Parkinson, J. E.; Keshavmurthy, S.; Chen, C. A. Ecologically differentiated stress-tolerant endosymbionts in the dinoflagellate genus *Symbiodinium* (Dinophyceae) Clade D are different species. *Phycologia* **2014**, *53*, 305–319.

45. Berkelmans, R.; van Oppen, M. J. . The role of zooxanthellae in the thermal tolerance of corals: a "nugget of hope" for coral reefs in an era of climate change. *Proc. R. Soc. B Biol. Sci.* **2006**, *273*, 2305–2312.

46. Pettay, D. T.; Wham, D. C.; Smith, R. T.; Iglesias-Prieto, R.; LaJeunesse, T. C. Microbial invasion of the Caribbean by an Indo-Pacific coral zooxanthella. *Proc. Natl. Acad. Sci.* **2015**, *112*, 7513–7518.

47. Hochberg, E. Spectral reflectance of coral reef bottom-types worldwide and implications for coral reef remote sensing. *Remote Sens. Environ.* **2003**, *85*, 159–173.

48. Torres-Pérez, J.; Guild, L.; Armstrong, R. Hyperspectral Distinction of Two Caribbean Shallow-Water Corals Based on Their Pigments and Corresponding Reflectance. *Remote Sens.* **2012**, *4*, 3813–3832.

49. Torres-Pérez, J. L.; Guild, L. S.; Armstrong, R. A.; Corredor, J.; Zuluaga-Montero, A.; Polanco, R. Relative Pigment Composition and Remote Sensing Reflectance of Caribbean Shallow-Water Corals. *PLOS ONE* **2015**, *10*, e0143709.

50. Hoegh-Guldberg, O.; Smith, G. J. Influence of the population-density of zooxanthellae and supply of ammonium on the biomass and metabolic characteristics of the reef corals *Seriatopora hystrix* and *Stylophora pistillata*. *Mar. Ecol. Prog. Ser.* **1989**, *57*, 173–186.

51. Browne, N. K.; Tay, J. K. L.; Low, J.; Larson, O.; Todd, P. A. Fluctuations in coral health of four common inshore reef corals in response to seasonal and anthropogenic changes in water quality. *Mar. Environ. Res.* **2015**, *105*, 39–52.

52. Fitt, W. K.; McFarland, F. K.; Warner, M. E.; Chilcoat, G. C. Seasonal patterns of tissue biomass and densities of symbiotic dinoflagellates in reef corals and relation to coral bleaching. *Limnol. Oceanogr.* **2000**, *45*, 677–685.

53. *Chlorophyll a Fluorescence in Aquatic Sciences: Methods and Applications*; Suggett, D. J.; Prášil, O.; Borowitzka, M. A., Eds.; Springer Netherlands: Dordrecht, **2010**.

2. Use of Hyperspectral Imagery to Assess Cryptic Color Matching in Sargassum Associated Crabs

This chapter was published in PloS ONE on September 9, 2015

Russell, BJ; Dierssen, HM. (2015) Use of hyperspectral imagery to assess cryptic color matching in *Sargassum* associated crabs. *PLOS ONE* doi:10.1371/journal.pone.0136260

PLOS | ONE

RESEARCH ARTICLE

Use of Hyperspectral Imagery to Assess Cryptic Color Matching in *Sargassum* Associated Crabs

Brandon J. Russell[1☯]*, **Heidi M. Dierssen**[1,2☯]

1 Department of Marine Science, University of Connecticut, Groton, CT, 06340, United States of America,
2 Department of Geography, University of Connecticut, Storrs, CT, 06268, United States of America

☯ These authors contributed equally to this work.
* Brandon.Russell@uconn.edu

Citation: Russell BJ, Dierssen HM (2015) Use of Hyperspectral Imagery to Assess Cryptic Color Matching in *Sargassum* Associated Crabs. PLoS ONE 10(9): e0136260. doi:10.1371/journal.pone.0136260

Editor: Eric James Warrant, Lund University, SWEDEN

Received: March 30, 2015

Accepted: August 3, 2015

Published: September 9, 2015

Data Availability Statement: All relevant data are within the paper and its Supporting Information files.

Funding: This work was funded by the Office of Naval Research (http://www.onr.navy.mil/) Multi-University Research Initiative (N000140911054). Ship time was donated by the Bermuda Alliance for the Sargasso Sea, and the Bermuda Aquarium, Museum, and Zoo.

Competing Interests: The authors have declared that no competing interests exist.

Abstract

Mats of the pelagic macroalgae *Sargassum* represent a complex environment for the study of marine camouflage at the air-sea interface. Endemic organisms have convergently evolved similar colors and patterns, but quantitative assessments of camouflage strategies are lacking. Here, spectral camouflage of two crab species (*Portunus sayi* and *Planes minutus*) was assessed using hyperspectral imagery (HSI). Crabs matched *Sargassum* reflectance across blue and green wavelengths (400–550 nm) and diverged at longer wavelengths. Maximum discrepancy was observed in the far-red (i.e., 675 nm) where Chlorophyll *a* absorption occurred in *Sargassum* and not the crabs. In a quantum catch color model, both crabs showed effective color matching against blue/green sensitive dichromat fish, but were still discernible to tetrachromat bird predators that have visual sensitivity to far red wavelengths. The two species showed opposing trends in background matching with relation to body size. Variation in model parameters revealed that discrimination of crab and background was impacted by distance from the predator, and the ratio of cone cell types for bird predators. This is one of the first studies to detail background color matching in this unique, challenging ecosystem at the air-sea interface.

Introduction

The need to hide is a potent evolutionary driver [1]. Biological camouflage, the ability to avoid detection or recognition by an observer, has evolved in multiple phyla as an adaptation to visually-orienting predators and prey. The study of marine camouflage systems has relevance to ecology and animal behavior as well as human naval operations, and to target discrimination in the water column [2, 3]. A wide variety of strategies exist, and the classification of camouflage techniques is a complex field [4]. One of the central topics of camouflage is color—Does an animal match the color of its background? The concept of general background color matching has been integral to the study of camouflage throughout its history, and this strategy is common in the marine environment [1, 4–11].

Early camouflage studies were typically biased towards human vision and subjective color assessment [4]. The use of calibrated Red-Green-Blue (RGB) and other forms of photography has effectively been applied to study color patterns and background matching [12–18], though it does not provide fully spectrally resolved light data. Spectroradiometry with fiber optic probes has been widely used in terrestrial and marine camouflage research to provide full spectral reflectance from an organism and address color discrimination by observers [8, 11, 19–22]. For animals and backgrounds which have small, highly contrasting color elements, however, sampling of the entire pattern with a spectroradiometer probe is difficult and provides isolated data points that may not always be statistically representative of the entire organism without equipment modification and rigorous technique [21]. An additional sampling concern is contamination of the signal from specular reflectance. While this can be greatly minimized through proper alignment of subject, light, and probe [20], it remains a concern particularly on smooth, curved animal surfaces like those under investigation here.

Hyperspectral imagery (HSI) represents a combination of these traditional techniques and is an invaluable tool for the objective study of spectral camouflage [23–25]. A hyperspectral imager provides a near-synoptic image with full spectral or "hyperspectral" information for every pixel covering an organism and its background habitat. Specular reflection can be easily identified and removed from the dataset. Moreover, the large volume of gridded data allows for statistical processing of both the spectral and spatial components of animal and background patterns which are impossible or difficult to sample with other methods [26]. Recent developments in highly portable imagers allow the use of hyperspectral imagery in the field and onboard small vessels to investigate dynamic changes in animal coloration. Here, a portable imager was used to investigate camouflage in two species of crab endemic to floating mats of the brown macroalgae *Sargassum* (*S. natans* and *S. fluitans*).

Sargassum mats cover vast areas of the ocean surface in the subtropical North Atlantic [27–29]. These mats serve as important primary producers [30, 31] and habitat in the open ocean. Several hundred species are known to associate with or utilize the mats, including an endemic faunal community [27, 32–36]. A *Sargassum* mat is a complex optical and structural environment. Mats contain both pelagic species in varying stages of age and biofouling, as well as other biological and artificial debris. Organisms adapted to this habitat have evolved a high degree of crypsis. There is no hard cover in which to hide, and animals may be detected simultaneously from any angle. Color and patterning which mimic the algae are common among endemics, as is the use of shapes which resemble fronds, stipes, or gas vesicles [37–39]. Animals seeking refuge within *Sargassum* are under threat of detection from multiple classes of visual system with differing spectral sensitivities. Important predators in the mats include several species of seabird [40], pelagic fish [31, 32, 41], and *Sargassum* endemics including the frogfish *Histrio histrio* and swimming crab *Portunus sayi* [27, 31, 42, 43]. Research on camouflage and predator avoidance in this environment has focused on crustaceans, which are among the most abundant *Sargassum* animals by species, number, and biomass [27]. The present study builds from pioneering work conducted 70–100 years ago focusing on chromatophore response to background in *Sargassum* crabs and shrimp [5, 9, 37], but employs the use of hyperspectral imagery to quantify the ability of predators to distinguish between the crab and its background based on color. As outlined in [6] and [26], quantitative studies of camouflage must consider three main factors: 1) the reflectance properties of the target and background, 2) the ambient light field and optical environment, and 3) the visual system of the observer. While multiple studies have investigated background matching under varying light fields [6, 19, 21, 22] and predator visual systems [11, 21, 23], this is one of the first studies to use hyperspectral imagery to investigate all of these components of spectral matching and crypsis in terms of predation from both in-water and airborne predators.

Methods

This study focused on camouflage of two different species of crab collected from the Sargasso Sea. The methods for capturing organisms, measuring the hyperspectral reflectance properties of crabs and background *Sargassum*, quantifying the ambient light field and optical environment, and for assessing background color matching from the perspective of different predators are discussed below.

2.1 Collection of Crabs and *Sargassum*

Organisms and spectra were collected aboard the sailing vessel *Sea Dragon* on two cruises (26–28 May 2013 and 2–5 June 2013) south of Bermuda in the vicinity of 31° 12.29'N, 64° 40.41'W. Collection took place under the auspices and protocols of the Bermuda Natural History Museum as part of a larger research effort. No specific permits were required for collection of *Sargassum* or associated invertebrates, and no protected or endangered species were collected. Samples of *Sargassum sp*. were collected using dip nets with hole size < 3mm [27, 33, 39]. *Sargassum* collections were hand-sorted in buckets of seawater on deck shortly after sampling. Crabs were separated into individual containers with water and placed in shade. Samples of the *Sargassum* immediately surrounding the crabs when found were also taken (approximately 300mL) in an attempt to identify the microhabitat in which the individual was located just prior to collection, i.e. the specific background it would have naturally been viewed against. When this was not possible due to displacement of an individual within the net, a random sample from within that collection was taken. Crabs and macroalgae were quickly imaged (typically < 30 minutes) to prevent possible effects from thermal or other stressors. Animals were returned to the water with live algae samples after imaging.

2.2 Hyperspectral Imaging and Analysis

Spectral information was collected using a tripod-mounted 710 Hyperspectral Imager (Surface Optics Corporation). This instrument collects an image (520 x 696 pixels) with spectral information at 128 bands with 5 nm spacing from 380 nm to1040 nm, known as a "data cube." Study organisms were gently restrained and imaged under daylight illumination on a diffusive, matte dark grey background (average $R = 0.12$) at approximately normal incidence. Every image included a Spectralon (LabSphere) standard for calculation of reflectance $R(\lambda)$, the ratio of incident photons scattered backwards off the target at each wavelength [44]. The calculated reflectance is independent of the light field and considered to be an inherent optical property of the target. For this study, the target was assumed to be Lambertian, reflecting light equally at all angles. While the surfaces of crabs and algae are most likely non-Lambertian, our assumption is reasonable when applied to the element of reflectance which includes color information (as opposed to glare or specular reflection off the carapace surface) [20] and was sampled by our approach.

ENVI (Exelis VIS) image analysis software was used to process data cubes. All spectra were interpolated from instrument and standard calibrations to 1 nm resolution. The image was converted to reflectance by normalizing to an average radiance obtained from non-saturated pixels centered on the Spectralon standard (generally >500 pixels). For each individual crab, Regions of Interest (ROIs) were hand selected to include the carapace surface and avoid visibly glare-contaminated pixels. Saturated pixels were identified and masked. Algae pixels were extracted from the imagery using a Normalized Difference Vegetation Index (NDVI), which contrasts reflectance in near infrared wavelengths (700 nm) to red wavelengths (670 nm) and has been previously used to identify *Sargassum* [44]. The NDVI identifies algal pixels containing a "red edge," the sharp rise in reflectance in far red wavelengths common to plant material.

Pixels with calcareous epibionts are not identified with an NDVI and were selected manually. For the statistical analyses, a random subset of *Sargassum* pixels equal to the number of available crab carapace pixels (~500–1500 pixels) was selected as representative of the background for that individual. Mean reflectance curves for each individual crab and corresponding algal background were then generated.

2.3 Discrimination by Predators

Color vision in vertebrates is the result of input from multiple classes of photoreceptive cone cell viewing the same visual field, each of which is sensitive to a different range of wavelengths [45]. The difference in signal from the receptor classes is then compared via an opponency mechanism to produce the sensation of color. Systems with two, three, and four classes are classified as di, tri, and tetrachromats, respectively [6, 45, 46]. To assess whether two colored targets might be distinguishable/discriminable to a given observer under given light conditions, the widely used Vorobyev and Osorio model [46] was applied. This model was used to investigate color matching in the view of two generalized predator types: fish and birds. Dichromat piscine (mahi mahi—*Coryphaena hippurus*) and tetrachromat avian (wedge-tailed shearwater —*Puffinus pacificus)* models were selected. *C. hippurus*, a blue/green sensitive pelagic fish [47, 48], is a frequent *Sargassum* visitor shown to consume *P. sayi* through gut content analysis [43] and is one of the only known predators of *Sargassum* crabs for which spectral sensitivity data is available. Multiple taxa of sea birds forage for fish and crustaceans in *Sargassum* lines [40]. *P. pacificus* was selected for visual modeling as it is perhaps the most comprehensively studied for spectral sensitivity in marine birds [49, 50], and it is broadly sensitive to wavelengths from the ultraviolet to far red.

To estimate the color contrast of crabs and algae to the predator visual system, the proportion of incident photons captured by each class or type of photoreceptor (quantum catch) was first calculated for each crab and algae spectrum according to the general form:

$$\begin{aligned} q_i &= k_i \int_{\lambda min}^{\lambda max} I(\lambda)T(\lambda)R(\lambda)S_i(\lambda)d\lambda \\ k_i &= 1 \div \int_{\lambda min}^{\lambda max} I(\lambda)T(\lambda)R^b(\lambda)S_i(\lambda)d\lambda \\ Q_i &= \ln q_i \end{aligned} \tag{1}$$

where λ_{min} and λ_{max} are the limits of the spectral region considered, i is the photoreceptor type (with higher numbers indicating longer λ sensitivity), q_i is the receptor quantum catch for a given photoreceptor type, k_i is the von Kries transformation for color constancy, $T(\lambda)$ is light transmission between target and observer, $R(\lambda)$ is the reflectance of a target, $R^b(\lambda)$ is the mean reflectance of the visual field, $S_i(\lambda)$ is the spectral sensitivity of the receptor, and finally Q_i is the coded, logarithmic quantum catch for that photoreceptor [11, 19, 23 46]. The lower bound, λ_{min}, was set at 400 nm due to the signal-to-noise limitation of the imager, while λ_{max}, 700 nm, represents the upper boundary of light sensitivity in the bird model. Photopigment absorption spectra $S(\lambda)$ for each predator were taken from published sources. Fish sensitivity spectra [47] were digitized and a transmission curve (T50 = 436nm [48]) was applied to produce final sensitivity spectra S_i. Bird spectral sensitivities [50, 51] were digitized and directly utilized in the model.

In this chromatic discrimination model, contrast between crab and algae quantum catch signals for each photoreceptor type are determined via a neural opponency mechanism [22, 23, 46]. It is assumed that detection is limited by physiological noise in the receptor channels themselves. Similarity between two target colors was calculated as chromatic contrast (ΔS).

For the fish predator:

$$\Delta S^2 = (\Delta Q_1 - \Delta Q_2)^2/(e_1^2 + e_2^2) \quad (2)$$

For the bird predator:

$$\begin{aligned}\Delta S^2 = {} & [(e_1e_2)^2(\Delta Q_4 - \Delta Q_3)^2 + (e_1e_3)^2(\Delta Q_4 - \Delta Q_2)^2 + (e_1e_4)^2(\Delta Q_3 - \Delta Q_2)^2 + \\ & (e_2e_3)^2(\Delta Q_4 - \Delta Q_1)^2 + (e_2e_4)^2(\Delta Q_3 - \Delta Q_1)^2 + (e_3e_4)^2(\Delta Q_2 - \Delta Q_1)^2] \\ & /[(e_1e_2e_3)^2 + (e_1e_2e_4)^2 + (e_1e_3e_4)^2 + (e_2e_3e_4)^2]\end{aligned} \quad (3)$$

where e is the estimate of receptor signal-to-noise and ΔQ_i is the difference in quantum catch between two spectra (crab and background) for a given receptor type. Noise is approximated by:

$$e_i = \omega_i/\sqrt{g_i} \quad (4)$$

where ω_i is the Weber fraction noise estimate and g_i is the relative abundance (or ratio) of the photoreceptor type. In the absence of species-specific information, ω_i was set at 0.05 which is appropriate for avian vision in high light situations [52] and also used in studies of fish visual systems [23, 53]. For each receptor type g_i, the relative abundance of each was used [11, 19, 23, 26]. For the fish model, the ratio was set at 1:1 ($g_1 = g_2$) [11, 19, 23]. In birds, the relative abundance of their four photoreceptor types has been found to increase with sensitivity to longer wavelengths, but is highly variable both between species and eye region [26, 49]. For the bird model, $g_1{:}g_2{:}g_3{:}g_4$ was initially set as 1.5:1:1.5:2 [49, 50, 51] which represents the mean for the entire eye in *P. pacificus*. The UV component of avian vision is not modeled by our method, but this is unlikely to influence our results, as later discussed.

The units of chromatic contrast (Δ*S*) are Just Noticeable Differences (JNDs). Larger JNDs indicate greater color contrast to the visual system of the observer [11, 22, 23, 46]. When this parameter was less than 1, the crab was considered indistinguishable from its background. The literature suggests that values between 1 and 4 are difficult to distinguish, while JNDs greater than 4 would indicate that the crab is readily distinguishable [46, 53–55].

Additionally, achromatic contrast (or difference in luminance) can be used to identify targets on small spatial scales [17, 19–23, 51]. This is accomplished through paired or double cones, while chromatic contrast is processed from input of single cone cells. We calculated achromatic contrast for all crabs, under both fish and bird predators, as:

$$(\Delta S_{AC}) = (\Delta Q)/e \quad (5)$$

where ΔQ is the difference in quantum catch for crab and algae to the longest wavelength cone, and e calculated as in Eq 4.

Light Environment and Attenuation. Light field and water optical property data were generated in Hydrolight 5.2 (Sequoia Scientific) radiative transfer software from user specified inputs. As visual systems are sensitive to photons and not energy, irradiances were converted to quanta. The optical properties of the water column were determined from the New Case 1 Model using satellite derived Chlorophyll *a* concentration values (NASA GES DISC, Giovanni Web Service) and should be representative of clear Sargasso Sea water. A second case was also

considered with high light attenuation comparable to conditions found in the Florida Keys coastal region, using previous local measurements of diffuse attenuation K_d (λ) [56].

Attenuation through the water column at each wavelength was modeled [6, 56, 57] from Beer's Law:

$$E_d(z) = \quad E_d(0^-)e^{-K_d z} \tag{6}$$

where E_d(z) and $E_d(0^-)$ are downward irradiance at depth z and just below the surface and K_d is the downward diffuse attenuation coefficient (with (λ) notation dropped for clarity). From this, a transmission factor T(λ) was calculated [6, 26, 56, 57] for use in predator visual modeling:

$$T(\lambda) = \frac{E_d(z)}{E_d(0^-)} = \quad e^{-K_d z} \tag{7}$$

Several of the above parameters (illumination, light transmission through the water column, and bird photoreceptor ratio) were varied to determine the impact of these factors on chromatic contrast. For all individual crabs, the impact of modifying model parameters was assessed by change in chromatic contrast, dividing the new chromatic contrast value by the initial values:

$$\text{Change } \Delta S = \frac{\Delta S_{mod}}{\Delta S_{ini}} \tag{8}$$

Results

First, we describe observations of floating algal mats and *Sargassum* crabs encountered in the Sargasso Sea. The reflectances obtained from hyperspectral imagery of crabs and algae taken in the field are presented and compared. Then, we develop a conceptual modeling framework from our field observations. Using the conceptual and reflectance data, color matching by crabs is assessed through two different visual models: a dichromat fish and tetrachromat bird.

3.1 Environment and Organism Description

Drifting mats of *Sargassum* were encountered sporadically throughout both cruises. *Sargassum* was observed in different densities and configurations, including expansive amorphous mats (Fig 1A), thin windrows, and isolated clumps of one or a few individual strands or "plants" (Fig 1B). Mats extended to different depths depending on the mean buoyancy of individual strands and the density of strands in a given mat. A "dense" mat was approximately 30 cm thick, though this was variable. Our observations revealed clumps penetrating to approximately 5 m below the sea surface. The upper surface of thick mats was often uniform and emergent (Fig 1C). The bottoms of the mats were more rugose, leading to a complex 3-dimensional environment (Fig 1D). For a camouflaging animal, this would allow for a multitude of depths and orientations in relation to the ambient light field.

Two species of crab were found in the mats and used as model organisms in this study (Fig 2). The *Sargassum* Swimming Crab *Portunus sayi (Gibbes 1850)* was the larger of the two and had a yellow/brown, mottled appearance on its dorsal carapace. Of the 8 individuals (4 male, 4 female) encountered, the carapace width ranged from 0.50 cm to 2.53 cm and averaged 1.04 cm. Subjectively, the background shade of the carapace varied from yellow to dark brown and the mottled patterns varied greatly between individuals. Small *P. sayi* were lighter yellow overall, with dark markings. All individuals possessed a dorsal saddle mark with a central white

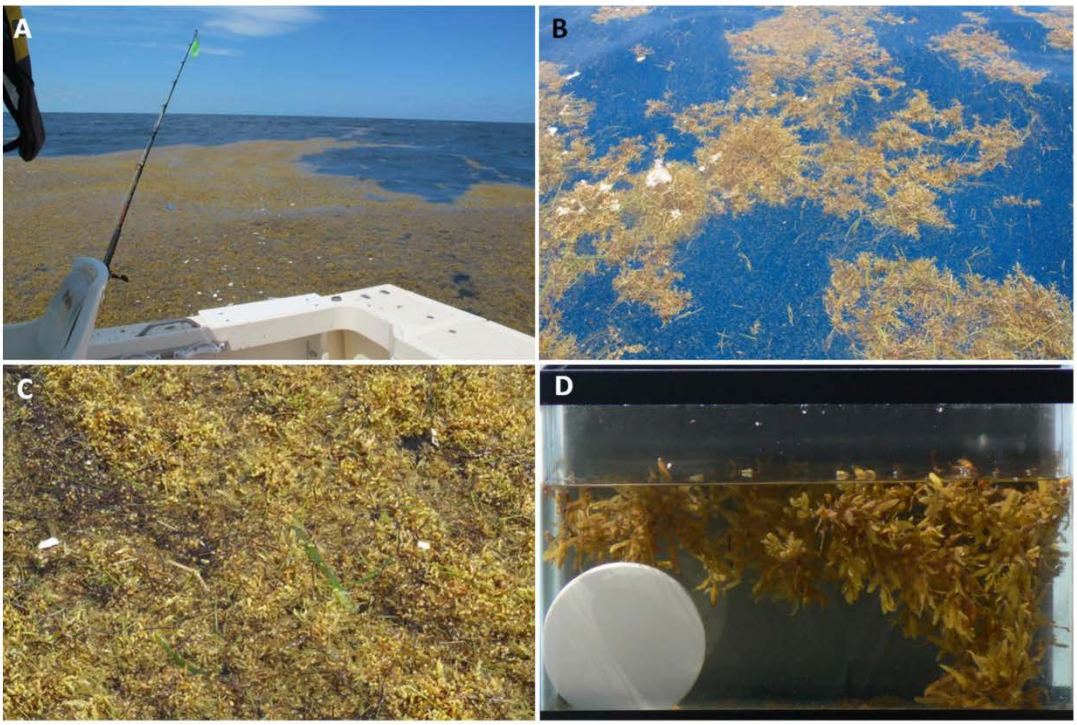

Fig 1. Photos of the floating macroalgae *Sargassum* encountered during this study in the Sargasso Sea, south of Bermuda. Individual aggregations can be extensive and densely packed (**A**) or more diffuse (**B**). Densely packed mats can be solid and partially emergent from the water column (**C**). The algae may float at several different depths and extend downwards from the surface by tens of centimeters, as depicted with a sample in a small tank (**D**).

doi:10.1371/journal.pone.0136260.g001

patch. The patch covered approximately 4% of the carapace (Fig 2A and 2B). Larger individuals possessed additional small white spots. Limbs were generally marked with light and dark stripes perpendicular to the appendage. The carapace of the largest individual (Fig 2B) was darker overall, but retained the saddle marking. We have observed the same trend of darkening with size in other regions (Greater Florida Bay, Gulf of Mexico).

The Gulf Weed or Columbus Crab *Planes minutus* (Linnaeus 1758) was generally yellow in color (Fig 2C), ranging to light orange for some individuals. Twenty three individuals were encountered on *Sargassum* (12 male, 11 female), and carapace widths ranged from 0.31 cm to 0.80 cm, with a mean of 0.53 cm. Conspicuous white spots were apparent on 8 *P. minutus*, ranging in size from ~1 mm^2 to the entire surface of the carapace. These were irregularly shaped, with 1–2 markings per individual. With the exception of these markings, individual *P. minutus* were generally uniform in color.

P. minutus were also found on a floating, red plastic bucket during the first cruise. These crabs were much darker in coloration than those in *Sargassum* (Fig 2D) and were treated as a separate subpopulation in this study. In the plastic bucket, 7 individuals (3 male, 4 female) ranged from 0.51 cm to 0.88 cm, with a mean of 0.69 cm. Six of these were dark red, with one

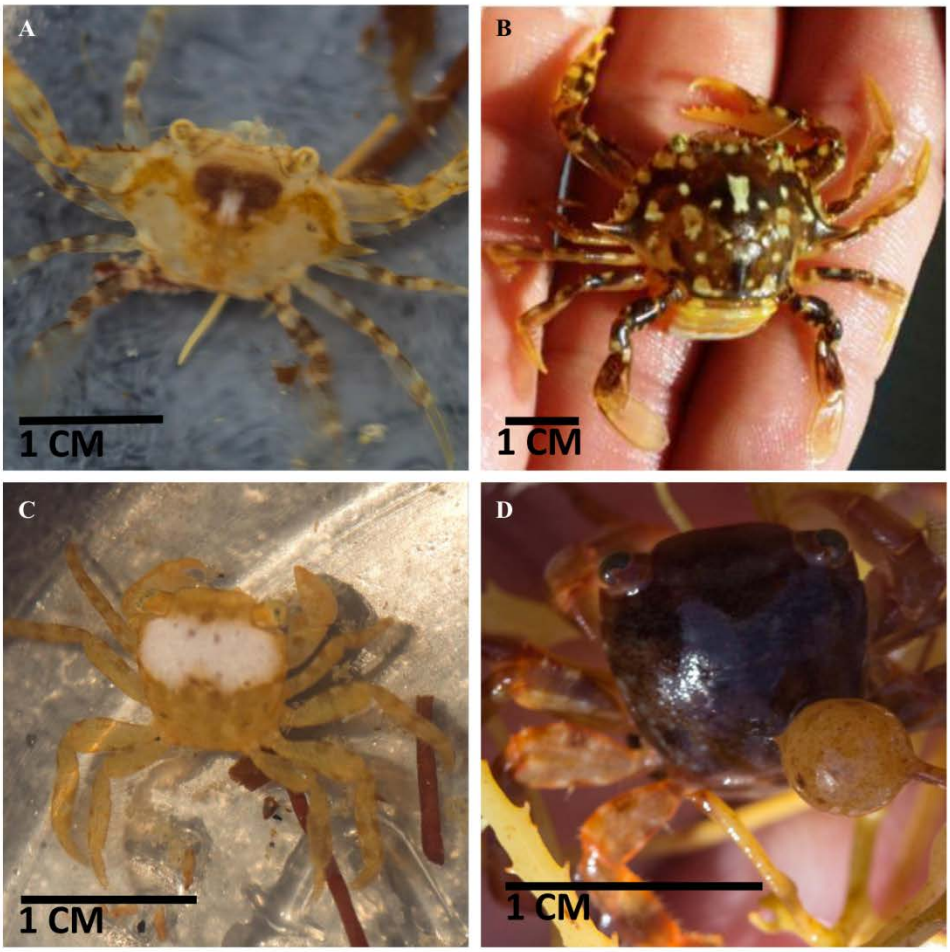

Fig 2. Photos of representative *Sargassum* crabs from two different species encountered in the Sargasso Sea. *Portunus sayi* display considerable variation in pattern from more uniform and pale (**A**, small adult male) to highly mottled (**B**, large adult female). Some aspects of patterning, such as the central dorsal white spot and m-shaped saddle marking, appeared in all adult individuals. The smaller species *Planes minutus* tended to have a more uniform coloration across the carapace (**C**, adult female). Some individuals had one or more white patches on the dorsal surface which ranged from small to covering the entire carapace and appendages. Several dark red *P. minutus* (**D**, adult male) were found drifting on a plastic bucket.

doi:10.1371/journal.pone.0136260.g002

possessing a large white spot covering approximately 75% of the carapace. One individual was brown in color, though darker than those found on algae. No significant difference in carapace width was observed between male and female for either species. For individuals collected on *Sargassum*, all crab colors were visually within those of algae samples. Ventral sides were pale yellow to white for both species.

The location and orientation of the crabs within the floating *Sargassum* mats were not directly observable with our collection methods. However, short term observations were made

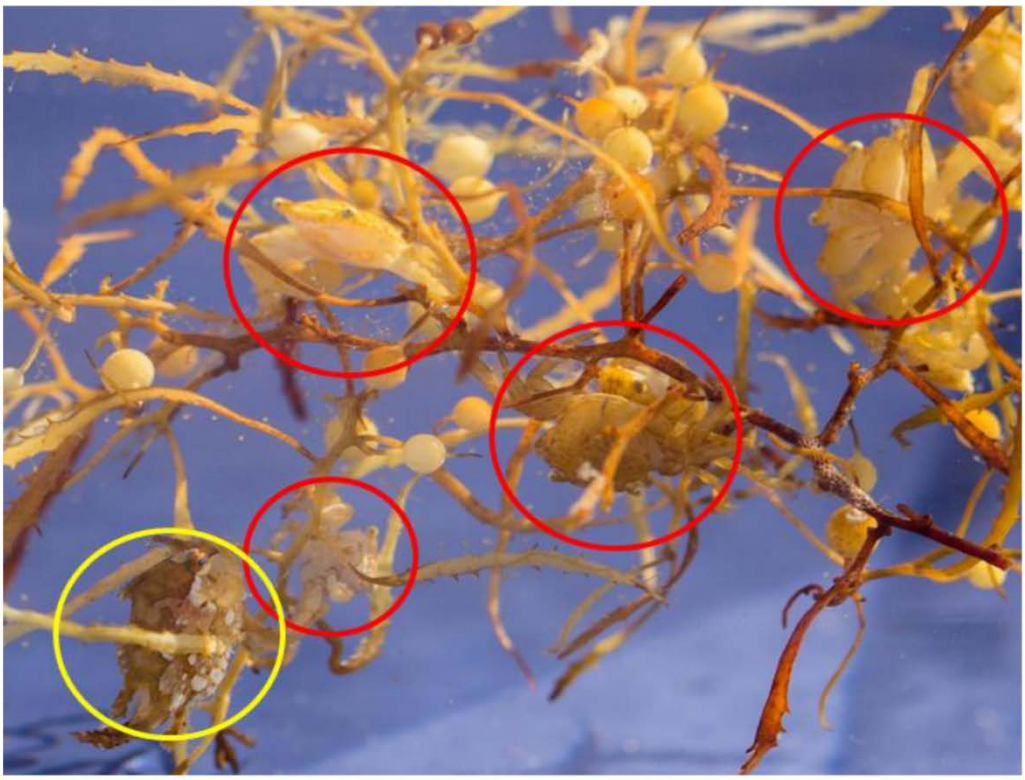

Fig 3. *Sargassum* crabs on algae in a small tank. Individual crabs (circled in red) did not show any preferred orientations relative to algae during short-term measurements in shipboard aquaria. Note the presence of a small frog fish, *Histrio histrio*, in the lower left (yellow circle).

doi:10.1371/journal.pone.0136260.g003

on deck in small tanks, where crabs were allowed to move freely within clumps of algae. Individuals were oriented in multiple directions clinging to algae fronds and stipes, with no clear trends in positioning or movement evident (Fig 3) for either species. Both species of crab appear to display counter-shading, though neither seemed to continually orient themselves to utilize this camouflage strategy. We have also observed adult *P. sayi* sitting emergent from the water column on top of mats in the Florida Keys, though this was not seen during the present study. While specific animal frequency data was not collected, multiple individuals were often encountered in the same dip sample, periodically in close proximity. Both species were encountered in the same sample on at least one occasion.

Water was clear without considerable amounts of phytoplankton or other light absorbing or scattering constituents. The mean Chlorophyll *a* concentration (Chl) in this region during the study period was estimated from the MODIS Aqua ocean color satellite to be ~0.1 mg m^{-3}. Water clarity in this region, although highest in the summer (Chl = 0.05 mg m^{-3}), was considered high throughout the year. During the study period, daylength was approximately 14 hrs with mostly clear sky conditions.

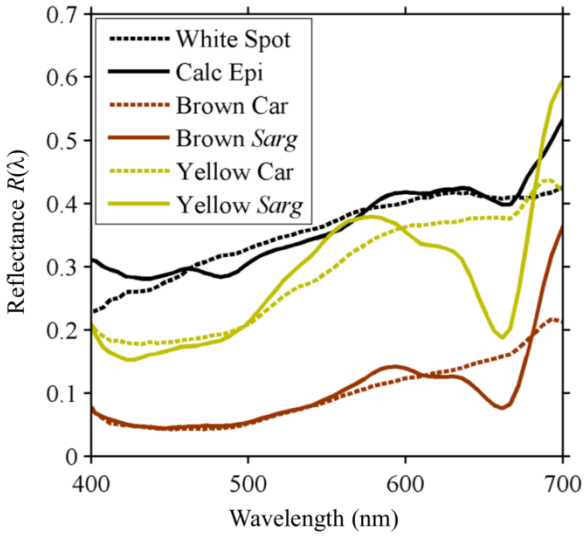

Fig 4. Reflectance of *P. sayi* pattern elements and subjectively corresponding habitat features. Reflectance *R*(λ) of the white, brown, and yellow areas on a randomly selected *P. sayi* carapace very closely matched the reflectance of calcareous epibionts, senescent brown, and healthy yellow *Sargassum*. Spectra of yellow and white areas on *P. minutus* showed similar correspondence. As with carapace and algae mean reflectance, maximum divergence appears in the far red.

doi:10.1371/journal.pone.0136260.g004

3.2 Reflectance of Organism and Background

Hyperspectral imaging (HSI) was conducted on each individual crab and the associated background of *Sargassum* or red plastic. For an individual crab, the reflectance of the different color and pattern elements (yellow, brown, white) show good matching to elements of the *Sargassum* environment (Fig 4). Over the entire carapace and algae ROIs, both crab and algae showed low mean reflectance in blue wavelengths (400–500 nm), with values rising steadily into the orange and red (500–600 nm) (Fig 5A and 5B). Crab reflectance continued to gradually increase monotonically, while *Sargassum* flattened due to characteristic absorption features and then dipped sharply at the Chlorophyll *a* secondary absorption band (675 nm) before rising exponentially at the vegetative "red edge". Standard deviation of *R*(λ) for both crabs and algae was lowest in short wavelengths, and increased into the red, representing the variability of *R*(λ) among all pixels in a ROI. *R*(λ) values were generally normally distributed for both species (S1 Fig).

Both *P. sayi* (Fig 6A, 6B and 6C) and *P. minutus* (Fig 6D, 6E and 6F) most closely matched the reflectance of their algal backgrounds in the blue, green, and yellow regions of the spectrum, with greater divergence appearing in the red. For all individuals of both species on algae, the largest difference was observed in a small region centered on the secondary chlorophyll absorption feature (Fig 6C and 6F) where the spectral differences were up to seven times greater than that at other wavelengths. For individual *P. minutus* with large white markings, enhanced reflectance was found in blue and green spectral regions (Fig 6D, black dotted lines) and resulted in abnormally high differences between crab and background in blue wavelengths (Fig 6F) as well as increasing the variation in *R*(λ) values for this species. Among the generally

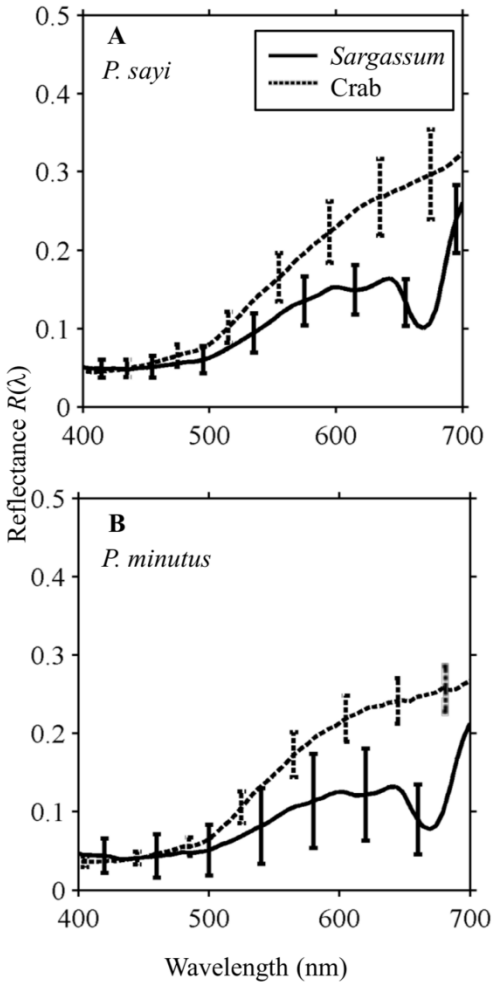

Fig 5. Mean and standard deviation of the measured reflectance spectra, *R*(λ), for a single randomly selected individual and its background obtained from a hyperspectral image of A) *P. sayi* and B) *P. minutus*. The greatest difference for both species appears around the secondary chlorophyll absorption dip (675 nm) present in *Sargassum* reflectance, but not observed for the crabs. Variation in *R*(λ) across the carapace is lowest in the blue and increases towards the red.

doi:10.1371/journal.pone.0136260.g005

dark red *P. minutus*–bucket subgroup, reflectance was flatter and lower across all wavelengths than for the other groups (Fig 6G). The corresponding reflectance of the plastic was also extremely low (Fig 6H), and the greatest difference between crab and background reflectance in this group was observed between 575 and 675 nm (Fig 6I).

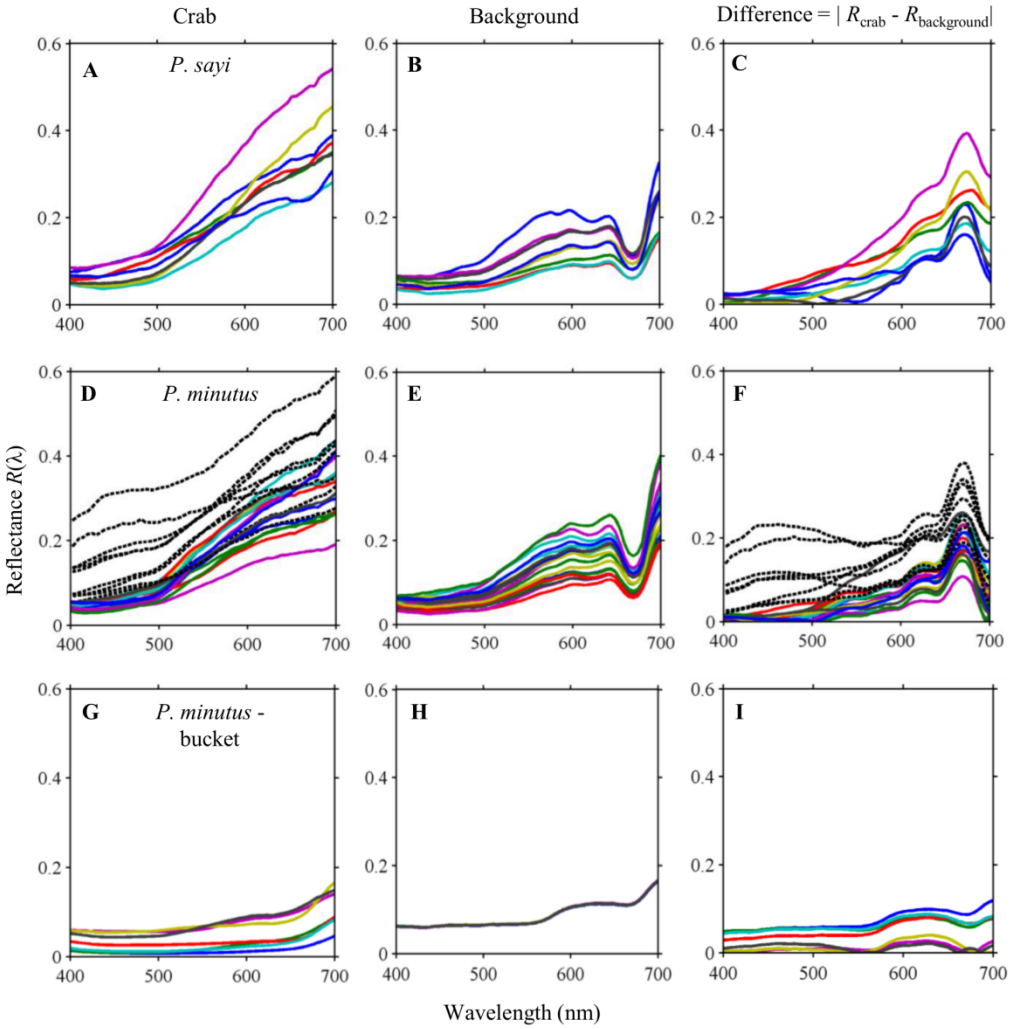

Fig 6. Reflectance *R(λ)* of individual crabs and associated backgrounds determined from hyperspectral imagery collected from the Sargasso Sea. Left panels show the reflectance spectra of individual crabs. Middle panels show spectra for the associated background (*Sargassum* or bucket). Right panels present the difference between the left (crab) and middle (background) panels. Error bars for each spectrum have been omitted for clarity, but were similar to that for the example individuals. Black dashed lines in panels (**D, F**) represent *P. minutus* with large white markings and higher reflectance than other crabs of both species. Individual *P. minutus* collected from a floating red bucket (**G**) all had substantially lower reflectance than crabs on natural algae. The greatest difference between crabs and algae was centered around the secondary absorption band of Chlorophyll *a* (675 nm) where a dip was found in the *Sargassum* reflectance spectrum.

doi:10.1371/journal.pone.0136260.g006

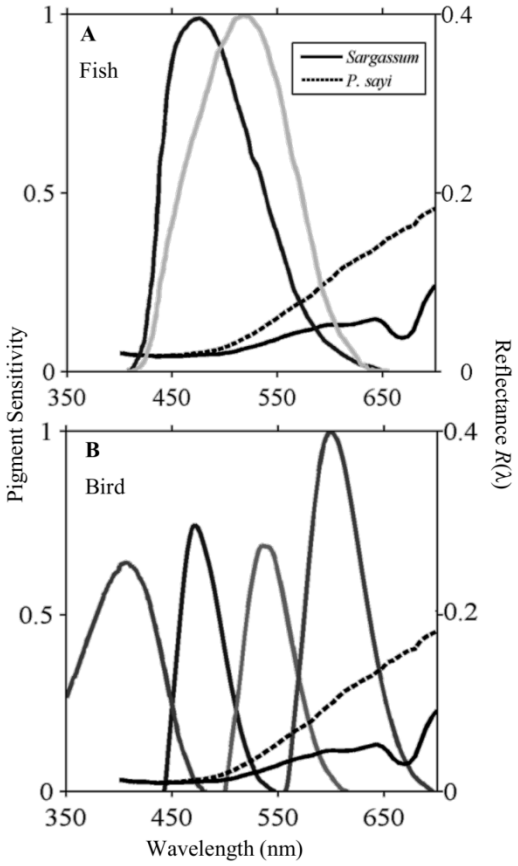

Fig 7. Normalized visual pigment sensitivities for dichromat fish mahi mahi (A), *Coryphaena hippurus* (Munz and McFarland 1979), and tetrachromat bird wedge-tailed shearwater (B), *Puffinus pacificus* (Hart 2004). *C. hippurus* is most sensitive to light in the blue and green wavelengths, while *P. pacificus* is also sensitive to red wavelengths. Sensitivity spectra (limited to 400–700 nm) are superimposed on sample *R(λ)* for crab and algae.

doi:10.1371/journal.pone.0136260.g007

3.3 Discrimination of Crab and Background by Predators

Following our observations of the environment and organisms (Sec. 3.1) and reflectance measurements of algae and crabs (Sec. 3.2), a conceptual framework was developed for assessing the color matching abilities of *Sargasum* crabs in the view of fish and bird predators (Fig 7). This framework allowed us to vary several of the parameters in the chromatic contrast model to emulate realistic environmental variation. Several "worst case" scenarios are presented for testing configurations of airborne and in-water predators, light field, and water column.

Two initial scenarios were considered based on predator type. Within the conceptual framework, the crab was placed on the background and observed with the dorsal surface facing

orthogonal to the predator. *Sargassum* was treated as a planar surface comprised of the fronds of algae and opaque to light. For the fish predator, the algal surface was placed vertically. This is consistent with the strategy of *C. hippurus*, which attacks prey parallel to the water surface [58]. Depth was arbitrarily set at 15 cm, within a reasonable depth range for floating *Sargassum*. The illumination spectrum $I(\lambda)$ was set as downward planar irradiance $E_d(\lambda)$ at 15 cm below the sea surface (S2 Fig).

In the bird predation scenario, the algal surface was placed horizontally at the surface of the water column with the crab emergent and observer in air, looking downward. The illumination $I(\lambda)$ was set as downward planar irradiance incident upon the sea surface $E_d(0^+)$ (S2 Fig). For both scenarios, $T(\lambda)$ was initially set at 1 for all wavelengths.

The parameter chromatic contrast, in units of Just Noticeable Differences (JNDs), quantified how discernible each crab was from its background given the visual capabilities of the predator and the chosen environmental scenario. On *Sargassum*, *P. sayi* and *P. minutus* achieved approximately equal contrast under initial conditions (Fig 8). The dichromat piscine predator was not able to reliably discriminate between background and crab for either species, though some individual crabs showed JNDs above the threshold detection value of 1 (Fig 8A). The tetrachromat avian predator, by contrast, was able to distinguish between crab and background for both species with no individuals below the threshold (Fig 8B). Mean contrasts were not significantly different ($p = 0.05$) between *P. sayi* and *P. minutus*. Within each group, individual crabs achieved a wide range of chromatic contrast with their background. For *P. sayi*, contrast was inversely correlated to carapace width for both dichromat fish and tetrachromat bird predators (Fig 9A and 9B), while *P. minutus* showed positive correlation (Fig 9C and 9D).

Achromatic contrast was an order of magnitude higher than chromatic contrast for the piscine model (Fig 10A) for both *P. sayi* and *P. minutus*, and approximately twice as high for most individuals as chromatic contrast for the avian predator (Fig 10B). Contrasts between crab species were not significantly different ($p = 0.05$). No contrast trends with body size were observed.

3.4 Discrimination of Crab and Background—Model Variation

Avian Photoreceptor Ratio. For the avian predator model, multiple photoreceptor ratios were considered. Initially, the mean ratio of 1.5:1:1.5:2 was used. A unity ratio 1:1:1:1 and two ratios found in birds were examined: 1:1:2:2 and 1:2:2:4 [26, 49]. Due to the presence of outliers, median chromatic contrast for each group was used in comparing the effects of receptor ratio. Median JND increased for all crab populations, as well as most individuals, with increasing relative numbers of long wavelength receptor types. *P. sayi* group median chromatic contrast was 22% lower than initially at 1:1:1:1, 8% lower at 1:1:2:2, and 14% higher at 1:2:2:4. For *P. minutus*, the corresponding changes were 20% lower, 7% lower, and 12% higher for the respective ratios (Fig 11A). Several individuals in both species showed decreased contrast (< 1) at the 1:2:2:4 ratio. These crabs had relatively low reflectance in the blue relative to most individuals.

Attenuation through Water Column. Attenuation by water with observer distance was investigated by varying $T(\lambda)$. For the fish, $T(\lambda)$ was calculated using horizontal distance through the water column in place of depth z (Eq 7). When evaluating attenuation by water for the bird, the predator was considered to have its head underwater during active foraging, and transmission across the air-water interface was not considered. An overlaying water column of varying depth was added to the initial scenario. Illumination $I(\lambda)$ as $E_d(\lambda)$ was generated for each depth, and $T(\lambda)$ calculated. Attenuation was estimated for two water types with differing optical characteristics, corresponding to the Bermuda Sargasso Sea and coastal Florida (S3 Fig) where we have also encountered *P. sayi*. Attenuation by the water column with increasing

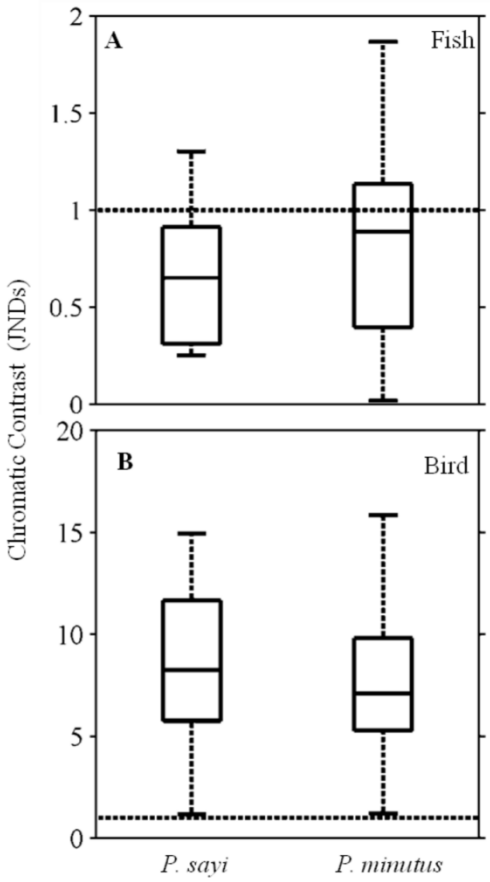

Fig 8. Crab chromatic contrast (Δ*S*) for initial model conditions when viewed by fish (A) and bird (B) predator models. Units are Just Noticeable Differences (JNDs), and values less than 1 (dashed line) indicate that the organism is not distinguishable from its background. Contrasts for the fish model were mostly below 1, while values for the bird were significantly higher.

doi:10.1371/journal.pone.0136260.g008

distance between target and observer decreased discriminability of crabs and algae for both predators. Low sensitivity was observed for the piscine predator (Fig 11B), which showed negligible (< 10%) decrease in chromatic contrast under all but the most attenuating Florida condition at 5 m depth, with reductions in median contrast of 29% for *P. sayi*, and 25% for *P. minutus*. The impact of attenuation on chromatic contrast was somewhat more pronounced for the bird predator model at intermediate attenuation than for the fish (Fig 11C). Under the most attenuating 5m Florida condition, reductions in median contrast were 33% for *P. sayi*, and 23% for *P. minutus*. Some individuals showed an increase in contrast with attenuation. This was restricted to those *P. minutus* with large, dorsal white spots and a single *P. sayi*. The effect of attenuation on achromatic contrast was negligible for the fish predator, and somewhat

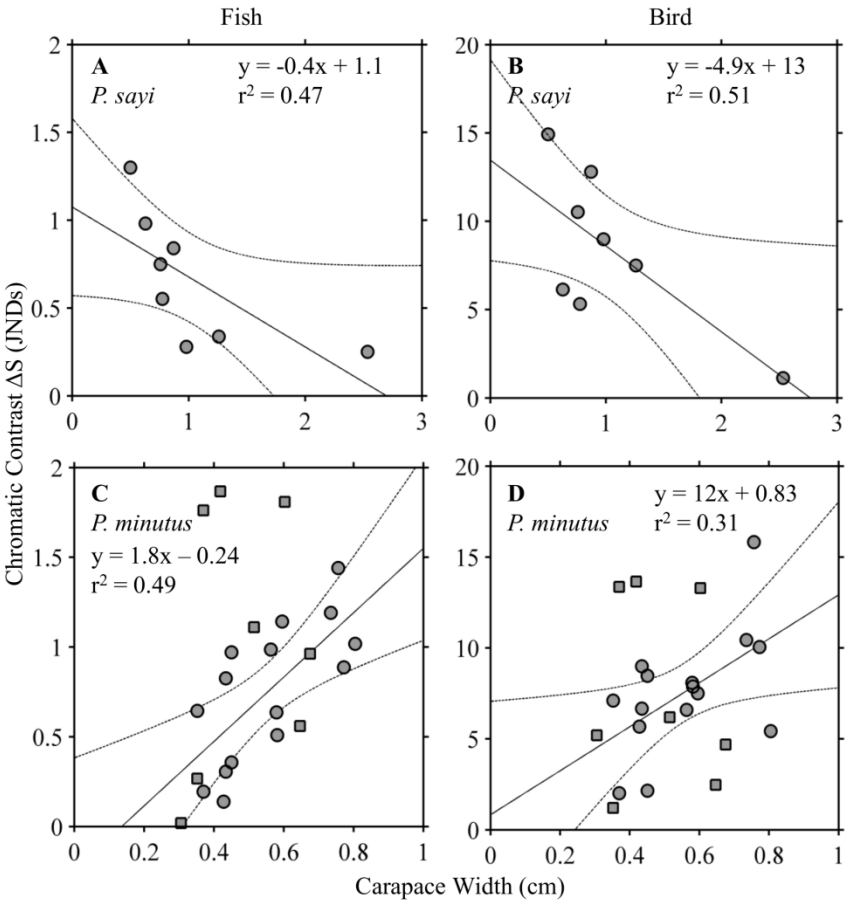

Fig 9. Chromatic contrast (Δ*S*) plotted against carapace width (CW) for each species under fish (left panels) and bird (right panels) visual models. A linear regression model was fit to each group. Δ*S* showed a strong, significant (p = 0.05) negative correlation to CW for both models in *P. sayi* (**A**, **B**). For *P. minutus* (**C**, **D**), significant positive correlation to CW was observed for individuals without large white patches (circles). This correlation was not observed for individuals with white patches (squares), which have been superimposed on the figure and were not used in calculating the regression. Dotted lines represent 95% confidence interval.

doi:10.1371/journal.pone.0136260.g009

more pronounced for the bird (Fig 12) with median reductions under 5% at 1 m for both water types, and of 16% (Bmd) and 15% (Fld) for *P. sayi* at 5 m, and 14% (Bmd) and 12% (Fld) for *P. minutus*. Physically, for both water types the discrepancy in reflected signals between crab and algae diminished with increasing absorption and scattering with distance through the water column, particularly in the highly absorbed red wavelengths (S4 Fig).

Illumination and Visual Scene Reflectance. When illumination spectra $I(\lambda)$ was altered from solar noon (initial scenario) to a red-shifted low solar angle (1 hour before sunset), a $< 1\%$ increase from the initial conditions in median contrast for each group of crab was

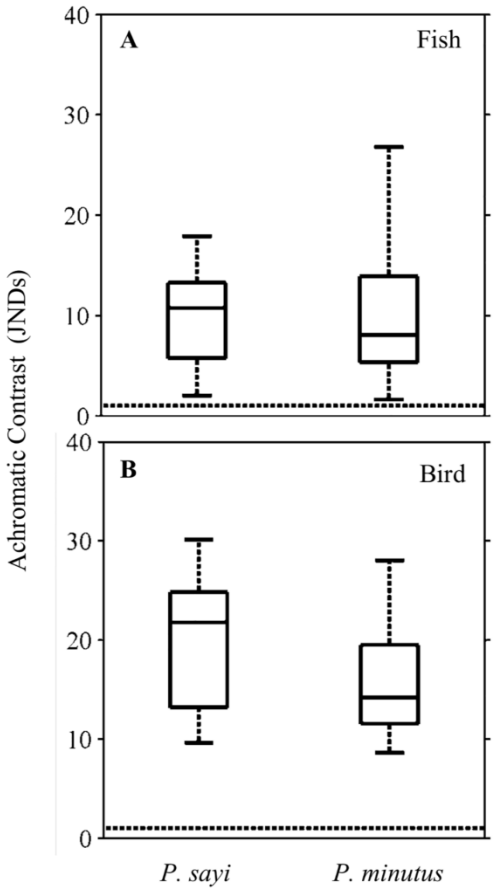

Fig 10. Achromatic contrast (ΔS_{AC}) for initial model conditions when viewed by fish (A) and bird (B) predator models. Units are Just Noticeable Differences (JNDs), and values less than 1 (dashed line) indicate that the organism is not distinguishable from its background. Achromatic contrast for both crab species were not significantly different (p = 0.05) for either predator model. All individuals were above the threshold value of 1 for both predators.

doi:10.1371/journal.pone.0136260.g010

observed for the bird visual model under sunset illumination, with no change in contrast evident for the fish at the given precision (1 decimal place). Varying $R^b(\lambda)$ as a linear mix of algae and water had no discernible impact on chromatic contrast at the level of precision used for either predator.

Discussion

We hypothesize that camouflage in the *Sargassum* ecosystem will be well developed due to its location at the air-water interface, the total lack of hard-cover retreats from predation, and the presence of multiple classes of visual systems. Indeed, we found that the spectra reflected from

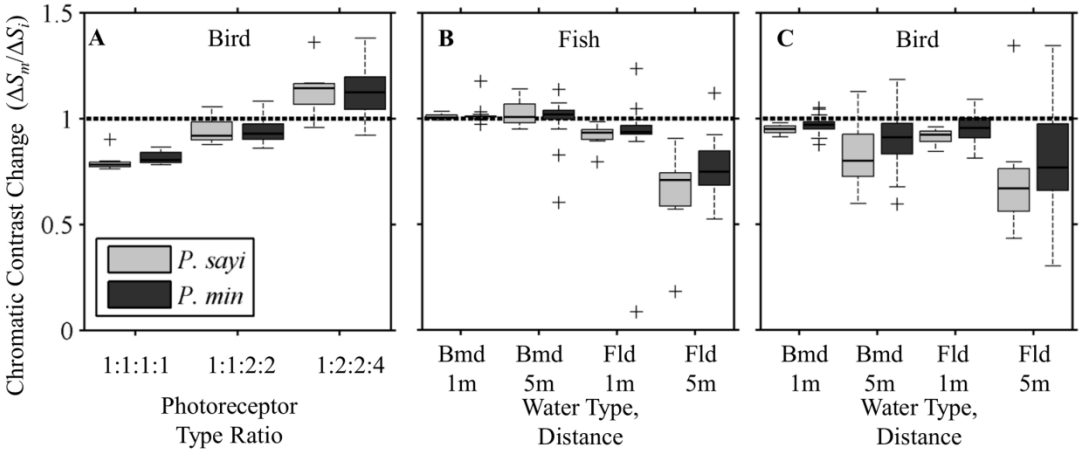

Fig 11. Impact of bird model photoreceptor ratios and water column attenuation on chromatic contrast (Δ*S*). Bars represent median contrast for each crab group relative to Δ*S* for the initial condition. Dashed line represents a ratio of 1 (no change). For bird photoreceptor ratios (**A**), the unity ratio achieved the lowest chromatic contrast. Contrast increased with increasing proportion of red-sensitive photoreceptor types. Chromatic contrast at 1 and 5 m distance in a low (Bermuda/Bmd) and high (Florida/Fld) attenuation water columns were compared to null attenuation (T = 1, Eq 1). Simulating attenuation of light with distance generally decreased contrast values for both fish (**B**) and bird (**C**) predators, though this was highly variable on an individual basis with some individuals becoming more distinguishable (> 1). Outliers (+) were observed for both crab species. Decrease in chromatic contrast was most pronounced for the highest attenuation condition (Fld, 5 m).

doi:10.1371/journal.pone.0136260.g011

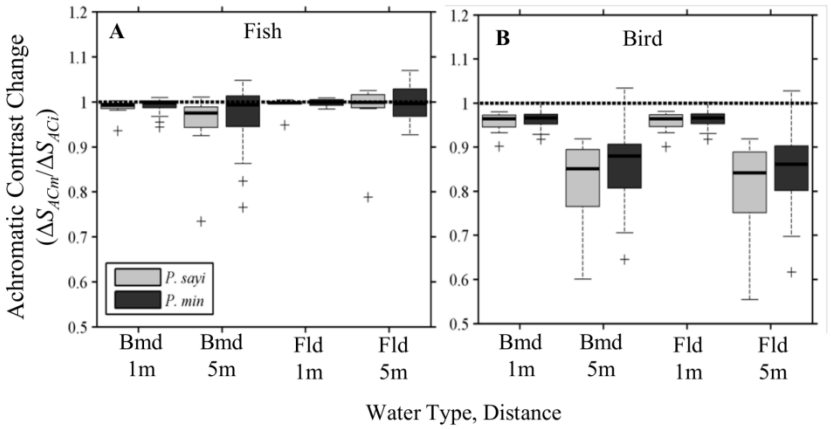

Fig 12. Impact of water column attenuation on achromatic contrast (ΔS_{AC}) to fish (A) and bird (B) models. Bars represent median contrast for each crab group relative to ΔS_{AC} for the initial condition. Dashed line represents a ratio of 1 (no change). Decrease in achromatic contrast was generally low, except for the avian predator under the 5 m conditions, where median ΔS_{AC} of both species decreased by 15% and up to 50% for some individuals. Outliers (+) were observed for both crab species.

doi:10.1371/journal.pone.0136260.g012

the crabs were very close to the background *Sargassum* (or red bucket), except at far red wavelengths. Important differences were found between the two species in terms of size when viewed by piscine and airborne predators.

Discrimination by Predators Relative to Body Size

For *P. sayi*, chromatic contrast showed a strong decrease with increasing carapace width. In other words, the larger crabs were able to better match their background color than the smaller crabs. The sample size (n = 8) was relatively small given the variation in $R(\lambda)$ for this species. Even though there was only a single very large *P. sayi* encountered in this study (2.5 cm wide), the correlation remained significant without this individual for body sizes from 0.5 to 1.3 cm ($p < 0.01$). *P. sayi* is known to change color on short (several hours) time scales, which may be employed in dynamic camouflage [59]. Expansion and contraction of chromatophores beneath the transparent carapace changes the color of the animal, and may provide a better match to its general surroundings [9, 60, 61]. Apparently, the background matching ability of *P. sayi* improves with size and/or age. The smaller crab, *P. minutus*, however, showed an opposite trend with body size, such that the larger individuals showed a greater contrast to their background than the smaller ones. Unlike *P. sayi*, coloration in *P. minutus* is not known to be dynamic and only changes over long time scales [5, 9]. As discussed further below, the individuals found on the dark red bucket had a significantly darker red color than those found on *Sargassum*, indicating an ability to acclimate to differently colored backgrounds. Color matching increased with carapace width in *P. sayi* and decreased in *P. minutus*. These results suggest that differences in body size, patterning, and camouflage strategy may be significant between these species [62]. Further research on color change in *P. sayi* and pattern heterogeneity in both species, determined from hyperspectral images, is forthcoming.

Planes minutus on Floating Debris

By a stroke of coincidence, the present work sheds light on a much earlier study. The *P. minutus* encountered on a drifting bucket were of a deep red color not found in the natural algal population, which mirrors an observation by Crozier [5] of "mahogany" *P. minutus* on a floating cedar log. Unable to induce color change in adult *P. minutus* by placing them on varying backgrounds in a series of experiments, he postulated that this species may change coloration to match substrate over long periods. Hitchcock [9] described the crabs' chromatophore responses, but found no clear indication that the species attempted to match new backgrounds over several days. In the present study, bio-fouling on the bucket indicates a significant period adrift. A prolonged duration within the bucket is supported by the significantly ($p = 0.02$) larger size of the bucket *P. minutus* as opposed to those from *Sargassum*. *P. minutus* is evidently capable of morphological color change on long time scales, possibly related to pigment deposition during molting [10, 61, 63], in contrast to the more rapid changes of *P. sayi* [59]. The present observation confirms Crozier's initial discovery that *P. minutus* possesses an ability to match backgrounds with a wide color range, even beyond those encountered on evolutionary time scales.

Predator Visual Systems

The ratio and spectral sensitivities of observer photoreceptor types can alter the chromatic contrast of a given target by an order of magnitude. *Sargassum* crabs match their algal background least closely in the red wavelengths. Model runs confirmed that the presence, as well as the relative abundance, of long wavelength sensitive photoreceptors increased chromatic discrimination between crab and background. While there is variation in cone cell sensitivity across bird

taxonomic groups [49], measured or modeled data is still lacking for many bird species. This variation is greatest in shorter wavelengths, where birds possess either an ultraviolet (UVS) or significantly long-shifted violet sensitive (VS) type. Variation is considerably lower in longer wavelengths, as the spectral sensitivities of the medium, short, and long wave cone pigments (SWS MWS, and LWS, respectively) are relatively conserved [49]. The model bird in this study, *P. pacificus*, has the violet type. Work by Chiao et al. [23] has shown that color discrimination may not be greatly affected by small shifts in maximum absorption by visual pigments, and so the potential differences between the model system selected and actual avian predators is likely negligible for the purposes of this study. It must be noted that *P. pacificus*, like all known birds, is sensitive to wavelengths shorter than 400 nm. This is the lower bound of our visual model, due to the technical limitations of the hyperspectral imager. Discrepancies in $R(\lambda)$ between crabs and algae in the ultraviolet would not be accounted for in our chromatic contrast calculations. However, inclusion of lower wavelengths would not significantly change our results. Crabs and *Sargassum* are very closely matched in $R(\lambda)$ at 400nm, and our study assumes that this relationship persists in the UV, and ΔQ_{VS} would remain unchanged. The enhanced discrimination ability of birds in this system is apparently due to sensitivities in red wavelengths. Any divergence in $R(\lambda)$ between crabs and background below 400 nm would only increase discrimination in the bird visual model, which is already clearly able to differentiate crab and algae by color.

In addition to chromatic contrast, birds, fish, and other animals are known to utilize achromatic contrast (or difference in luminance) to identify targets on small spatial scales. Many studies of animal camouflage have investigated this visual channel [17, 19, 20–23, 51, 54, 70, 73]. Our results indicate that the achromatic contrast between crabs and algae is up to an order of magnitude higher than the chromatic contrasts calculated in this study, and less affected by attenuation. The luminance channel may therefore be important for predators trying to detect crabs which are well matched to the algae in terms of chromatic contrast.

The visual systems of other important predators, like the Sargassum frogfish *Histrio histrio*, have yet to be studied and may be drivers of camouflage in this environment. *H. histrio* is a voracious ambush predator, and gut contents frequently contain *P. sayi*, *P. minutus*, and shrimp [64]. Visual sensitivity data is not available for *H. histrio*, but prey survival experiments on red, green, and yellow artificial *Sargassum* indicate that *H. histrio* may utilize color discrimination and camouflage breaking to detect prey [65]. The fish we modeled in this study, *C. hippurus*, is a widely distributed pelagic predator not endemic to the mats. Pelagic fish such as *C. hippurus* have visual pigments adapted to open-ocean ambient light fields [43, 48]. Visual pigments in fish adapted to *Sargassum* mats may be sensitive to longer wavelengths. Behavioral and molecular evidence for color discrimination by crabs, as well as the use of this ability in behavioral tasks like mate and habitat selection, is increasing [66–68]. Whether either *Sargassum* crab is able to utilize color information in guiding behavior is unknown, but seems possible in light of evidence for visual habitat discrimination by *Sargassum* crustaceans [39, 69].

Chromatic Modeling

Multiple models exist for estimating discrimination of color. The Vorobyev and Osorio model is widely used and supported by experimental data [4, 11, 16, 19, 21–23, 26, 46, 53, 54], and was considered appropriate for this study. Color constancy is here modeled by the von Kries transformation [21–23, 46, 54, 70], which incorporates both illumination $I(\lambda)$ and the mean reflectance of a scene, $R^b(\lambda)$. Varying the light field between noon and sunset conditions showed virtually no impact on the chromatic contrast of crabs for either predator. For this reason, there would likely be little difference in chromatic contrast between the horizontal

downwelling irradiance used in the conceptual model and a more realistic sidewelling illumination. This has been observed [22] when measured downwelling and sidewelling irradiances were compared using the Vorobyev and Osorio model. Effects at the air-water interface may impact chromatic discrimination by birds beyond what has been considered here. While the red shifted light at sunset may slightly increase contrast for the bird, enhanced glint with low sun angle [71] would make target detection more difficult. Other surface effects like bubble production, spatial resolution, and signal loss through transmission across the air-water interface for submerged crabs would also make it more difficult for flying birds to detect prey.

A radiative transfer model was used to generate illumination data for both the surface and depth. Such sophisticated light modeling might not be necessary for deep, clear oceanic "type 1" water columns where simple estimates of illumination can be sufficient for most applications. However, more refined treatment of the spectral absorption and scattering properties of the water column can be important for assessing camouflage in many ecosystems. In optically shallow waters, for example, reflectance from the seafloor impacts the spectral shape, magnitude, and polarization characteristics of the light field [2]. Organisms that hide in such environments have to match downwelling light from the sun, as well as upwelling light reflected from the seafloor (sediment, seagrass, corals, etc.) and often match the polarization conditions that may be visible to certain predators [2].

Here, different spectral light attenuation properties were important to show the influence of water depth on background matching. The differences in reflected radiance between the crab and *Sargassum* became less pronounced with predator distance (S4 Fig). This is because water preferentially absorbs red photons [56]. Therefore, the reflected light from the crab and *Sargassum* in red wavelengths is absorbed by water molecules and primarily green photons (500–550 nm) reach the predator. This means that for fish swimming at the mats from a distance (e.g., *C. hippurus*), the crabs will be much harder to detect than for small fish endemic to the mats (*H. histrio*). Similarly, the crab was much less discernible at 5 m distance to a bird foraging at the sea surface in both Bermuda and particularly in the more turbid Florida waters.

The background reflectance, $R^b(\lambda)$, used in this study was the average reflectance of a *Sargassum* sample imaged on deck, and is not fully representative of the true environment. A more accurate spectrum would possibly include dark water or glint, and require knowing the field of view of the predator. Simple linear mixing of algae and water spectra (Sec. 3.4), however, indicated that variation in $R^b(\lambda)$ played a minimal role in overall chromatic contrast.

Comparable Camouflage Systems

While direct comparison between studies is difficult, it appears that *Sargassum* crabs generally demonstrate similar or lower contrast to their natural background than multiple other cryptic species. In crabs, perhaps the most studied groups in regards to color, camouflage, and patterning are fiddler and shore crabs. For example, the fiddler crab *Uca vomeris*, when subject to predation by birds, achieves a similar color match to *Sargassum* crabs on a more static background (mud flat). When under low pressure from birds, these crabs showed significantly higher chromatic contrast (and therefore a poorer color match) compared to either high-predation *U. vomeris*, or the *Sargassum* crabs *P. sayi* and *P. minutus* [8]. However, a different fiddler crab, *U. tangeri*, has been shown to achieve much lower contrast (and better matching) against birds [21]. The shore crab *Carcinus maenas* has similar chromatic contrast to *Sargassum* crabs against natural backgrounds to an avian visual model [17]. In this study, *C. maenas* also showed a color change response to background albedo. Similarly, the horned ghost crab *Ocypode ceratophthalmus* exhibits both dynamic color change and a significant degree of background matching [16], though direct comparison to the present study is difficult as the authors

did not quantify color matching in either tetrachromat or dichromat visual space. Like *P. Sayi* and *P. minutus*, the kelp crab *Pugettia producta* is also found closely associated with macroalgae. This crab exhibits an ontogenetic color shift: juveniles are found in red algae turf habitat and are generally dark red, and then migrate to off shore kelp beds and change to a brown or amber coloration [63] during adulthood. While we are unaware of any research on background color matching in this species, survivorship studies indicate that the distinct color morphs of *P. producta* are well camouflaged against macroalgae [10, 62]. In a comparable terrestrial paradigm, researchers found that crab spiders hiding on flowers had similar or higher chromatic contrast values against both trichromatic prey and tetrachromat avian predators than *Sargassum* crabs [72, 73]. Extensive research on cuttlefish has yielded a range of contrasts relative to background, but *Sargassum* crabs appear to achieve a comparable match to their background in the view of fish predators [19, 22, 23].

Conclusions

Sargassum crabs were found to be extremely well matched to their background over most of the visible spectrum and were not distinguishable from algae in the view of a dichromat fish predator. Tetrachromat birds, by contrast, were able to discriminate between the color of *Sargassum* crabs and algae because of photoreceptors at far red wavelengths, corresponding to the chlorophyll absorption maximum. Interestingly, only one species of crab previously studied had better background matching to avian predators than the *Sargassum* crabs, but that species was found in mud flats without a noticeable chlorophyll absorption peak [21]. The ability to more closely match their algal background from visual detection by a fish compared to a bird potentially suggests that *Sargassum* crab camouflage may be driven more by predation by fish than birds.

Chromatic contract was considered under multiple environmental scenarios including diurnal variation in illumination, signal attenuation by water with distance, predator visual adaptation to patch size, and predator photoreceptor ratios. Photoreceptor ratio in avian predators and signal attenuation over distance had the largest effects on chromatic contrast. Attenuation of the light reflected from the crab and *Sargassum* generally decreased the chromatic contrast of crab and background with distance for both the fish and bird predators. With increasing distance in the real environment, factors such as veiling light, observer spatial resolutions, and occlusion of the target by algal fronds will also play a role in discrimination by predators [6, 26]. Additionally, some of the unique properties of air-water interface such as sun glint, internal reflection of photons and the presence of waves, bubbles and foam may also play a role that has yet to be considered [74, 75].

Sargassum crabs have convergently evolved coloration and patterning to match their background in an environment with no hard cover refuge and predation from both above and below the water surface. High resolution spectral measurements in the far red wavelengths ($>$ 650 nm) were necessary to model chromatic contrast in this ecosystem. Hyperspectral imaging provided information on the variability associated with an individual carapace or algal sample that could not be effectively quantified using fiber optic spectrometry, and allowed for modeling the effects of variation in light field and visual system parameters on chromatic contrast. Forthcoming studies will utilize the spatially resolved information from this imagery to study patterning and heterogeneity in *Sargassum* crabs.

Supporting Information

S1 Data. Mean reflectance spectra for individual crabs and associated algae samples, with notations and crab metadata. Spectra are organized by spreadsheet with spectra in columns.

The first row of all spectral spreadsheets is a header.
(XLSX)

S1 Fig. Distribution of $R(\lambda)$ values. Histograms of reflectance values at selected wavelengths corresponding to the visual sensitivities of fish and a region of close spectral matching (430 nm), a region of crab visual sensitivity [67] (490 nm), and high $R(\lambda)$ discrepancy (660 nm) for an individual **A**) *P. sayi* and **B**) its associated *Sargassum* sample. Reflectance for an individual image was generally normally distributed, indicating the suitability of using mean reflectance spectra for chromatic modeling.
(TIF)

S2 Fig. Illumination as downwelling irradiance $E_d(\lambda)$ at the surface (solid line) and at 15cm depth (dashed line). Irradiances are very similar in blue and green (400–550 nm) wavelengths, but diverge at longer wavelengths due to preferential attenuation and transmission across the air-sea interface.
(TIF)

S3 Fig. Diffuse attenuation (K_d) used in predator visual models for Bermuda (solid line) and Florida (dashed line) water types. Attenuation for Bermuda waters is low and characteristic of clear oceanic waters, with attenuation increasing exponentially in the red wavelengths. Florida waters attenuate much more strongly, particularly in the blue, due to the presence of colored dissolved organic matter (CDOM) and sediments.
(TIF)

S4 Fig. Impact of water column on target signal ($R(\lambda)^* I(\lambda)$) for a sample *P. sayi* and associated *Sargassum* in Bermuda water type. Attenuation with distance decreased the difference between reflected light from crab and algae that is available to the observer, modeled here for the avian predator at 1 and 5 m depth. This is particularly true in the highly absorbed red wavelengths, where the spectral signatures of both animal and background converge.
(TIF)

Acknowledgments

Ship-time was donated by the Bermuda Alliance for the Sargasso Sea, and the Bermuda Aquarium, Museum, and Zoo. We wish to thank Eric Heupel of the University of Connecticut for assistance in sample collection, imagery, and photography. We thank Dr. Wolfgang Sterrer and Dr. R. Struan Smith of BAMZ for co-ordination efforts, as well as the crew and researchers aboard *Sea Dragon* for assistance in collecting animals. We would like to thank two anonymous reviewers for comments on an earlier version of this paper.

Statement concerning study animals: All live animals in this study were invertebrates and not subject to University of Connecticut IRB/IACUC requirements. All measures were taken to minimize suffering or stress of subjects.

Author Contributions

Conceived and designed the experiments: BJR. Performed the experiments: BJR. Analyzed the data: BJR HMD. Contributed reagents/materials/analysis tools: BJR HMD. Wrote the paper: BJR HMD.

References

1. Cott HB (1940) Adaptive coloration in animals. Oxford University Press, New York

2. Gilerson AA, Stepinski J, Ibrahim AI, You Y, Sullivan JM, Twardowski MS, et al. (2013) Benthic effects on the polarization of light in shallow waters. Applied Optics 52: 8685–8700 doi: 10.1364/AO.52.008685 PMID: 24513934
3. Brady P, Travis K, Maginnis T, Cummings ME (2013) The polaro-cryptic mirror: a biological adaptation for open-ocean camouflage. Proc Natl Acad Sci USA 110: 9764–9769 doi: 10.1073/pnas.1222125110 PMID: 23716701
4. Stevens M, Merilaita S Eds. (2011) Animal Camouflage: Mechanisms and Function. Cambridge University Press, Cambridge
5. Crozier WJ (1918) Note on the Coloration of *Planes minutus*. Am Nat 52, 262–263
6. Endler JA (1990) On the measurement and classification of colour in studies of animal colour patterns. Biol J Linn Soc 41: 315–352
7. Hanlon RT, Chiao CC, Mathger LM, Barbosa A, Buresch KC, Chubb C (2009) Cephalopod dynamic camouflage: bridging the continuum between background matching and disruptive coloration. Phil Trans Roy Soc B 364: 429–437
8. Hemmi JM, Marshall J, Pix W, Vorobyev M, Zeil J (2006) The variable colours of the fiddler crab *Uca vomeris* and their relation to background and predation. J Exp Biol 209: 4140–4153 PMID: 17023607
9. Hitchcock HB (1941) The coloration and color changes of the Gulf-Weed Crab, *Planes minutus*. Biol Bull 80: 26–30
10. Hultgren KM, Stachowicz JJ (2008) Alternative camouflage strategies mediate predation risk among closely related co-occurring kelp crabs. Oecologia 155: 519–528 PMID: 18084779
11. Cheney KL, Skogh C, Hart NS, Marshall NJ (2009) Mimicry, colour forms and spectral sensitivity of the bluestriped fangblenny, *Plagiotremus rhinorhynchos*. Proc R Soc B 276: 1565–1573 doi: 10.1098/rspb.2008.1819 PMID: 19324827
12. Barnard ME, Strandburg-Peshkin A, Yarett IR, Merz RA (2012) The blue streak: a dynamic trait in the mud fiddler crab, *Uca pugnax*. Invertebr Biol 131: 52–60
13. Detto T, Hemmi JM, Backwell PRY (2008) Colouration and colour changes of the fiddler crab, *Uca capricornis*: a descriptive study. PLoS ONE 3(2): e1629 doi: 10.1371/journal.pone.0001629 PMID: 18286186
14. Josef N, Amodio P, Fiorito G, Shashar N (2012) Camouflaging in a complex environment—octopuses use specific features of their surroundings for background matching. PLoS ONE 7: e37579 doi: 10.1371/journal.pone.0037579 PMID: 22649542
15. Silbiger N and Munguia P (2008) Carapace color change in *Uca pugilator* as a response to temperature. J Exp Mar Biol Ecol 355: 41–46
16. Stevens M, Rong CP, Todd PA (2013) Colour change and camouflage in the horned ghost crab *Ocypode ceratophthalmus*. Biol J Linn Soc 109: 257–270
17. Stevens M, Lown AE, Wood LE (2014) Colour change and camouflage in juvenile shore crabs *Carcinus maenas*. Front Ecol Evol 2: 14
18. Troscianko J, Stevens M (2015). Image Calibration and Analysis Toolbox—a free software suite for objectively measuring reflectance, colour, and pattern. Methods Ecol Evol
19. Akkaynak D, Allen JJ, Mäthger LM, Chiao CC, Hanlon RT (2013) Quantification of cuttlefish (*Sepia officinalis*) camouflage: a study of color and luminance using in situ spectrometry. J Comp Physiol A 199: 211–225
20. Baldwin J, Johnsen S (2012) The male blue crab, *Callinectes sapidus*, uses both chromatic and achromatic cues during mate choice. J Exp Biol 215: 1184–1191 doi: 10.1242/jeb.067512 PMID: 22399664
21. Cummings ME, Jardao JM, Cronin TW, Oliveira RF (2008) Visual ecology of the fiddler crab, *Uca tangeri*: effects of sex, viewer and background on conspicuousness. Anim Behav 75:175–188
22. Hanlon RT, Chiao CC, Mathger LM, Marshall NJ (2013) A fish-eye view of cuttlefish camouflage using in situ spectrometry. Biol J Linnean Soc 109: 535–551
23. Chiao CC, Wickiser JK, Allen JJ, Genter B, Hanlon RT (2011) Hyperspectral imaging of cuttlefish camouflage indicates good color match in the eyes of fish predators. Proc Natl Acad Sci U S A. 108: 9148–9153 doi: 10.1073/pnas.1019090108 PMID: 21576487
24. Manolakis D, Marden D, Shaw GA (2003) Hyperspectral image processing for automatic target detection applications. IEEE Signal Processing Magazine, 14: 79–116
25. Pinto F, Mielewczik M, Liebisch F, Walter A, Greven H, Rascher U (2013) Non-invasive measurement of frog skin reflectivity in high spatial resolution using a dual hyperspectral approach. PLoS ONE 8(9): e73234. doi: 10.1371/journal.pone.0073234 PMID: 24058464
26. Endler JA, Mielke PW (2005) Comparing entire colour patterns as birds see them. Biol J Linnean Soc, 86: 405–431

27. Butler JN, Morris BF, Cadwallader J, Stoner AW (1983) Studies of *Sargassum* and the *Sargassum* community. Bermuda Biological Station Research, *Special Publication* 22: 1–307
28. Gower JFR, Hu CM, Borstad G, King S (2006) Ocean color satellites show extensive lines of floating *Sargassum* in the Gulf of Mexico. IEEE T. Geosci Remote Sens 44: 3619–3625
29. Parr AE (1939) Quantitative observations on the pelagic *Sargassum* vegetation of the western North Atlantic. Bull Bingham Oceanogr Collect 6: 1–94
30. Peres JM (1982) Specific pelagic assemblages. In: Kinne O, editor. Marine ecology, vol. 5, pt. 1, John Wiley and Sons, New York. pp. 314–372
31. Rooker JR, Turner JP, Holt SA (2006) Trophic ecology of *Sargassum*-associated fishes in the Gulf of Mexico determined from stable isotopes and fatty acids. Mar Ecol Prog Ser 313: 249–259
32. Coston-Clements L, Settle LR, Hoss DE, Cross FA (1991) Utilization of the *Sargassum* habitat by marine invertebrates and vertebrates—A review. NOAA Tech Mem NMFS-SEFSC-296
33. Dooley JK (1972) Fishes associated with the pelagic *Sargassum* complex, with a discussion of the *Sargassum* community. Contrib Mar Sci 16: 1–32
34. Fine ML (1970) Faunal variation on pelagic *Sargassum*. Mar Biol 7: 112–122
35. Morris BF, Mogelberg DD (1973) Identification manual to the pelagic *Sargassum* fauna. Bermuda Biological Station for Research, St. George's West
36. Weis JS (1968) Fauna associated with pelagic *Sargassum* in the Gulf Stream. Am Midl Nat 80: 554–558
37. Brown FA (1939) The coloration and color changes of the Gulf-Weed Shrimp, *Latreutes fucorum*. Amer Nat 73: 564–568
38. Hacker SD, Madin LP (1991) Why habitat architecture and color are important to shrimps living in pelagic *Sargassum*: use of camouflage and plant-part mimicry. Mar Ecol Prog Ser 70: 143–155
39. Jobe CF, Brooks WR (2009) Habitat selection and host location by symbiotic shrimps associated with *Sargassum* communities: The role of chemical and visual cues. Symbiosis 49: 77–85
40. Moser ML, Lee DS (2012) Foraging over *Sargassum* by Western North Atlantic Seabirds. Wilson J Ornithol 124: 66–72
41. Wells RJD, Rooker JR (2009) Feeding ecology of pelagic fish larvae and juveniles in slope waters of the Gulf of Mexico. J Fish Biol 75:1719–1732 doi: 10.1111/j.1095-8649.2009.02424.x PMID: 20738644
42. Brooks WR, Hutchinson KA, Tolbert MG (2007) Pelagic *Sargassum* mediates predation among symbiotic fishes and shrimps. Gulf of Mexico Sci 2: 144–152
43. Palko BJ, Beardsley GL, Richards W (1982) Synopsis of the Biolological Data on Dolphin-Fishes, *Coryphaena hippurus* Linnaeus and *Coryphaena equiselis* Linnaeus. FAO Fisheries Synopsis (130); NOAA Technical Report NMFS Circular (443)
44. Dierssen HM, Chlus A, Russell B (2015) Hyperspectral discrimination of floating mats of seagrass wrack and the macroalgae *Sargassum* in coastal waters of Greater Florida Bay using airborne remote sensing. Remote Sens Environ doi: 10.1016/j.rse.2015.01.027
45. Chronin TW, Johnsen S, Marshall JN, Warrant EJ (2014) Visual Ecology. Princeton University Press, Princeton. doi: 10.1186/1472-6785-14-14 PMID: 24886170
46. Vorobyev M, Osorio D (1998) Receptor noise as a determinant of colour thresholds. Proc R Soc B 265: 351–358 PMID: 9523436
47. Munz FW, McFarland WN (1975) Part I. Presumptive cone pigments extracted from tropical marine fishes. Vision Res 15:1045–1062 PMID: 1166604
48. Fritsches KA, Partridge JC, Pettigrew JD, Marshall NJ (2000). Colour vision in billfish. Phil Trans R Soc B 355, 1253–1256 PMID: 11079409
49. Hart NS (2001) Variations in cone photoreceptor abundance and the visual ecology of birds. J Comp Physiol A 187: 685–697 PMID: 11778831
50. Hart NS (2004) Microspectrophotometry of visual pigments and oil droplets in a marine bird, the wedge-tailed shearwater *Puffinus pacificus*: topographic variations in photoreceptor spectral characteristics. J Exp Biol 207: 1229–1240 PMID: 14978063
51. Hart NS, Hunt DM (2007) Avian visual pigments: Characteristics, spectral tuning, and evolution. Am Nat 169: S7–S26. doi: 10.1086/510141 PMID: 19426092
52. Langmore N, Stevens M, Maurer G (2011) Visual mimicry of host nestlings by cuckoos, Proc R Soc B 278: 2455–2463 doi: 10.1098/rspb.2010.2391 PMID: 21227972

53. Hurtado-Gonzales JL, Loew E, Uy JAC. (2014) Variation in the visual habitat may mediate the maintenance of color polymorphism in a poeciliid fish. PLoS One 9 (7): e101497 doi: 10.1371/journal.pone.0101497 PMID: 24987856

54. Siddiqi A, Cronin TW, Loew ER, Vorobyev M, Summers K (2004) Interspecific and intraspecific views of color signals in the strawberry poison frog *Dendrobates pumilio*. J Exp Biol 207: 2471–2485 PMID: 15184519

55. Stevens M (2007) Predator perception and the interrelation between different forms of protective coloration. Proc R Soc B 274: 1457–1464 PMID: 17426012

56. McPherson ML, Hilll VJ, Zimmerman RC, Dierssen HM (2011) The optical properties of Greater Florida Bay: Implications for seagrass abundance. Estuar Coasts 34: 1150–1160

57. Mobley CD (1994) Light and Water: Radiative Transfer in Natural Waters. Academic Press, San Diego.

58. Barbosa P, Castellanos I Eds. (2005) Ecology of predator-prey interactions. Oxford University Press, New York.

59. Russell BJ and Dierssen HM (2012) Hyperspectral Imaging as a Tool for Camouflage Evaluation of the Sargassum Crab *Portunus sayi*. Ocean Optics Conference XXI. October 8–12. Glasgow, Scotland

60. Darnell MZ (2012) Ecological physiology of the circadian pigmentation rhythm in the fiddler crab *Uca panacea*. J Exp Mar Biol Ecol 426–427: 39–47

61. Green JP (1963) An analysis of morphological color change in two species of brachyuran crustaceans. Ph.D. Thesis, University of Minnesota, Minneapolis

62. Hultgren KM, Stachowicz JJ (2012) Camouflage in decorator crabs: integrating ecological, behavioural and evolutionary approaches. In: Stevens M, Merlaita S, editors. Animal Camouflage: Mechanisms and Function. Cambridge University Press, Cambridge

63. Iampietro PJ (1999) Distribution, diet, and pigmentation of the northern kelp crab, *Pugettia producta* (Randall) in central California kelp forests. Master's thesis, California State University, Stanislaus

64. Smith KL (1973) Energy transformations by the Sargassum fish, *Histrio histrio* (Linnaeus). J Exp Mar Biol Ecol 12: 219–227

65. Hutchinson KA (2004) Prey selectivity of the fishes *Stephanolepis hispidus* and *Histrio histrio* on the *Sargassum* shrimps *Latreutes fucorum* and *Leander tenuicornis*. MS Thesis, Florida Atlantic University

66. Bursey CR (1984) Color recognition by the blue crab, *Callinectes Sapidus* Rathbun (Decapoda, Brachyura). Crustaceana 47: 278–284

67. Detto T (2007) The fiddler crab *Uca mjoebergi* uses colour vision in mate choice. Proc Roy Soc B 274: 2785–2790

68. Hyatt GW (1975) Physiological and behavioral evidence for color discrimination by fiddler crabs (Brachyura, Ocypodidae, genus *Uca*) In: Vernberg FJ, editor. Physiological ecology of estuarine organisms. University of South Carolina Press, Columbia

69. West L (2012) Habitat location and selection by the Sargassum Crab *Portunus sayi*: The role of sensory cues. Master's Thesis, Florida Atlantic University

70. Johnsen S, Kelber A, Warrant E, Sweeney AM, Widder EA, Lee RL Jr, et al. (2006) Crepuscular and nocturnal illumination and its effects on color perception by the nocturnal hawkmoth *Deilephila elpenor*. J Exp Biol 209: 789–800 PMID: 16481568

71. Chang GC, Dickey TD (2004) Coastal ocean optical influences on solar transmission and radiant heating rate. J Geophys Res 109, 10.

72. Théry M, Casas J (2002) Predator and prey views of spider camouflage. Nature 415: 133

73. Defrize J,Théry M, Casas J (2010) Background colour matching by a crab spider in the field: a community sensory ecology perspective. J Exp Biol 213: 1425–1435 doi: 10.1242/jeb.039743 PMID: 20400626

74. Monahan EC, Mac Niocaill G (1986) Oceanic Whitecaps: And Their Role in Air-Sea Exchange Processes. Springer Science & Business Media

75. Randolph K, Dierssen HM, Twardowski M, Cifuentes-Lorenzen A, Zappa CJ (2014) Optical measurements of small deeply penetrating bubble populations generated by breaking waves in the Southern Ocean. J Geophys. Res Oceans 119: 757–756

3. Color change in the Sargassum Crab, *Portunus sayi*: Response to diel illumination cycle and background albedo

This chapter is prepared for submission to PloS ONE.

Color change in the Sargassum Crab, *Portunus sayi*: Response to diel illumination cycle and background albedo

Russell, Brandon J; Dierssen, Heidi M

University of Connecticut, Department of Marine Sciences

1080 Shennecossett Rd, Groton CT 06340

Abstract

Physiological color change has been observed in many crab species, and allows relatively rapid change in overall coloration and patterning. Change can be both rhythmic and acute. This has relevance to thermal regulation, communication, and camouflage. The Sargassum crab *Portunus sayi* possesses a heterogeneous yellow and brown patterning which matches its algal background. Here, we show that this coloration can be altered within hours. *P. sayi* held in a naturalistic illumination and temperature regime displayed a distinct diel cycle of coloration, being pale at night and darker during the day. Individuals under constant illumination did not show this cycle, becoming progressively paler over time. Individuals held on monochromatic black, grey, and white containers showed an ability to change coloration in response to their backgrounds, as integrated reflectance (ΣR) of crabs generally followed background albedo. Dynamic color change in this species may play roles including photoprotection, with possible use in enhancing cryptic color matching.

1. INTRODUCTION

Somatic color change in Crustacea has received a great deal of attention as a conspicuous and quantifiable phenomenon related to physiological and ecological factors. Both dramatic and subtle examples can be found which function in a variety of important biological responses, e.g. thermoregulation [1,2], background matching [3–6], and intra-specific communication [7,8]. Two general categories of reversible color change are present [9–11]. Morphological change involves the deposition or destruction of pigment in the dermal tissue or cuticle and production of new chromatophore cells, while physiological color change results from expansion and contraction of chromatophores and melanophores (reviewed in [9,11]). Physiological change occurs far more quickly than morphological (seconds to hours versus days to months), and can be utilized in timely response to acute demands.

In crabs, color response to factors such as background, temperature and light levels are frequently superimposed on endogenous and exogenous diel, tidal, and lunar cycles [1,12–16]. Accordingly the control of somatic coloration in a given crab species is complex, depending upon specific adaptive pressures, and thus the full significance of observed pigmentation patterns often remains unclear [5,17]. Diel signals of pigment dispersion during the day and concentration at night are commonly observed, and some success has been made in linking these to behavior and ecological demands [2,5,9,14–16,18]. Pigmentation cycles and response to environmental stimulus has been extensively researched in a few species of the semi-terrestrial fiddler crabs *Uca* [1,2,4,7,8,13,16,17,19–32], while other groups remain comparatively unstudied (but see [5,6,14,33–38]).

Floating mats of pelagic *Sargassum* macroalgae form expansive yet variable habitat in the western North Atlantic, with a highly cryptic macrofaunal community [33,39–44]. These animals lack hard cover and must therefore rely largely on cryptic coloration to avoid detection by predators with distinct visual systems, making this a useful system for camouflage or animal color research in a unique and challenging habitat at the air/water interface [41,43–46]. Among the *Sargassum* macrofauna, crustaceans are perhaps the most abundant by biomass, number, and species [40], and have received the most attention in regards to coloration and crypsis [33,34,39,41,43,44,46].

Two species of crab are present in these mats: *Portunus sayi* and *Planes minutus*. *Portunus sayi* (Gibbes 1850) has a yellow/brown, mottled appearance which, to the human eye, blends into its algae habitat. Adults display varied pattern and shading on the dorsal surface, with a conspicuous central white spot that may mimic barnacles or calcareous tubes formed by worms. The smaller *P. minutus* is generally more uniform, ranging from light yellow to orange, with some individuals possessing irregular white patches [42,43,47]. In a previous study [43], we demonstrated that both species match their algal background well in the blue and green wavelengths (400 – 550 nm), but diverged at longer orange and red wavelengths. A visual model showed that while the crabs effectively matched the color of *Sargassum* against blue/green sensitive fish predators, birds were able to discriminate between crab and algae due to the presence of a far-red sensitive cone type [43].

Color change in response to background has previously been studied in *P. minutus* [33,34]. While this species appears to match the color of its background over long periods, i.e. morphological color change, the crabs failed to change appreciably when placed on colored backgrounds for short periods [33,43]. We are aware of no published studies on cryptic color

change in *P. sayi*. Preliminary investigations [45] revealed that *P. sayi* is able to rapidly change color, alternating between dark coloration during the day and paler shading at night. For a crab like *P. sayi* that has little protection from predators aside from camouflage, dynamic color change could have important ramifications for crypsis.

We investigated physiological color change in *P. sayi*. We compared the color of individuals exposed to both natural and constant illumination over multiple diel cycles. Further, we exposed crabs to monochrome backgrounds to determine if dynamic color change in this species might be used to improve cryptic color matching.

2. METHODS

P. sayi were captured from *Sargassum* in the field and transferred to the laboratory in order to study somatic coloration in response to background albedo and ambient light cycles. Coloration was assessed using spectral reflectance $R(\lambda)$, the ratio of photons back scattered from a target relative to a standard at each wavelength [43,48]. This is an inherent property of the target and is independent of the light field. Patterns of color change in relation to time and background albedo were then examined.

2.1 Collection of Crabs and Algae

Data collection took place during June 2012 at Keys Marine Lab in Layton, Florida, USA. Two days sampling effort yielded a total of 27 adult and large juvenile *P. sayi* (carapace width ≥ 8mm, size at which abdomen shape was discernible) from floating *Sargassum* mats in the vicinity of Long Key. Collection took place in accordance with permits (FL Fish and Wildlife Scientific Research SAL, NOAA National Marine Sanctuaries) and protocols established for a larger related study. No specific permits or protocols were required for collection of *Sargassum*

or associated invertebrates, and no protected or endangered species were collected. All care was taken to ensure humane treatment of animals, which were returned to the wild on clumps of live algae after experimentation. Mesh nets (hole size < 3 mm) were used to take samples of algae, which were then sorted by hand in buckets of seawater. Crabs were placed in a shaded, bubbled container for transport to the laboratory. Representative samples of both species of pelagic *Sargassum (S. fluitans* and *S. natans)* were also collected. Animals were maintained on live *Sargassum* in flow-through tanks prior to the start of experimentation. Males and females, both with and without egg masses, were included and randomly distributed among treatments.

2.2 Diel Color Change

Seven individuals were held in transparent, shaded outdoor tanks with unfiltered flow-through sea water. Crabs were maintained on clumps of *Sargassum* which contained other associated organisms and allowed to move and feed freely. This set-up matched natural conditions as closely as possible while still allowing for regular retrieval and imaging of crabs. Individuals were tracked through the course of the experiment by sex and carapace width. Every 12 hours (starting at 12:00 EST), crabs were removed from the containers and imaged. Experimental duration was 48 hours, for a total of 5 measurements. These were compared to crabs held on live *Sargassum* under constant illumination. Following this, the group under constant illumination was returned to a natural light cycle for an additional 48 hours.

2.3 Response to Background

Portunus sayi response to background albedo was assessed indoors under constant illumination (Philips Agro-Lite BR30 incandescent lamps). Twenty individuals were selected randomly from the collected crabs (acclimated in outdoor tanks on live *Sargassum*) and distributed among 4

groups. Individuals were placed on black, grey, and white backgrounds, with a control group remaining on a sample of algae in transparent containers. Colored plastic containers with nylon mesh were used as artificial substrate. The backgrounds were spectrally flat over the region considered, with reflectance values of approximately 0.04 (black), 0.16 (grey), and 0.73 (white). All crabs were placed in individual, aerated containers to avoid intra-specific interactions. Containers were kept in a flow-through seawater bath for temperature control. Crab color was assessed during transfer from the holding tanks to treatment backgrounds (initial measurements) and at 12 hour intervals for 48 hours, for a total of 5 measurements.

2.4 Spectral Reflectance

Collection of Spectral Data

Collection and processing of reflectance data for *P. sayi* and *Sargassum* followed a previously described method [43]. Crabs and algae were scanned with a 710 Hyperspectral Imager (Surface Optics Corp.). The instrument collects a 520 x 696 pixel image with radiance information for every pixel at 5 nm intervals between 380 – 1040 nm, known as a "data cube." Imaging occurred under solar (day) or artificial (night) illumination with a diffusive, matte black cloth background. A 12% Spectralon (LabSphere) reflectance standard was included in every frame for calculation of spectral reflectance $R(\lambda)$. Crabs were restrained using elastic bands, gently dried to minimize glare, and imaged in air. The spectral region initially considered is 400 – 700 nm. A comparison of crab images made under artificial light and then immediately under solar illumination showed good agreement of reflectance values at wavelengths longer than 450nm. At lower wavelengths, the illumination source produced insufficient photons for the imager, resulting in low signal-to-

noise ratio and reflectance artifacts. Therefore, spectra collected at night and reflectance-based metrics were restricted to 450 – 700 nm.

Spectral Data Processing

Data cubes were analyzed using ENVI (Exelis VIS) software. Cubes were converted from raw, dimensionless radiance data to $R(\lambda)$ using the in-frame standard. Regions of Interest (ROIs) were generated for the carapace of each crab, from which mean $R(\lambda)$ was extracted. Visibly glare contaminated pixels were avoided, and saturated pixels automatically masked. The reflectance of monochrome backgrounds was similarly determined from imagery of the containers. For the control group, *Sargassum* $R(\lambda)$ was determined as the mean from all algal pixels in each of the control samples. A modified Normalized Difference Vegetation Index (NDVI) contrasting near infrared (700 nm) to red (660nm) wavelengths was used to automatically select *Sargassum* pixels.

To quantify the overall shade of individuals, i.e. how light or dark it is, we calculated integrated reflectance [20,32,49] for each crab:

$$\sum R = \int_{450}^{700} R\,(\lambda) d\lambda \qquad [2]$$

3. RESULTS

Portunus sayi have a largely translucent cuticle, with their overall color patterns apparently determined by the distribution of chromatophores in the dermal tissue (Fig 1A, B). When molted, the cuticle shows a tint and may play a large role in the overall color of the animal (Fig 1C). The central dorsal white spot, as well as other smaller bright markings, is mirrored on the discarded

molt. The molted outer carapace is significantly more reflective across the region considered than the intact individual (Fig 1D).

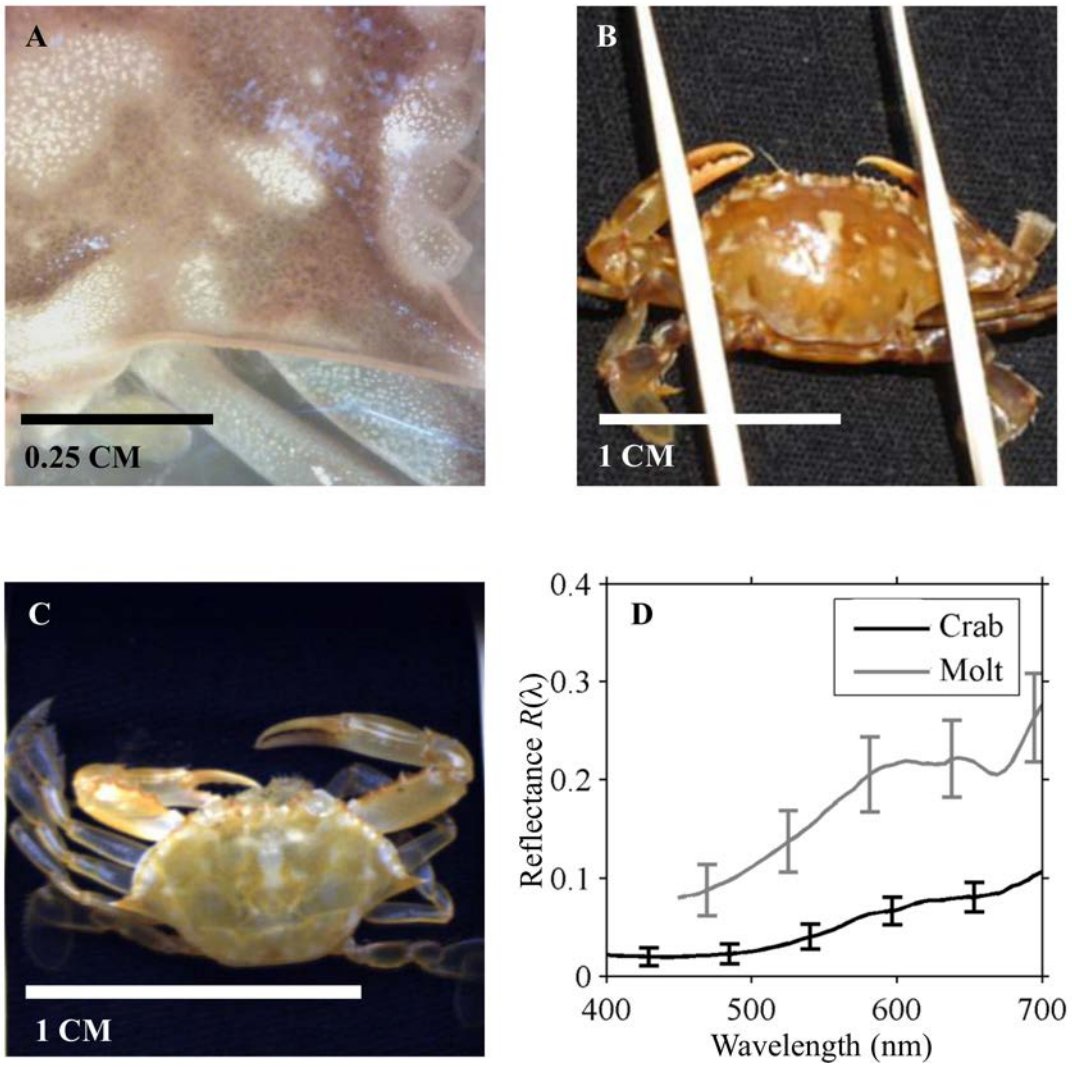

Figure 1. *Portunus sayi* translucent cuticle. **A:** Magnified view of juvenile *P. sayi*. Chromatophores are evident beneath semi-translucent outer cuticle. **B:** RGB image of adult male, < 12 hrs before ecdysis. **C:** Psuedo RGB image of discarded cuticle. **D:** Mean carapace reflectance $R(\lambda)$ for the pre-ecdysis individual (black line) is much lower than for the discarded cuticle (grey line), which displays a slight chlorophyll-like reflectance feature at 675 - 700 nm. Error bars are +/- 1 standard deviation.

3.1 Diel Color Change

Five individuals survived for the duration of the experiment. Among these, a clear trend of dark, melanistic coloration during the day and paler shading at night was observed for individuals exposed to natural illumination (Fig 2). Median carapace reflectance spectra (Fig 2A) illustrate diurnal melanism (Fig 2B) with associated low reflectance, and pale nocturnal coloration (Fig 2C) with significantly higher $R(\lambda)$. Spectrally, reflectance showed the greatest change in the red wavelengths, and lowest change in the blue.

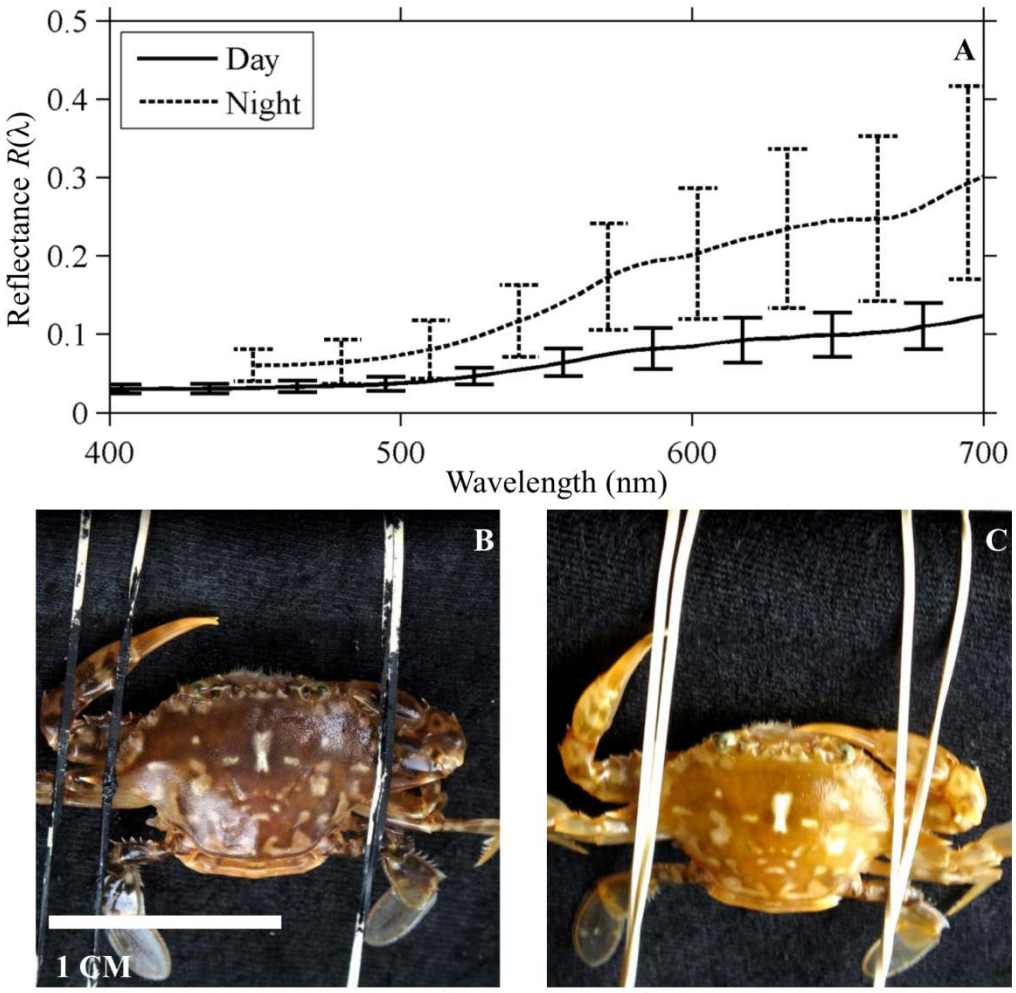

Figure 2. Diurnal/nocturnal coloration of *Portunus sayi*. Median carapace reflectance of all individuals **(A)** was significantly higher at all wavelengths at night (dashed line) than during the day (solid line). Spectra are a median carapace $R(\lambda)$ for all individuals, averaged over 2 observations. Error bars are +/- 1 pooled standard deviation. Subjectively, individuals (adult female shown for example) are considerably darker during daylight hours **(B)** than at night **(C)**.

Crabs held on live *Sargassum* under constant illumination did not show the same diel cycle (Fig 3) as those in natural light. Integrated reflectance ΣR was low during daytime measurements (Fig

3A) and significantly higher at night for individuals under natural illumination. For those under constant illumination, ΣR increased over the experimental period regardless of time of measurement (Fig 3B). After being returned to a natural illumination cycle, crabs exposed to constant illumination darkened and returned to initial ΣR values by 96 hours.

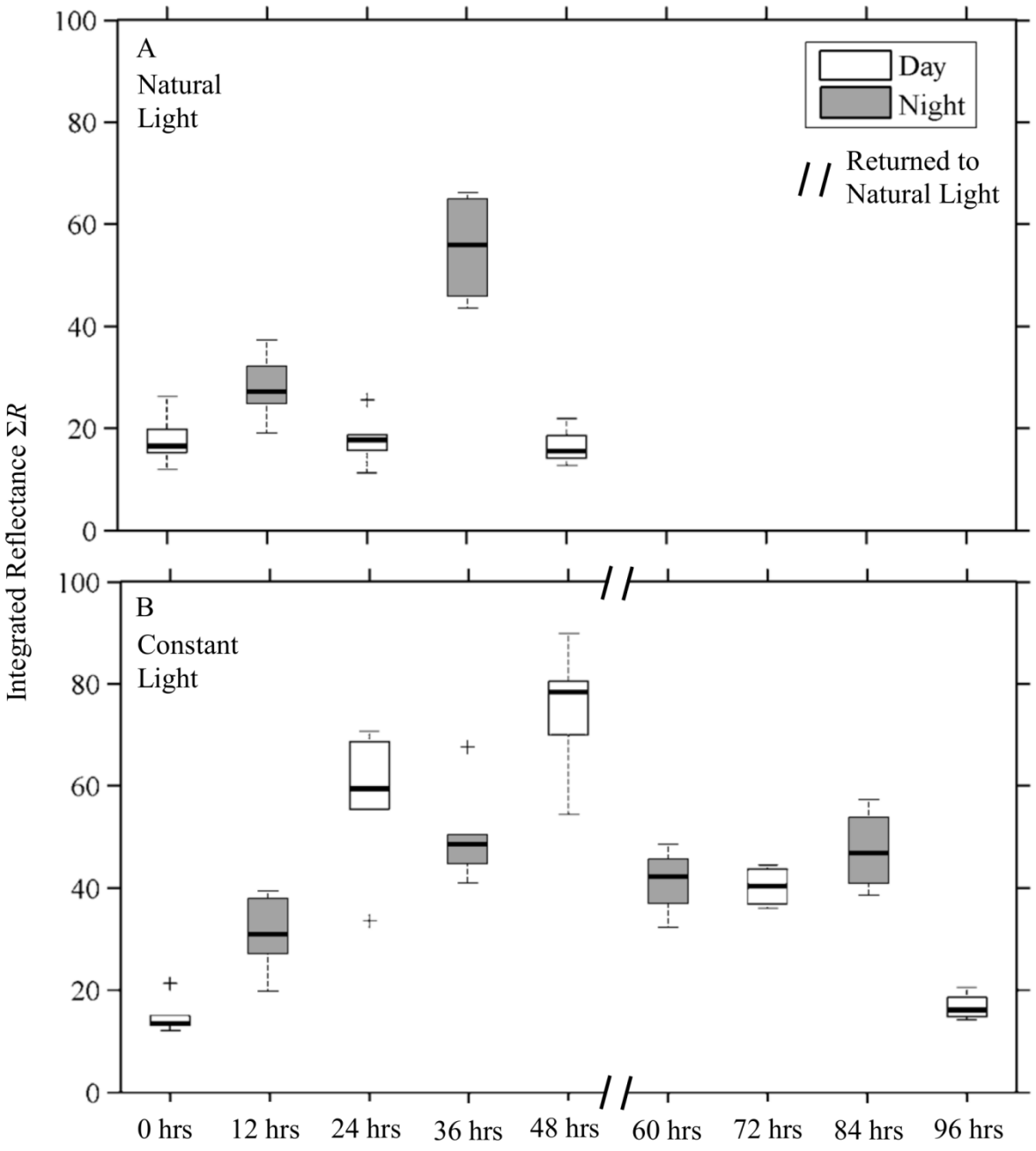

Figure 3. Integrated reflectance Σ*R* of crabs exposed to natural illumination (**A**) and constant illumination (**B**). A clear cycle of low *R* during the day and higher *R* at night was observed for crabs exposed to natural lighting, which was absent from individuals under constant illumination. Double bars indicate return of crabs under constant illumination to natural light cycle. Outliers are marked by crosses.

3.2 Response to Background

Aggregate reflectances do indicate group differences in coloration with background albedo after acclimation (Fig 4). Responses were highly variable on the individual level, and all individuals regardless of treatment group increased reflectance over time. At 36 hours however, crab reflectances were lower than at 24 hours, but increased by 48 hours.

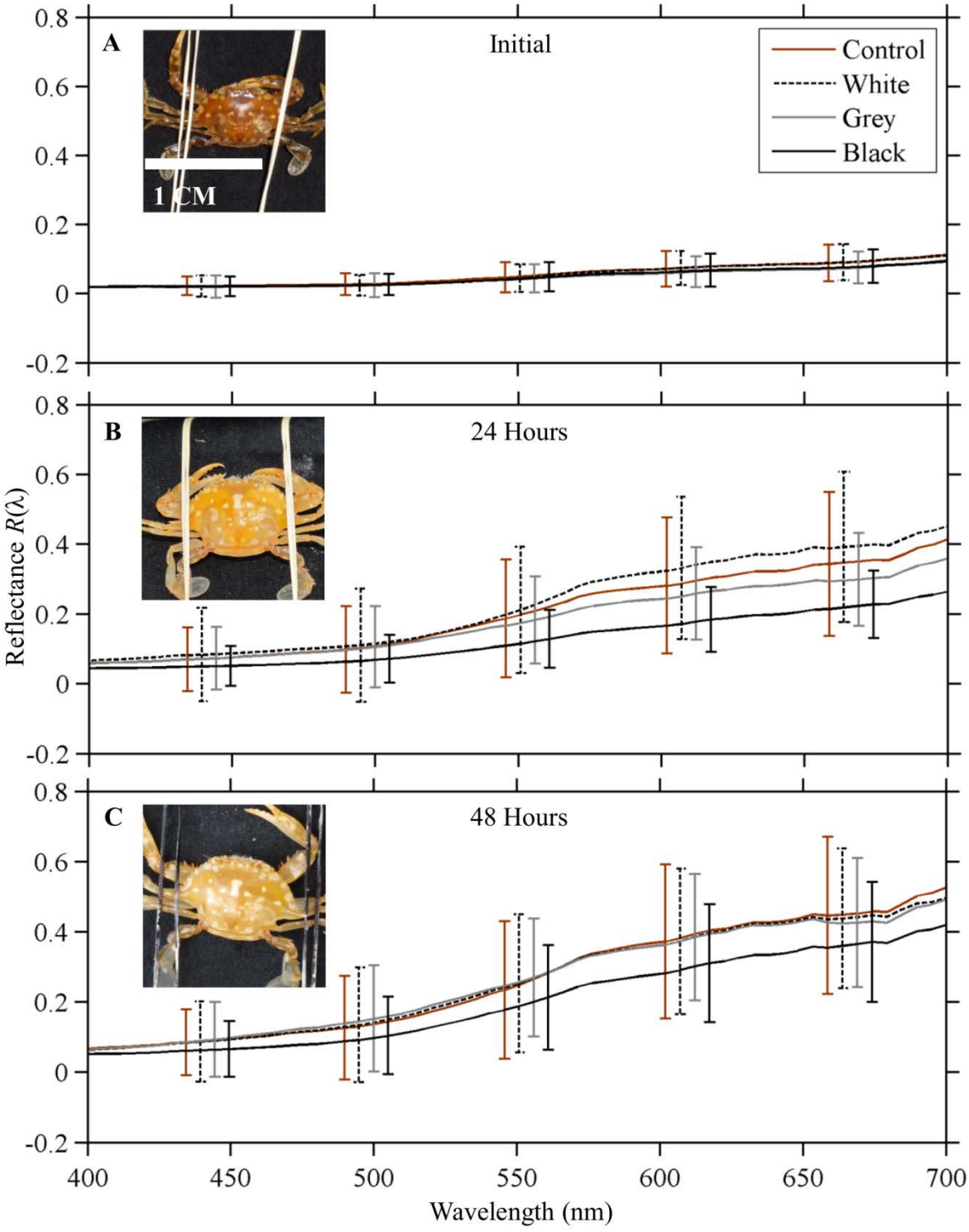

Figure 4. Group mean reflectance *R*(λ) of *P. sayi* initially (**A**), and after exposure to *Sargassum*, white, grey, and black backgrounds for 24 (**B**) and 48 (**C**) hours. While individual response was

highly variable, group spectra do indicate a graded background albedo response. Reflectance of all individuals increased over time. Error bars are +/- 1 pooled standard deviation. For illustration, crabs acclimated to white backgrounds were significantly lighter than their initial state (inset photos).

Mean reflectance of all groups was equal initially (Fig 4A). After 24 hours (Fig 4B), black maintained crabs showed the lowest reflectance values, and acclimated reflectances were lower than the control group at all wavelengths ($p < 0.05$ 400 – 440 nm, $p < 0.1$ 400 – 700 nm). Grey crab reflectance was (non-significantly) lower than the control at wavelengths > 550 nm. Crabs maintained on white backgrounds showed (non-significantly) higher reflectance than the control at wavelengths > 550 nm by 24 hours (Fig 4B), and were noticeably lighter than their initial state (Fig 4 inset images). After 48 hours (Fig 4C), control, white, and grey treatment mean reflectance was virtually identical at all wavelengths. Black treatment reflectance was lower than the control at all wavelengths, significantly ($p < 0.1$) at < 500 nm.

Integrated reflectance ΣR was not significantly different among treatments during initial measurements (Fig 5), and increased over time for all groups. At 12, 24, and 36 hours, ΣR of treatment groups followed background albedo. That is, median ΣR was greatest for white crabs and lowest for black treated crabs. Black treated crabs showed the lowest ΣR of all groups after acclimation at each measurement time, and was different from the control (Mann-Whitney U test) at 24 ($p = 0.09$), and 36 ($p = 0.01$) hours.

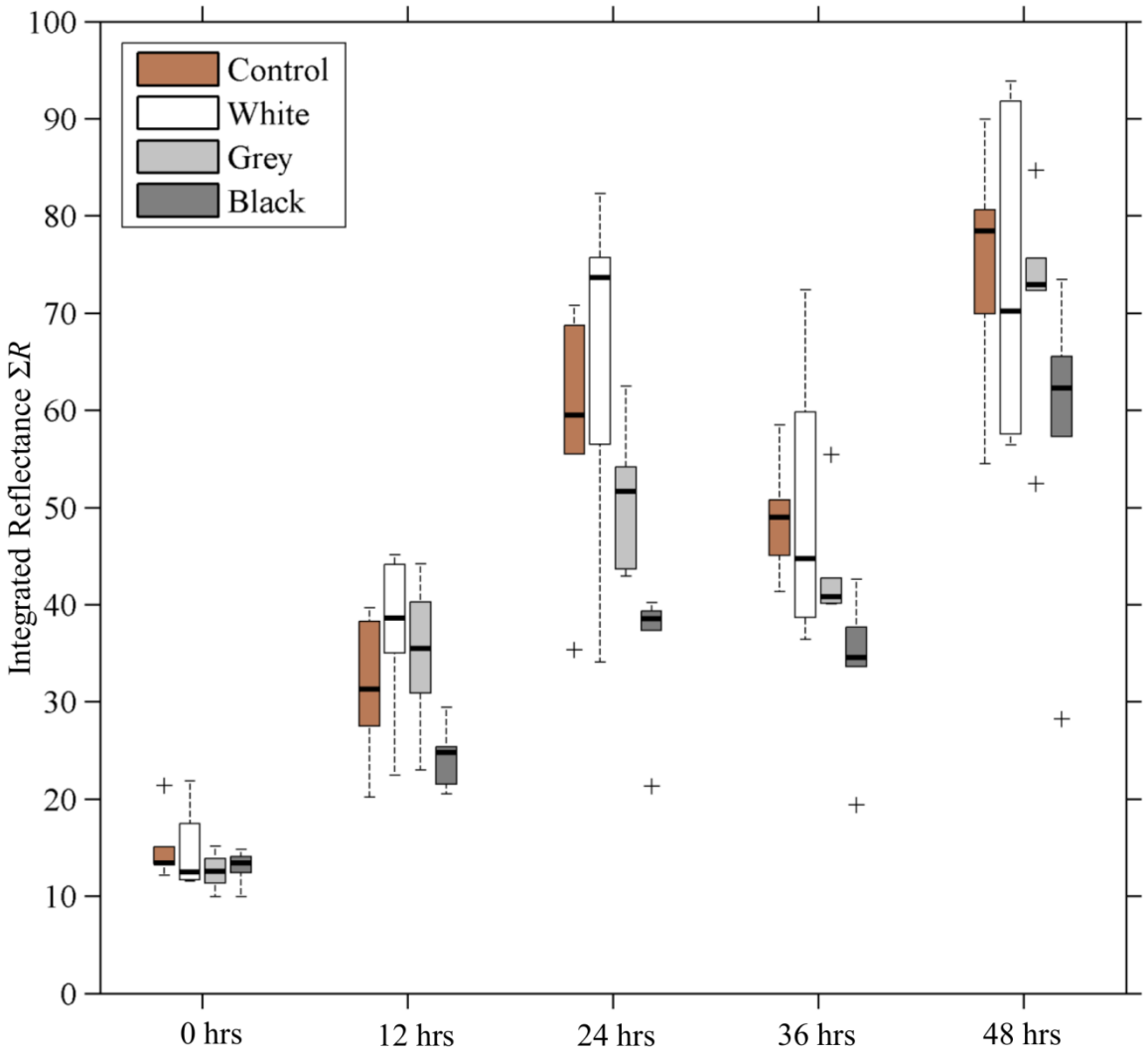

Figure 5. Integrated reflectance Σ*R* of crabs exposed to monochrome backgrounds. All crabs showed increased Σ*R* over time. Median Σ*R* of treatment groups followed background albedo at 12, 24, and 36 hours. Outliers are marked by crosses.

4. DISCUSSION

4.1 Color Change in Response to Environmental Conditions

Data presented here show that *P. sayi* have the ability to drastically alter their overall carapace coloration within several hours. The absence of regular diel melanistic/pale cycles as seen in crabs exposed to constant illumination demonstrates that such cycles are partially controlled by ambient light and are at least largely non-circadian, unlike similar cycles in some other crabs [14,15,28].

The possibility of protection from ultra violet radiation has been posited for diel cycles involving a dark phase during daylight hours [9,12,22], particularly in semi-terrestrial *Uca*, in which direct melanistic response to exposure to wavelengths between 300 – 400 nm [23] and visible wavelengths [22,24] has been studied. For *P. sayi*, which are subject to high irradiance in low-latitude surface waters, expanded chromatophores could serve a protective role by absorbing damaging UV photons [50]. The apparent cycle in coloration observed here may potentially be the result of energetic costs associated with pigmentation [51,52]. Maintaining expanded dark chromatophores, including the potential replacement of pigments damaged or destroyed by UV absorption, will presumably impose some metabolic cost. At night, the benefit for this cost (i.e. photoprotection) would be absent and paler nocturnal coloration would represent a simple decrease in metabolic expenditure. Further, visual predation is presumably reduced at night [53–55] and trade-offs between body color, thermoregulation, photoprotection and crypsis could be largely irrelevant.

Thermoregulation represents a possible function for light/dark pigmentation cycles. *Uca* fiddler crabs on exposed mudflats, for example, are subject to large temperature variation on short time

scales. *U. pugilator* changes from dark to light coloration in response to increasing temperature, with a demonstrated difference in body temperature between chromatic states [1,21]. A cycle of darker coloration during the day and lighter color at night has been observed in this species [12,13,21], similar to that seen here. Detailed temperature information was not collected during the present study, and is a possible factor influencing color change in *P. sayi*.

An albedo response, where the individual changes shading in response to the reflectance of the background, has been observed to varying extents in crab species including multiple in the genus *Uca* [13,19,25], *C. sapidus* [37], *Sesarma reticulatum* [38,56], *Carcinus maenas* [57], *Ocypode ceratophthalmus* [5] and a variety of other crustaceans [9,11,39,58]. The trends in reflectance relative to certain backgrounds observed here indicates that physiological color change may have potential for dynamic camouflage in *P. sayi*, but further research is required. We are aware of a small number of previous studies on color change in *Sargassum* crustaceans. The other species of associated crab, *Planes minutus*, possesses three chromatophore classes: white, yellow, and black [34]. However, overall coloration of the animals was not adequately reported and no appreciable response to the reflectance of the background was observed. This was suggested to be due to “extra-chromatophoral” pigments in the dermal cells and faint coloration of the exoskeleton, observed upon molting. The shrimp *Latreutes fucorum* is extremely abundant in the pelagic *Sargassum* complex [40,42]. *L. fucorum* are found in a wide variety of colors and patterns, and responded to background albedo with chromatophore expansion on black backgrounds and contraction on white [39].

Chromatophore response in crabs can be divided into two mechanisms [11,59]. Primary chromatophore responses involve non-ocular pathways, such as the action of light directly on the chromatophore. Secondary responses in crustaceans are initiated by light perceived by the eye

and mediated by the sinus gland in the eyestalks [15,60,61]. This is the mechanism involved in albedo response [11,13,59,62]. As with other crustacean species, color change in *P. sayi* is likely controlled by a complex interaction of factors including background albedo, illumination, temperature, and possibly circadian or other rhythms [2,11,14,15,17,19,25]. At 36 hours, all crabs in the albedo treatment showed a decrease in reflectance from 24 hours, diverging from the otherwise linear increase observed. This could be the result of a factor outside of experimentation such as those previously discussed. Sex and reproductive status may also be relevant [1,2,35], and future work should examine color change in respect to such factors. The majority of individuals used in this study were female. It is unknown if this results from actual population dynamics or an unidentified bias in collection procedure.

The impact of laboratory light levels seems to be a compounding variable when testing color response to background. The present observation of lighter coloration in crabs exposed to laboratory illumination was not expected, and may be due to physiological stress from experimental conditions. Interestingly, this response was opposite to the natural condition of paler shading in response to darkness and may indicate a response to lower light intensity in the lab compared to typical day-time light levels in the region. This and similar complications have been observed in other studies [13,37]. Those crabs exposed to constant illumination began to regain their diel color cycle after being returned to natural lighting. This would indicate that the progressive increase in ΣR was part of a response to experimental conditions, and not likely the result of any permanent degeneration or health issues induced by experimental stress.

4.2 Camouflage Through Morphological Color Change

The slower acting mechanism of morphological color change, in which new pigments are created, has been observed to serve in background color matching for several crab species [63–67]. The other *Sargassum* associated crab, *Planes minutus*, also appears to employ morphological color change. Crozier [33] noted that *P. minutus* was able to "harmonize" with the deep mahogany color of a drifting cedar log. Later, Hitchcock [34] documented their chromatophore response on different colored backgrounds, but found that extracellular pigmentation in hypodermis and exoskeleton prevented rapid color change. We have similarly found that *P. minutus* were able to achieve a deep red color when found on a red plastic bucket [43], though the time period required to match this background is unknown. The degree to which pigmentation in the cuticle impacts overall coloration in *P. sayi* has yet to be determined, but examination of the molts seen during this study indicates it is likely to play a role.

5. CONCLUSIONS

Like many other marine crustaceans, *Portunus sayi* exhibits physiological color change in response to environmental conditions. Under natural illumination, the species displays a clear diel cycle of coloration through a physiological pathway. During daylight hours, adults have a highly contrasting pattern of light and dark, with brown, yellow, and white elements. This shifts to mostly yellow and white at night. Crabs exposed to continuous illumination did not show such a cycle. When placed on backgrounds of varying albedo, *P. sayi* appears to change coloration according to the background, being less reflective on black backgrounds and more reflective on brighter ones, though individual response was highly variable. Further research is needed to determine if sex or body size are important to camouflage or pigmentation cycles in *P. sayi* as in

other species, or if morphological change might function to improve background matching as in *P. minutus*.

REFERENCES

1. Munguia P, Levinton JS, Silbiger NJ. Latitudinal differences in thermoregulatory color change in *Uca pugilator*. J Exp Mar Biol Ecol. 2013 Feb;440:8–14.

2. Silbiger N, Munguia P. Carapace color change in *Uca pugilator* as a response to temperature. J Exp Mar Biol Ecol. 2008 Feb;355(1):41–6.

3. Fingerman M. Chromatophores. Physiol Rev. 1965;45:296–339.

4. Hemmi JM, Marshall J, Pix W, Vorobyev M, Zeil J. The variable colours of the fiddler crab *Uca vomeris* and their relation to background and predation. J Exp Biol. 2006 Oct 15;209(20):4140–53.

5. Stevens M, Rong CP, Todd PA. Colour change and camouflage in the horned ghost crab *Ocypode ceratophthalmus*. Biol J Linn Soc. 2013;109(2):257–70.

6. Stevens M, Lown AE, Wood LE. Camouflage and Individual Variation in Shore Crabs (*Carcinus maenas*) from Different Habitats. Eklöv P, editor. PLoS ONE. 2014 Dec 31;9(12):e115586.

7. Detto T, Backwell PR., Hemmi JM, Zeil J. Visually mediated species and neighbour recognition in fiddler crabs (*Uca mjoebergi* and *Uca capricornis*). Proc R Soc B Biol Sci. 2006 Jul 7;273(1594):1661–6.

8. Detto T. The fiddler crab *Uca mjoebergi* uses colour vision in mate choice. Proc R Soc B Biol Sci. 2007 Nov 22;274(1627):2785–90.

9. Umbers KDL, Fabricant SA, Gawryszewski FM, Seago AE, Herberstein ME. Reversible colour change in Arthropoda: Arthropod colour change. Biol Rev. 2014 Nov;89(4):820–48.

10. Horst MN, Freeman JA. The Crustacean Integument: Morphology and Biochemistry. Boca Raton, FL: CRC Press; 1993. 240 p.

11. Fingerman M. The Control of Chromatophores. New York: Macmillan; 1963. 192 p. (International series of monographs on pure and applied biology. Zoology division).

12. Abramowitz AA. The chromatophorotropic hormone of the Crustacea: Standardization, properties and physiology of the eye-stalk glands. Biol Bull. 1937 Jun;72(3):344.

13. Brown FA, Sandeen MI. Responses of the chromatophores of the fiddler crab, *Uca*, to light and temperature. Physiol Zool. 1948;361–71.

14. Fingerman M. Persistent daily and tidal rhythms of color change in *Callinectes sapidus*. Biol Bull. 1955;109(2):255–64.

15. Thurman CL. Rhythmic physiological color change in crustacea: A review. Comp Biochem Physiol PART C Comp Pharmacol. 1988;91:171–85.

16. Fingerman M. Phase Difference in the Tidal Rhythms of Color Change of Two Species of Fiddler Crab. Biol Bull. 1956 Jun;110(3):274.

17. Detto T, Hemmi JM, Backwell PRY. Colouration and Colour Changes of the Fiddler Crab, *Uca capricornis*: A Descriptive Study. Rands S, editor. PLoS ONE. 2008 Feb 20;3(2):e1629.

18. Fingerman M, Lowe ME, Mobberly WC. Environmental Factors Involved in Setting the Phases of Tidal Rhythm of Color Change in the Fiddler Crabs *Uca pugilator* and *Uca minax*. Limnol Oceanogr. 1958;3(3):271–82.

19. Brown FA. Studies on the Physiology of *Uca* Red Chromatophores. Biol Bull. 1950 Jun;98(3):218.

20. Kronstadt SM, Darnell MZ, Munguia P. Background and temperature effects on *Uca panacea* color change. Mar Biol. 2013 Jun;160(6):1373–81.

21. Wilkens JL, Fingerman M. Heat tolerance and temperature relationships of the fiddler crab, *Uca pugilator*, with reference to body coloration. Biol Bull. 1965;128(1):133–41.

22. Coohill TP, Fingerman M. Relative effectiveness of ultraviolet and visible light in eliciting pigment dispersion in melanophores of the fiddler crab, *Uca pugilator*, through the secondary response. Physiol Zool. 1975;57–63.

23. Coohill TP, Bartell CK, Fingerman M. Relative effectiveness of ultraviolet and visible light in eliciting pigment dispersion directly in melanophores of the fiddler crab, *Uca pugilator*. Physiol Zool. 1970;43(3):232–9.

24. Coohill TP, Fingerman M. Comparison of the effects of illumination on the melanophores of intact and eyestalkless fiddler crabs,*Uca pugilator*, and inhibition of the primary response by cytochalasin B. Experientia. 1976;32(5):569–70.

25. Barnwell FH. Comparative Aspects of the chromatophoric responses to light and temperature in fiddler crabs of the genus *Uca*. Biol Bull. 1968 Apr;134(2):221.

26. Herreid CF, Mooney SM. Color change in exercising crabs: evidence for a hormone. J Comp Physiol B. 1984;154(2):207–12.

27. Thurman CL. Adaptive coloration in Texas fiddler crabs (*Uca*). In: Wickstein M, editor. Adaptive coloration in invertebrates. Texas: Texas A&M University Press; 1990. p. 109–26.

28. Brown FA, Fingerman M, Sandeen MI, Webb HM. Persistent diurnal and tidal rhythms of color change in the fiddler crab, *Uca pugnax*. J Exp Zool. 1953;123(1):29–60.

29. Zeil J, Hofmann M. Signals from “crabworld”: cuticular reflections in a fiddler crab colony. J Exp Biol. 2001;204(14):2561–9.

30. Crane J. On the color changes of fiddler crabs in the field. Zoologica. 1944;29:161–8.

31. Shih H-T, Mok H-K, Chang H-W, Lee S-C. Morphology of *Uca formosensis* Rathbun, 1921 (Crustacea: Decapoda: Ocypodidae), an endemic fiddler crab from Taiwan, with notes on its ecology. Zool Stud-TAIPEI-. 1999;38:164–77.

32. Darnell MZ. Ecological physiology of the circadian pigmentation rhythm in the fiddler crab *Uca panacea*. J Exp Mar Biol Ecol. 2012 Sep;426-427:39–47.

33. Crozier WJ. Note on the coloration of *Planes minutus*. Am Nat. 1918 May;52(616/617):262–3.

34. Hitchcock HB. The coloration and color changes of the gulf-weed crab, *Planes minutus*. Biol Bull. 1941;26–30.

35. Jensen GC, Egnotovich MS. A whiter shade of male: Color background matching as a function of size and sex in the yellow shore crab *Hemigrapsus oregonensis* (Dana, 1851). Curr Zool. 2015;61(4):729–38.

36. Granato FC, Tironi TS, Maciel FE, Rosa CE, Vargas MA, Nery LEM. Circadian rhythm of pigment migration induced by chromatrophorotropins in melanophores of the crab *Chasmagnathus granulata*. Comp Biochem Physiol A Mol Integr Physiol. 2004 Jul;138(3):313–9.

37. Fingerman M. Physiology of the black and red chromatophores of *Callinectes sapidus*. J Exp Zool. 1956;133(1):87–105.

38. Fingerman M, Nagabhushanam R, Philpott L. Physiology of the melanophores in the crab *Sesarma reticulatum*. Biol Bull. 1961;337–47.

39. Brown FA. The coloration and color changes of the gulf-weed shrimp, *Latreutes fucorum*. Am Nat. 1939;73:564–8.

40. Butler JN, Morris BF, Cadwallader J, Stoner AW. Studies of *Sargassum* and the *Sargassum* community. Bermuda Biological Station for Research, St Georges 22; 1983.

41. Hacker SD, Madin LP. Why habitat architecture and color are important to shrimps living in pelagic *Sargassum*: use of camouflage and plant-part mimicry. Mar Ecol Prog Ser. 1991;70:143–55.

42. Morris BF, Mogelberg DD. Identification manual to the pelagic *Sargassum* fauna. Bermuda Biological Station for Research, St Georges 22; 1973. 61 p. (Special Publication).

43. Russell BJ, Dierssen HM. Use of hyperspectral imagery to assess cryptic color matching in *Sargassum* associated crabs. PloS One. 2015;10(9):e0136260.

44. Brooks WR, Hutchinson KA, Tolbert MG. Pelagic *Sargassum* mediates predation among symbiotic fishes and shrimps. Gulf Mex Sci. 2007;2:144–52.

45. Russell BJ, Dierssen HM. Hyperspectral imaging as a tool for camouflage evaluation of the *Sargassum* crab *Portunus sayi*. In Glasgow, Scotland; 2012.

46. Jobe CF, Randy Brooks W. Habitat selection and host location by symbiotic shrimps associated with *Sargassum* communities: The role of chemical and visual cues. Symbiosis. 2009 Oct;49(2):77–85.

47. Chace FA. The oceanic crabs of the genera *Planes* and *Pachygrapsus*. Proc U S Natl Mus. 1951;101(3272).

48. Dierssen HM, Chlus A, Russell B. Hyperspectral discrimination of floating mats of seagrass wrack and the macroalgae *Sargassum* in coastal waters of Greater Florida Bay using airborne remote sensing. Remote Sens Environ. 2015 Sep;167:247–58.

49. Russell B, Dierssen H, LaJeunesse T, Hoadley K, Warner M, Kemp D, et al. Spectral reflectance of Palauan reef-building coral with different symbionts in response to elevated temperature. Remote Sens. 2016 Feb 23;8(3):164.

50. Gouveia GR, Lopes TM, Neves CA, Nery LEM, Trindade GS. Ultraviolet radiation induces dose-dependent pigment dispersion in Crustacean chromatophores. Pigment Cell Res. 2004;17(5):545–8.

51. Emery CJ. The ecological impact of near ultraviolet radiation on *Daphnia pulex*. [Master's]. [Ontario]: University of Windsor; 1984.

52. Korínek V, Frey DG, editors. Biology of Cladocera: Proceedings of the Second International Symposium on Cladocera, Tatranska Lomnica, Czechoslovakia, 13–20, September 1989. Vol. 71. Springer Science & Business Media; 2013.

53. De Robertis A. Size-dependent visual predation risk and the timing of vertical migration: an optimization model. Limnol Oceanogr. 2002;47(4):925–33.

54. Ballance L, Pitman R. S34. 4: Foraging ecology of tropical seabirds. In: Proc 22 Int Ornithol Congr, Durban. Citeseer; 1999. p. 2057–71.

55. Oro D, Martínez-Abraín A. Ecology and behavior of seabirds. In: Duarte CM, Lota A, editors. Marine Ecology, Encyclopedia of Life Support Systems (EOLSS). Oxford: Eolss Publishers-UNESCO;

56. Fingerman M, Nagabhushanam R, Philpott L. Photomechanical responses of the proximal pigment in *Palaemonetes* and *Orconectes*. Biol Bull. 1962 Aug;123(1):121.

57. Stevens M, Lown AE, Wood LE. Color change and camouflage in juvenile shore crabs *Carcinus maenas*. Front Ecol Evol. 2014;2.

58. Hultgren KM, Mittelstaedt H. Color change in a marine isopod is adaptive in reducing predation. Curr Zool. 2015;6(4):739–48.

59. Fingerman M, Tinkle DW. Responses of the white chromatophores of two species of prawns (*Palaemonetes*) to light and temperature. Biol Bull. 1956;110(2):144–52.

60. Brown FA. The controlling mechanism of chromatophores in *Palaemonetes*. Proc Natl Acad Sci. 1933;19(3):327–9.

61. Welsh JH. Diurnal rhythms. Quart Rev Biol. 1938;13:123–39.

62. Powell BL. The responses of the chromatophores of *Carcinus maenas* (L., 1758) to light and temperature. Crustaceana. 1962;4(2):93–102.

63. Iampietro PJ. Distribution, diet, and pigmentation of the northern kelp crab, *Pugettia producta* (Randall) in central California kelp forests. [Master's]. California State University, Stanislaus; 1999.

64. Hultgren KM, Stachowicz JJ. Alternative camouflage strategies mediate predation risk among closely related co-occurring kelp crabs. Oecologia. 2008 Mar;155(3):519–28.

65. Green JP. Morphological color change in the fiddler crab, *Uca pugnax* (S. I. Smith). Biol Bull. 1964 Oct;127(2):239.

66. Green JP. Morphological color change in the Hawaiian ghost crab, *Ocypode ceratophthalma* (Pallas). Biol Bull. 1964 Jun;126(3):407.

67. Kolwalkar DG, Rangnekar PV. Morphological color change in the marine crab *Portunus pelagicus*. J Bombay Nat Hist Soc. 1979;76(3):540–3.

ACKNOWLEDGEMENTS

This work was funded by the Office of Naval Research Multi-
University Research Initiative (N000140911054), and by a pre-doctoral award from the Unviersity of Connecticut Department of Marine Sciences.

Statement concerning study animals: All live animals in this study were invertebrates and not subject to University of Connecticut IRB/IACUC requirements. All measures were taken to minimize suffering or stress of subjects.

Author Contributions

Conceived and designed the experiments: BJR. Performed the experiments: BJR. Analyzed the data: BJR, HMD. Contributed reagents/materials/analysis tools: BJR, HMD. Wrote the paper: BJR, HMD.

4. Spectral Reflectance of Palauan Reef-Building Coral with Different Symbionts in Response to Elevated Temperature

This chapter was published in Remote Sensing on February 23, 2016. It appeared in the special issue “Remote Sensing for Coral Reef Monitoring."

Russell, BJ; Dierssen, HM; LaJeunesse, TC; Hoadley, KE; Warner, ME; Kemp, DW; Bateman, TG. Spectral Reflectance of Palauan Reef-Building Coral with Different Symbionts in Response to Elevated Temperature. *Remote Sens.* **2016**, *8*(3), 164; doi:10.3390/rs8030164

remote sensing

MDPI

Article

Spectral Reflectance of Palauan Reef-Building Coral with Different Symbionts in Response to Elevated Temperature

Brandon J. Russell [1,*], Heidi M. Dierssen [1,2], Todd C. LaJeunesse [3], Kenneth D. Hoadley [4], Mark E. Warner [4], Dustin W. Kemp [5] and Timothy G. Bateman [1]

1 Department of Marine Science, University of Connecticut, Groton, CT 06340, USA; heidi.dierssen@uconn.edu (H.M.D.); timothy.bateman@uconn.edu (T.G.B.)
2 Department of Geography, University of Connecticut, Storrs, CT 06268, USA
3 Department of Biology, Pennsylvania State University, University Park, PA 16802, USA; tcl3@psu.edu
4 School of Marine Science and Policy, University of Delaware, Newark, DE 19716, USA; khoadley@udel.edu (K.D.H.); mwarner@udel.edu (M.E.W.)
5 Odum School of Ecology, University of Georgia, Athens, GA 30602, USA; dkemp1@uga.edu
* Correspondence: Brandon.Russell@uconn.edu; Tel.: +1-203-241-7253

Academic Editors: Stuart Phinn, Chris Roelfsema, Xiaofeng Li, Raphael M. Kudela and Prasad S. Thenkabail
Received: 15 December 2015; Accepted: 13 February 2016; Published: 23 February 2016

Abstract: Spectral reflectance patterns of corals are driven largely by the pigments of photosynthetic symbionts within the host cnidarian. The warm inshore bays and cooler offshore reefs of Palau share a variety of coral species with differing endosymbiotic dinoflagellates (genus: *Symbiodinium*), with the thermally tolerant *Symbiodinium trenchii* (*S. trenchii*) (= type D1a or D1-4) predominating under the elevated temperature regimes inshore, and primarily Clade C types in the cooler reefs offshore. Spectral reflectance of two species of stony coral, *Cyphastrea serailia* (*C. serailia*) and *Pachyseris rugosa* (*P. rugosa*), from both inshore and offshore locations shared multiple features both between sites and to similar global data from other studies. No clear reflectance features were evident which might serve as markers of thermally tolerant *S. trenchii* symbionts compared to the same species of coral with different symbionts. Reflectance from *C. serailia* colonies from inshore had a fluorescence peak at approximately 500 nm which was absent from offshore animals. Integrated reflectance across visible wavelengths had an inverse correlation to symbiont cell density and could be used as a relative indicator of the symbiont abundance for each type of coral. As hypothesized, coral colonies from offshore with Clade C symbionts showed a greater response to experimental heating, manifested as decreased symbiont density and increased reflectance or "bleaching" than their inshore counterparts with *S. trenchii*. Although no unique spectral features were found to distinguish species of symbiont, spectral differences related to the abundance of symbionts could prove useful in field and remote sensing studies.

Keywords: coral reef; reflectance spectroscopy; *Symbiodinium trenchii*; *Cyphastrea serailia*; *Pachyseris rugosa*; hyperspectral imaging; coral bleaching

1. Introduction

To a remote sensing scientist, the idea of a "coral reef" is an assemblage of different species of corals that can potentially be represented by unique spectral endmembers in a classification algorithm. Indeed, a variety of models and applications have been used to assess coral reefs from satellite and airborne multispectral imagery [1–4]. However, the concept of a "species" of coral is not quite accurate when considering spectral reflectance characteristics. Most reef-building corals are symbiotic with

dinoflagellate symbionts (photosynthetic unicellar eukaryotes), and a calcium carbonate skeleton is overlain by host tissues containing dense populations of their endosymbionts. While coral species can contain host tissue pigments, the dominant spectral reflectance patterns for the coral arise from the pigments of symbiont populations within them [5]. Therefore, remote sensing of corals is largely remote sensing of the dinoflagellates.

The symbionts of corals are "morphologically cryptic" dinoflagellates assigned to the genus *Symbiodinium* [6]. Research over the past few decades has shown that the diversity of endosymbiotic dinoflagellates associated with corals is tremendous and regionally diverse [7–9]. Indeed, the symbiont assemblages associated with coral communities in the Western Pacific differ significantly from the Greater Caribbean in the Western Atlantic [10]. Moreover, coral communities from reef habitats separated by several kilometers or less may be dominated by symbiont species that are very different [7,8,11]. We are aware of no published research on whether communities of corals dominated by different lineages of symbiont can be distinguished based on their inherent reflectance properties. Recently, two different coral species were analyzed from the Caribbean and significant differences were found between the auxiliary pigment concentrations and the measured reflectance spectra [12], though the identities of the symbionts were not investigated.

Warming sea surface temperatures have led to frequent episodes of coral bleaching and mortality. Coral bleaching or whitening occurs when symbiotic algae are expelled from the host, however, tolerance to environmental stress varies among *Symbiodinium* species, and thereby colonies with thermally tolerant symbionts may avoid bleaching [13–19]. Thus changes in the resident symbiont can substantially shift the thermal tolerance of a coral colony [20]. For example, background populations of the thermally tolerant symbiont species *Symbiodinium trenchii* (*S. trenchii*) increased in the weeks leading up to and during a bleaching episode as well as subsequent to bleaching [14]. The stability of a symbiont population within a coral can be influenced by the environmental conditions under which it lives, such as temperature and irradiance. Such conditions vary with latitude, depth in the water column, and water clarity. *S. trenchii* is known for being a generalist inhabiting corals in marginal conditions [16], and coral colonies with this symbiont can often tolerate higher temperatures than conspecific counterparts [13,15,20–22].

When corals lose endosymbionts, their tissues become more transparent and the white and highly structured skeleton enhances colony reflectance [23–25]. Additionally, the influence of pigments from endolithic algae may then contribute to the reflectance signal [26–28]. Many studies have therefore investigated reflectance as a method of non-invasively assessing the status of both corals and symbionts. Reflectance has been used to study a variety of parameters, including discrimination between healthy, bleached, and dead coral, as well as other reef constituents like sand and macroalgae [24–26,29–31], coral diversity [5,12,32–35], disease state [36], and pigment concentration [12,37].

Hyperspectral imaging (HSI) produces a digital image with full radiance information for every pixel. In marine sciences, this technology has been primarily applied to remote sensing of large areas [38]. More recently, HSI has been applied to biological studies at small spatial scales, such as the level of a single animal or plant [39–43] and has been used to measure reflectance of individual coral fragments in the lab [44–46] and even small areas of reefs *in situ* [32,33]. Underwater HSI systems therefore have extreme utility in mapping, classifying and in monitoring complex benthic environments at large spatial scales that would be practically impossible for divers [47,48]. Small, portable imaging systems have been developed which can be used in the field to rapidly collect large quantities of both spectrally and spatially resolved data which cannot be practically measured with other methods like fiber optic spectroradiometry [43,49].

Here, we used a portable hyperspectral imager to investigate reflectance of the mounding coral *Cyphastrea serailia* (*C. serailia*) and the laminar *Pachyseris rugosa* (*P. rugosa*) from two disparate environments in Palau, Micronesia. Palau has a diverse and abundant coral system with bay, patch, barrier, and fringing reefs. These reefs are exposed to distinct temperature and water quality regimes [50,51]. We explored whether coral-dinoflagellate mutualisms from warm turbid bays or

cooler clear-water offshore reefs harbor distinct lineages of algal symbionts, and whether these associations possess unique reflectance features which may be useful from a remote sensing perspective. As part of a larger study, we also examined if inshore corals possessed greater tolerance to elevated temperatures (*i.e.*, avoid bleaching) than the same species from offshore reefs through the use of reflectance measurements.

2. Materials and Methods

2.1. Study Sites

The Republic of Palau is a 700 km long archipelago in the western Pacific (Figure 1A), that has a great variety of coral taxa and symbionts [15,50,52]. Several thermally induced bleaching events have occurred in recent years (1998 and 2010), and the subsequent recovery surveyed [50,51]. Temperatures in the bays of the Rock Islands are significantly higher than those at patch or outer reefs, and yet bleaching during the 2010 thermal anomaly was highest for patch and outer fore reef corals [49].

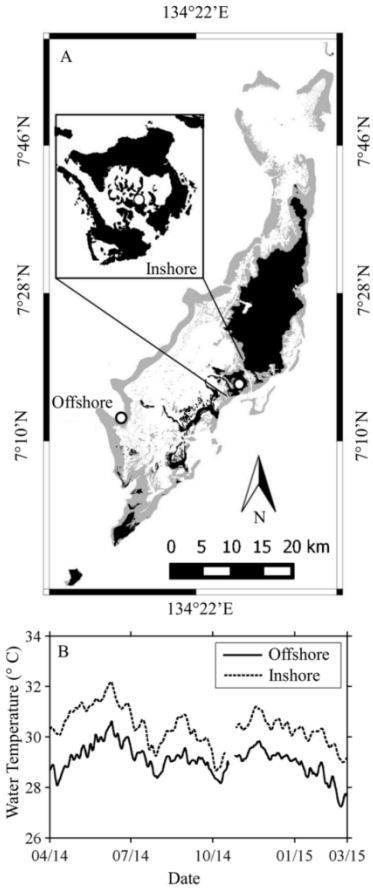

Figure 1. Study location. Palau is a Micronesian archipelago (**A**) with a variety of coral environments including bay, patch, barrier, and fringing reefs. The Inshore site at Nikko Bay is a shallow, warm bay near the city of Koror. The Offshore site is a barrier reef with more oceanic type water and consistently cooler temperatures (**B**) than the Inshore site.

2.1.1. Nikko Bay—Inshore

Nikko Bay is a shallow, warm embayment within the Rock Islands and located in close proximity to the city of Koror (Figure 1A). Light attenuation at this site is significantly higher than for offshore reefs [50]. The temperature regime in Nikko Bay is approximately 0.5–2 °C higher (Figure 1B) than at the Offshore site, Rebotel Reef [51]. Preliminary research indicated that many coral taxa at this site (hereafter referred to as "Inshore") are host to *S. trenchii*.

2.1.2. Rebotel Reef—Offshore

This location (hereafter referred to as "Offshore") is a shallow to moderate depth site on Rebotel Reef, with relatively minimal influence from human activities (Figure 1A). The water is clear and oceanic with high light transmission [50], cooler temperatures, higher pH [53] and lower dissolved inorganic carbon [53] than Nikko Bay (Table 1). Initial genetic assays at this location showed a variety of *Symbiodinium* spp. associated with coral taxa, however, very few instances of symbioses with *S. trenchii* have been found from this habitat.

Table 1. Water quality of study locations.

	Parameter			
Site	**Temp (°C)**	**pH (Total) [53]**	**DIC (μmol· kg^{-1}) [53]**	**K_{PAR} (m^{-1}) [50]**
Inshore—Nikko Bay	30.3 ± 0.8	7.84 ± 0.00	1782.7 ± 4.1	0.129
Offshore—Barrier Reefs	29.0 ± 0.7	8.05 ± 0.01	1835.3 ± 15.6	0.085

The inshore Nikko Bay reef experiences higher temperatures (yearly mean), lower pH [53], lower Dissolved Inorganic Carbon (DIC) [53], and greater diffuse light attenuation (K_{PAR}) [50] than offshore barrier reefs. Data for offshore reefs is from multiple locations in Palau. Temperatures were collected during this study at Nikko Bay and Rebotel Reef.

2.2. Coral Collection and Maintenance

Eight independent colonies of *C. serailia* and *P. rugosa* were sampled by divers at depths between 5 and 10 m Inshore and 5–15 m Offshore. Samples were returned to the lab in shaded containers. Experiments were conducted at the Palau International Coral Reef Center (PICRC). Colonies were maintained in a thermally regulated, natural seawater flow-through system (27.5 °C) during processing. Colonies were cut into approximately 3 cm × 3 cm fragments using a tile saw, transferred to shaded experimental tanks, and allowed to acclimate for >48 h before mounting to plastic tiles using Z-Spar 2 part marine epoxy. After mounting, fragments acclimated to ambient treatment conditions for an additional 10 days.

2.3. Experimental Setup

Each treatment system consisted of between 7 and 12 (56 L) plastic treatment bins connected to a central (~1200 L) sump. Each sump was continuously supplied with seawater collected directly off of the PICRC pier at a depth of 3 m. Seawater passed through a pressurized sand-bed and aquarium filter pads prior to reaching the sump. Seawater was heated to desired temperatures within the sump via titanium heating elements and then pumped to treatment bins. Treatment bins were setup outdoors, underneath a 60% shade cloth allowing for a peak midday light intensity of 800 μmol quanta m^{-2}· s^{-1}. Treatment bins were regularly scrubbed to prevent algal fouling throughout the experiment. For each treatment, three replicate fragments from each colony were placed within separate treatment bins. Within the high temperature treatment, temperature was gradually ramped from 27.5 °C to 32 °C over 96 h, and then maintained at 32 °C for an additional 10 days (14 days total). Temperature within the ambient temperature treatment was maintained at 27.5 °C throughout the full 14 day experiment.

Symbiotic algae density and genotype was assessed initially (Day 0), and then again after 9 and 14 days under experimental conditions.

2.4. Symbiont Species and Density

To determine the density of symbionts in host tissue, fragments representative of each coral colony from treatment and control tanks were sacrificed at Days 0, 9, and 14. Tissue was removed from fragments using a pressurized blast of air and seawater [54]. The resulting cell slurry was centrifuged at 1000 *g*, the supernatant discarded, and the resulting pellet of symbiont cells preserved with 10 µL of 1% glutaraldehyde for cell enumeration [55] and DNA extractions [10]. Symbionts were identified through amplification of the internal transcribed spacer 2 region (ITS2) of the ribosomal array, and analyzed by previously published protocols for denaturing gradient gel electrophoresis (DGGE) and sanger sequencing [7], relying on the ribosomal internal transcribed spacer sequences as proxies for species resolution. Cell density was recorded by light and fluorescence microscopy. Four independent replicate counts were performed for each algal sample on a hemocytometer. Samples were photographed using an EVOS digital microscope (4× magnification) and analyzed using the software Image J (NIH) with the Analyze Particles function using methods similar to Suggett *et al.* [56]. Surface area was determined via the foil method [57].

2.5. Imaging and Reflectance Processing

Spectral reflectance, the ratio of light backscattered from a target to that incident on it at every wavelength, of a coral sample results from the interaction of animal and endosymbiont pigments. A subset of fragments was selected for reflectance measurements. Spectral data was collected with a 710 VP (Surface Optics Corp, San Diego, CA, USA) hyperspectral imager. The imager collects a data cube, a 520 × 696 pixel image with full spectral radiance information at 5 nm increments between 380 and 1040 nm. Final spatial resolution was on the order of 10,000 pixels per cm^2. The imager was mounted on a tripod at an approximately normal viewing angle (*i.e.*, with the sensor looking vertically downward) with data collected under solar illumination between 10:00 a.m. and 2:00 p.m. local time.

During imaging, coral fragments were submerged (approximately 10 cm depth) in a tank lined with black cloth. To minimize stress and thermal effects on corals, fragments were gently and rapidly transferred from flow-through experimental tanks to the imaging tank, scanned (typically 30 s), and returned to the experimental system. Water in the imaging tank was taken from the treatment for that fragment group (heated or control). Water was changed frequently to avoid excessive heating. A Spectralon (LabSphere) 10% reflectance standard was included in every data cube for calculation of reflectance $R(\lambda)$ at the same depth as the coral sample. A 10% standard was selected to maximize the signal-to-noise ratio for reflectance of relatively dark coral samples [30]. Bubbles were removed from the standard by gentle polishing with 400-grit wet/dry sandpaper while submerged. Coral fragments were mounted horizontally, providing a near laminar surface.

ENVI (Exelis VIS) image analysis software was used for the processing of data cubes (Figure 2). Regions of Interest (ROIs) were generated manually with visual inspection so as to avoid glare contaminated and saturated pixels. Cubes with heavy glare or contamination from surface reflectance were discarded from analysis. ROIs were created for 3 elements in all remaining images: a Spectralon standard, the black background, and the coral. For coral ROIs, pixels near to the edge of the marine epoxy were avoided. From these ROIs, mean spectra (as dimensionless numbers) were extracted for processing. These signals were corrected for sensor noise using a dark signal collected during imaging. Due to signal to noise limitations of the imager, the spectral region considered is limited to 400–700 nm, interpolated to 1 nm using Piecewise Cubic Hermite Interpolating Polynomial (PCHIP).

As the reflectance of the standard under water diverged from the calibrated value [58], we therefore measured its reflectance relative to a 99% Spectralon standard (with bubbles removed from both standards) independently from data collection. This value, R_{std} (λ), was then used in

calculating coral reflectance (Table 2). All parameters in calculating reflectance are fully spectral, with (λ) dropped for clarity.

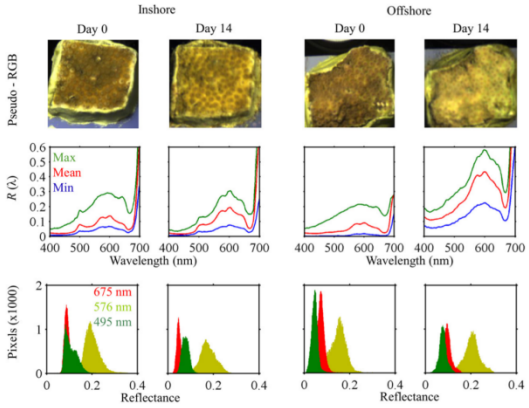

Figure 2. Hyperspectral imaging of *Cyphastrea serailia* at Day 0 and 14. Pseudo-RGB images (**top row**) illustrate the different degrees of pigment loss evident between Inshore and Offshore colonies after heating. Mean fragment reflectance (**middle row**) shows an increase in $R(\lambda)$ for the Inshore fragment, and a pronounced increase for Offshore. The shift in pixel histograms for reflectance at select wavelengths (**bottom row**) with bleaching are evident from the hyperspectral imagery, and HSI is far more efficient at revealing the distribution of variability of reflectance than techniques like fiber-optic spectroradiometry.

Table 2. Summary of symbols, definitions, and units.

Symbol	Definition	Unit
L_{crl}	Radiance of coral pixels	$W \cdot m^{-1} \cdot sr^{-1}$
L_{glr}	Radiance from surface reflectance	$W \cdot m^{-1} \cdot sr^{-1}$
L_{std}	Radiance of Spectralon pixels	$W \cdot m^{-1} \cdot sr^{-1}$
R_{std}	Reflectance of Spectralon	Dimensionless number
R_{blk}	Reflectance of black background	Dimensionless number
R_{crl}	Reflectance of coral	Dimensionless number

Coral fragments were submerged in seawater, while the imager was in air above the imaging tank. As such, contamination of radiance spectra by surface reflection represents a potentially non-trivial source of error, hereafter referred to as glare. This signal must be removed from coral and reflectance standard radiance spectra before calculating coral reflectance. Consistent with ocean color remote sensing, we consider the radiance from glare to be an additive component to the total radiance measured at the sensor. Glare radiance L_{glr} was set equal to the raw radiance L_{blk} of black background pixels over the spectral region where R_{blk} is near zero (400–638 nm). This signal also includes any photons that were reflected from within the water column itself. At longer wavelengths (639–700 nm), L_{glr} (λ) = L_{blk} (638 nm) because there was some non-negligible reflectance from the black cloth at far red wavelengths. Finally, coral radiance spectra extracted from the imagery were converted to Lambertian equivalent reflectance as:

$$R_{crl} = \left[\left(L_{crl} - L_{glr}\right) \times R_{std}\right] / \left(L_{std} - L_{glr}\right) \quad (1)$$

where L_{crl} is the raw signal of coral pixels. To remove noise due to environmental factors including capillary waves due to non-flat water surface and low signal in some wavelengths, spectra were smoothed 3 times with a Savitsky–Golay filter of order 3 and 15 nm width [5,12,25,26]. Standard deviation of R_{crl} was also generated for each fragment from the imagery.

2.6. Reflectance and Symbiont Density Comparison

An exponential regression was fit to symbiont density and integrated reflectance for fragments on Day 0. Reflectance spectra were integrated as:

$$\sum R = \int_{400}^{700} R_{crl}(\lambda)\, d\lambda \quad (2)$$

Colonies of both species were grouped by reef/symbiont type for analysis.

2.7. Reflectance Analysis

Differences in reflectance between species, sites, and temperature treatment were tested for significance at each wavelength (Mann–Whitney U test) for significance, utilizing mean reflectance for each fragment.

The location of peaks in the 2nd derivative of reflectance has been linked to the absorption spectra of specific endosymbiont and host pigments and can be utilized to locate important reflectance features [12,24–26,30,36]. The 2nd derivative of reflectance $\left(\frac{d^2R}{d\lambda^2}\right)$ was calculated for each fragment at Day 0 and peaks located during processing.

3. Results

3.1. Symbiont Species and Density

Symbionts in Inshore colonies for both *C. serailia* and *P. rugosa* were identified as *Symbiodinium trenchii* [15]. Offshore, seven *C. serailia* colonies harbored *Symbiodinium* type C3u and one colony contained C40 (ITS2 type designations). Of the eight Offshore *P. rugosa* colonies, five contained *Symbiodinium* C40 symbionts, one hosted Cunk (Clade C unknown), and two were associated with *S. trenchii*. As the purpose of this study was to examine spectral reflectance with regard to symbiont type, those Offshore *P. rugosa* colonies containing *S. trenchii* were excluded from analysis of Offshore *P. rugosa* and instead included in the "Inshore" group containing *S. trenchii*.

Median symbiont densities, on the order of 10^6 cells per cm^2 of coral surface area, were similar (Figure 3) for *C. serailia* colonies from both Inshore (labeled "NCs") and Offshore (labeled "OCs"), as well as Inshore *P. rugosa* colonies (labeled "NPr"). Corals from Inshore reefs, containing *S. trenchii*, had (non-significantly) higher densities than their Offshore counterparts (with multiple C type symbionts) for both coral species. Offshore *P. rugosa* (labeled "OPr") colonies had lower densities than Inshore corals (Mann–Whitney U test, NCs: $p = 0.03$, NPr: $p = 0.05$) and Offshore *C. serailia* ($p = 0.1$).

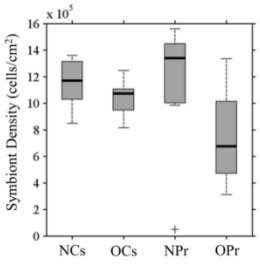

Figure 3. Initial symbiont cell density in coral colonies. Density of symbiont cells per cm^2 of coral fragments are given for Inshore (N) and Offshore (O) colonies of *Cyphastrea serailia* (Cs) and and *Pachyseris rugosa* (Pr). Horizontal bars are colony median density (on the order of 10^6 cells/ cm^2), crosses represent outliers.

3.2. Spectral Reflectance

3.2.1. *Cyphastrea serailia*

The reflectance of Inshore and Offshore *C. serailia* share several spectral features (Figure 4, top). In particular, peaks at 580 and 605 nm, and a shoulder at 655 nm were observed for colonies from both locations. These are similar to features in other published coral spectra [5,30,35]. However, Inshore colonies show a distinct reflectance peak, likely due to fluorescence, at 490–505 nm that was not observed for Offshore colonies. Inshore and Offshore colonies were similarly reflective in the blue (400–490 nm), while Inshore $R(\lambda)$ was significantly (Mann–Whitney U test, $p < 0.05$) higher than Offshore between 492 and 547 nm. Additionally, mean reflectance of *C. serailia* from Inshore showed a higher standard deviation than Offshore at most wavelengths.

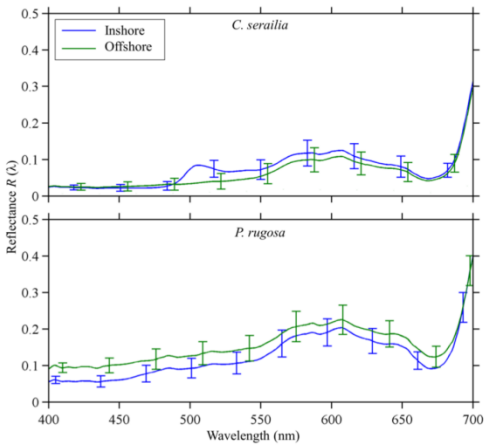

Figure 4. Mean reflectance of colonies from Inshore (*S. trenchii*) and Offshore (Clade C) reefs for *Cyphastrea serailia* (**top**) and *Pachyseris rugosa* (**bottom**). Spectral shapes from both locations are similar for both species, with the exception of green fluorescence at approximately 490–500 nm present in the Inshore *C. serailia*. Error bars represent ±1 standard deviation, as the square root of the pooled variances for each fragment in the species/site group. Eight fragments were averaged for each curve, except Offshore *P. rugosa* where two fragments with *S. trenchii* were omitted.

3.2.2. *Pachyseris rugosa*

The reflectance of Inshore and Offshore *P. rugosa* were very similar in spectral shape (Figure 4, bottom), though Offshore colonies were significantly ($p < 0.05$) more reflective than Nikko Bay in lower (400–471 nm) wavelengths. As with *C. serailia*, standard deviation was generally higher for Nikko Bay colonies. The features seen in *C. serailia* at 580, 605, and 655 nm were also observed in *P. rugosa*, with the addition of two slight peaks at 480 and 512 nm. A very slight peak was observed in all treatments at 405 nm.

3.2.3. Derivative Analysis

The major spectral features were found to be common to colonies of both species and locations (Figure 5). Second derivative peaks at 412, 420, 434, 455, 492, 524, 550, 559, 579, 593, 617, and 636 nm were found (±1 nm) in the mean second derivative spectra of all groups (Table 3). Additional peaks at 474 and 505 nm were present in all colonies except Inshore *C. serailia*. A peak at 536 nm was present in Offshore *C. serailia* and Inshore *P. rugosa*, at 668 nm in all colonies except Offshore *P. rugosa*, and at 689 nm in all but Inshore *P. rugosa*. The locations of all peaks were not different when using normalized

or non-normalized spectra. For *P. rugosa*, the magnitude of Offshore peaks was greater in the lower (400–500 nm) wavelengths.

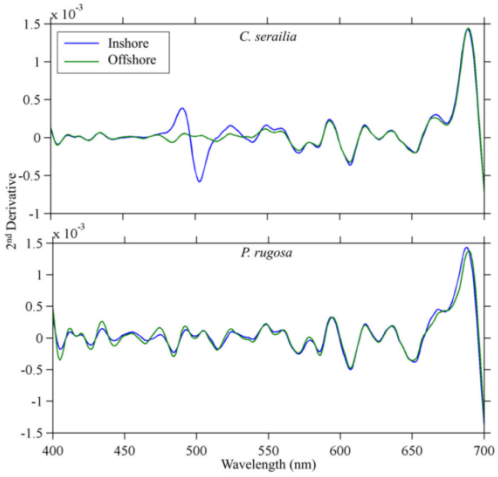

Figure 5. Mean second derivative of $R(\lambda)$ for both species. For *Cyphastrea serailia* (**top**), second derivative peak location and magnitude are almost identical except from 475–550 nm, due to the presence of a large $R(\lambda)$ feature in Inshore colonies. *Pachyseris rugosa* (**bottom**) colonies showed peaks at identical locations between sites. Error bars have been omitted for clarity.

Table 3. Second derivative peak wavelengths in mean reflectance spectra for coral species and site/symbiont combinations. Presence of a peak at given wavelength is indicated by +, absence by -.

	C. serailia		*P. rugosa*	
Wavelength (nm)	**Inshore**	**Offshore**	**Inshore**	**Offshore**
	S. trenchii	**C Type**	***S. trenchii***	**C Type**
412	+	+	+	+
420	+	+	+	+
434	+	+	+	+
455	+	+	+	+
474	-	+	+	+
492	+	+	+	+
504	-	+	+	+
524	+	+	+	+
536	-	+	+	-
549	+	+	+	+
559	+	+	+	+
579	+	+	+	+
593	+	+	+	+
617	+	+	+	+
636	+	+	+	+
666	+	+	+	-
689	+	+	-	+

3.2.4. Inshore *vs.* Offshore

Reflectance spectra of Inshore (*S. trenchii*) and Offshore (Clade C) colonies were grouped for inter-site comparison. No wavelengths were found to be significantly different (Mann–Whitney U test, $\alpha = 0.05$) between sites. This result remained true when spectra were normalized to their maximum value in the region considered due to significant differences in overall magnitude of reflectance and

initial symbiont cell density between some species/site combinations. There were no unique second derivative features common across both Inshore corals when compared to both Offshore corals.

3.3. Reflectance and Symbiont Density Comparison

Inverse exponential relationships between symbiont density (cells/cm^2) and integrated reflectance ΣR were observed for both coral species and dinoflagellate type (*S. trenchii vs.* Clade C). Exponential regressions between ΣR and the density differed for host/dinoflagellate combinations (Figure 6). Predictability ranged between 47% and 75%, with distinct relationships depending on coral/symbiont.

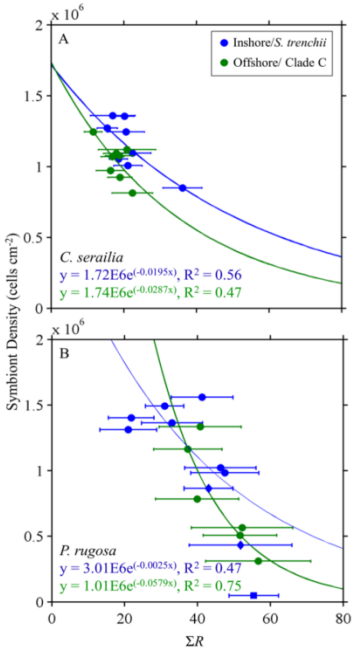

Figure 6. Integrated reflectance and symbiont density for colonies of *Cyphastrea serailia* (**A**) and *Pachyseris rugosa* (**B**). For each coral, both kinds of symbiont showed an inverse relationship for each coral with a range of predictability. Error bars are ±1 standard deviation of ΣR. Blue diamonds are *P. rugosa* from Offshore that contained *Symbiodinium trenchii*, and so were included with Inshore *P. rugosa* for analysis. Blue square represents a sample of Inshore *P. rugosa* whose symbiont density was considered to be an outlier and was excluded from regression.

3.4. Response to Heating

3.4.1. Symbiont Density

Cyphastrea serailia control fragments from Inshore (Figure 7A) had lower (Mann–Whitney U test, $p = 0.05$) cell density (*S. trenchii*) on Day 14 than Day 0, but control and heated densities were not different ($p = 0.16$). A slight increase in median density was observed for heated fragments between Days 9 and 14. Offshore *C. serailia* (Figure 6B) cell density (Clade C types) decreased significantly for both control and heated fragments by Day 14 ($p < 0.001$), but the heated fragments had approximately 50% less algal cells than the control fragments ($p = 0.001$).

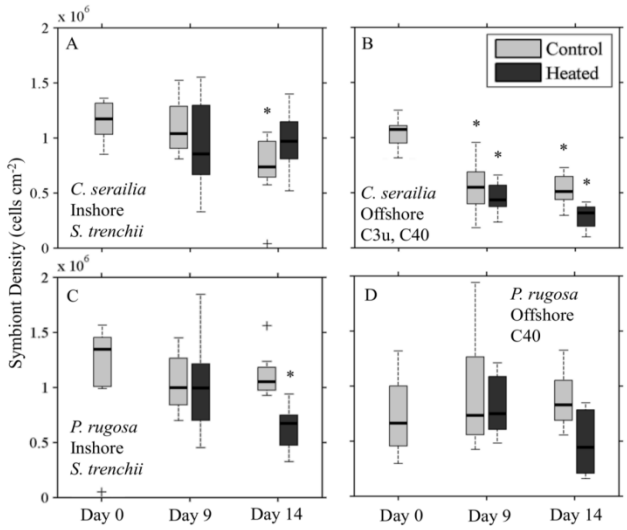

Figure 7. Symbiont cell density for coral colonies over time for control and heated treatments. *Cyphastrea serailia* contained *Symbiodinium trenchii* Inshore (**A**); with C3u and C40 Offshore (**B**); *Pachyseris rugosa* was associated with *S. trenchii* Inshore (**C**) and C40 and C3u Offshore (**D**). Asterisk denotes that the treatment is significantly different ($p < 0.05$) from the initial condition at Day 0.

For *P. rugosa*, Inshore symbiont (*S. trenchii*) densities decreased over time for both control and heated fragments (Figure 7C), though this decline was significant only for heated fragments ($p = 0.02$) on Day 14. Cell density in heated fragments was 44% percent lower than for control fragments ($p < 0.001$). Offshore, heated fragments (Figure 7D) had lower cell density (C types) on Day 14 from Day 0 ($p = 0.18$), and were 48% lower than control density ($p = 0.06$). For both species and sites, Day 0 densities for heated and control fragments were not collected separately.

3.4.2. Reflectance

Cyphastrea serailia

Colonies of *C. serailia* from Inshore and Offshore locations showed distinct responses to heating (Figure 8). On Day 0, there was no difference in mean reflectance spectra $R(\lambda)$ for all fragments for either Inshore or Offshore colonies. By Day 9, all fragment groups showed overall increased $R(\lambda)$, with Offshore colonies having a slightly higher mean reflectance at all wavelengths in response to heating. By Day 14, heated Inshore colonies had a slightly higher mean $R(\lambda)$ than the control at wavelengths above 511 nm. Heated Offshore colonies, by contrast, showed a higher mean reflectance at all wavelengths, significant at the $\alpha = 0.05$ level from 559–618 nm.

Pachyseris rugosa

Response to heating in *P. rugosa* followed the same general trend as observed in *C. serailia* (Figure 9). Colonies from both Inshore and Offshore increased in reflectance by Day 9 for both control and heated fragments. Day 14 mean $R(\lambda)$ was not significantly different between heated and control fragments for Inshore at any wavelength. For Offshore colonies, Day 14 mean $R(\lambda)$ of heated fragments was higher at all wavelengths than for the control, but this was not significant ($\alpha = 0.05$).

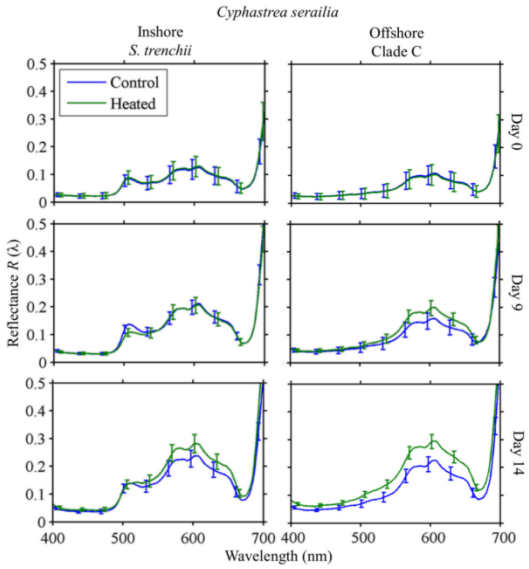

Figure 8. *Cyphastrea serailia* $R(\lambda)$ time series. Mean reflectance spectra at Days 0, 9, and 14 for control and heated fragments from Inshore/*S. trenchii* (**left column**) and Offshore/Clade C (**right column**) reefs. Error bars represent ± 1 standard deviation, as the square root of the pooled variances for each fragment in the species/site group.

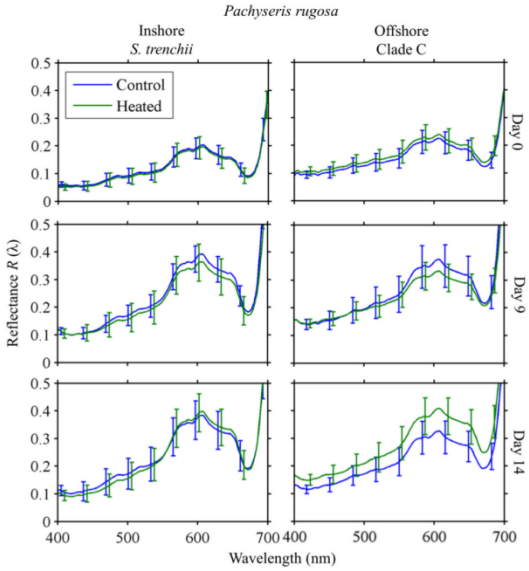

Figure 9. *Pachyseris rugosa* $R(\lambda)$ time series. Mean reflectance spectra at Days 0, 9, and 14 for control and heated fragments from Inshore/*S. trenchii* (**left column**) and Offshore/Clade C (**right column**) reefs. Error bars are ± 1 standard deviation, as the square root of the pooled variances for each fragment in the species/site group.

4. Discussion

We assessed the spectral features of two common species of reef-building coral in relationship to their symbiont species and response to thermal stress. The results are discussed in the context of spectral variability with coral species and symbiont type, areal density of symbionts, and to the effect of environmental temperature stress.

4.1. Reflectance of Different Coral/Symbiont Systems

The spectral shape and magnitude of reflectance of corals can be directly related to absorption, backscattering, and fluorescence features of both the host and dinoflagellate symbionts. A dip or local minima in a reflectance spectrum results from absorption by pigments, both within the photosynthetic symbionts and host tissues. Reflectance peaks can appear due to a lack of absorption compared to neighboring wavelengths or can result from pigment fluorescence. The spectral reflectance patterns of all the corals sampled were consistent with the large database of corals sampled from tropical reefs throughout the world ocean [5,59]. These corals followed the basic "triple-peaked pattern" [30] or "brown coral mode" [30] with generally low reflectance in the blue and green wavelengths (400–450 nm) rising in the red with local peaks around 575, 600, and 650 nm. The triple peaked patterns were conserved regardless of symbiont genetic identity or treatment and are the result of absorption dips in neighboring wavebands due common pigments of *Symbiodinium*. In particular, Torres-Pérez *et al.* [12,60] found that common pigments in two species of Caribbean corals included chlorophyll *a* with peaks at 427, 665, and 685 nm, chlorophyll c_2 at 634 nm, and diadino/diatoxanthin at 442 nm. Peridinin, a diagnostic pigment for many dinoflagellates [12] has an absorption maximum at 475 nm that creates an upward slope in reflectance between 500 and 550 nm [24], which is evident in our measurements though partially masked in Inshore *C. serailia* (Figure 4) by a large fluorescence feature. The concentrations and identities of symbiont pigments in this system will be the subject of forthcoming research.

The primary spectral difference observed occurred in *C. serailia* colonies from our Inshore site at Nikko Bay with the symbiont *S. trenchii* as a distinct broad reflectance peak from 498 to 520 nm. This feature is due largely to Green Fluorescent Proteins (GFPs) and is noted in naturally occurring reflectance measurements from other studies [24,61,62]. While present in all *C. serailia* Inshore colonies and absent from Offshore, a small feature in this region was observed in only a single colony of *P. rugosa* from both locations. However, it is possible that the GFP is a host derived photoprotection mechanism, plays an important part in thermal tolerance, and may indicate host acclimatization to the Nikko Bay environment [63,64]. The presence of GFPs will hinder discrimination of coral or symbiont taxa *in situ* due to a lack of predictability for the strength of the GFP signal and ecological parameters [59,65].

High backscattering from the underlying coral skeleton, combined with a sharp decrease in absorption by symbiont and host pigments in the far red, results in the rising reflectance at 700 nm also referred to as the red edge of reflectance common to vegetation [38]. Torres-Pérez *et al.* [12] were able to discern variability in the magnitude of near infrared reflectance related to different species of coral. Our analysis however was not able to reliably estimate the reflectance beyond 700 nm because of the experimental setup where the near infrared was highly absorbed due to water molecules. However, differences in near infrared are more challenging to observe in remote sensing imagery due to water absorption and may not be useful for discrimination of coral species.

4.2. Spectral Variability with Symbiont Concentration

Spectral reflectance was related to the symbiont concentration and the initiation of bleaching observed in offshore colonies. We investigated whether reflectance properties could be used to estimate the concentration of symbiont within coral samples. For the initial, newly collected coral samples, there was an inverse relationship between integrated reflectance and the symbiont concentration, as the photosynthetic symbionts absorb light and lower the overall reflectance of the coral. In addition

to symbiont areal density, the concentration of pigmentation per dinoflagellate cell will have a significant impact on ΣR. The relatively low correlation between ΣR and symbiont density in Inshore (*S. trenchii*) *P. rugosa* may be the result of significantly different photoacclimation and pigment status of the symbiont cells. Previous research found a strong inverse relation with high predictability ($R^2 \geqslant 0.80$) for ΣR and total tissue pigment concentration [12,60]. Integrated reflectance shows potential as a remote sensing tool for rough estimation of symbiont cell densities, however preceding parameterizations will be required for symbiont and coral species, as illustrated here by the higher overall reflectance of *P. rugosa* compared to *C. serailia* and corresponding distinct relationships between ΣR and symbiont density.

4.3. Spectral Response to Heating

Following the 1998 thermal bleaching event in Palau, Golbuu *et al.* [50] found that coral communities in protected bays and deep slopes were substantially less effected and recovered much more quickly than those on either shallow exposed fringe or patch reefs in Palau. This same trend was also observed after a thermal stress event in 2010 [51]. Increased heat and high irradiance can act synergistically to induce coral bleaching [2,66–70]. Both studies attributed the relative resilience of the bay communities to thermal resistance in the animal and symbionts, and reduced irradiance due to high light attenuation in bay water compared to the clear oceanic waters found at fringe and patch reef sites. Bleaching in corals results in the flattening of reflectance features and an overall increase in the magnitude of $R(\lambda)$ [24,25] as photosynthetic dinoflagellates are expelled and the bright, broadly reflective calcium carbonate skeleton influences reflectance.

Previous studies in Palau showed relative resistance to bleaching from elevated temperatures for inshore "bay" reefs [50,51]. Therefore, we expected coral fragments of both of *C. serailia* and *P. rugosa* from the Offshore site to show a larger increase in reflectance resulting from greater decrease in symbiont densities after heating relative to fragments from Inshore. We found that colonies of both *C. serailia* and *P. rugosa* from Inshore showed a negligible change in spectral reflectance with heating, while those colonies from the Offshore patch reef were more reflective than control fragments, where over the duration of the experiment they began to noticeably pale. Symbiont cell density in *C. serailia* conformed to the observed reflectance patterns, in that lower densities coincided with increased magnitude of $R(\lambda)$. Offshore colonies had significantly lower densities following heating, while Inshore colonies containing the thermally resistant *S. trenchii* did not significantly expel symbionts in response to elevated temperatures. By contrast, *P. rugosa* colonies from both Inshore and Offshore reefs showed a significant decline in endosymbiont density. Interestingly, the reflectance of heated Inshore *P. rugosa* with *S. trenchii* was not distinguishable from control fragments, despite having significantly lower cell densities. The degree to which the change in reflectance observed here is the product of symbiont expulsion or photoacclimation and pigment modification by the symbionts themselves is unknown, and will be the subject of future work.

Work on Palauan and Caribbean reefs indicate that corals with *S. trenchii* have greater thermal tolerance to increased seawater temperatures [13,14]. In the Caribbean, there is some evidence that the symbiosis is sub-optimal for some coral species as these colonies showed a lower level of calcification [16], though this may not be the case in Palau. The present study seems to indicate a lower level of thermal bleaching (as increased reflectance or loss of symbionts) in colonies with *S. trenchii*, compared to C3u or C40 symbionts. An examination of calcification rates and photosynthesis in the coral–symbiont pairings studied here is forthcoming.

5. Conclusions and Outlook for Remote Sensing

We evaluated the *in vivo* spectral reflectance from two Palauan species of coral (host cnidarian) with different species of dinoflagellate (symbionts) exhibiting different thermal tolerances. The use of an imager rather than a point spectrometer allowed us to measure the range and variability in spectral reflectance across an entire coral sample. Reflectance across all treatments showed similar features,

characteristic of brown mode reflectance [59]. A large fluorescence feature was observed in one cnidarian/dinoflagellate combination, but this could not be linked to symbiont or coral species. Under heating conditions, the magnitude of spectral reflectance increased for colonies of both coral species associated with Clade C symbionts, but not those with *S. trenchii*. Symbiont concentration decreased to some degree with heating for both coral species with Clade C, while *S. trenchii* concentrations remained constant in one coral species and decreased with heating for the second.

The inability to find a spectral signature unique to the thermally tolerant generalist *S. trenchii* relative to the other *Symbiodinium* types encountered here suggests that it will be challenging to use reflectance spectroscopy to distinguish different symbionts. The similarity of the reflectance spectra from distinct host species and symbionts further supports past remote sensing studies employing inversion of a representative endmember (where an optical model is applied to field reflectance data) to identify coral and benthic constituents [1–4,71,72]. The relationship between integrated reflectance and symbiont concentration may prove useful to assess or monitor reef condition and the potential for bleaching. Such algorithms may be implemented using hyperspectral sensors from airborne platforms like the Portable Remote Imaging Spectrometer (PRISM) [1,38], proposed future satellite sensors, and through the use of underwater hyperspectral imagers [32,33,47,48]. However, the implementation of the algorithms will be complicated by the effects of the intervening water column, sea-surface, and atmosphere, as well as the spectral and spatial resolution of the sensor itself [24,35]. Future studies to assess how these results compare to other species of coral and symbiont from various regions are warranted.

Acknowledgments: This research was supported by National Science Foundation (IOS-1258058, -1258065, and -1258063), Office of Naval Research Multi-University Research Initiative grant N000140911054, National Aeronautics and Space Administration Biological Diversity and Ocean Biology funding to H.M.D. Award # NNX15AC32G, and the NASA Earth Science Technology Instrument Incubator Program (IIP) for Snow and Water: Imaging Spectroscopy for Coasts and Snow Cover. We wish to thank the staff of the Palau International Coral Reef Center where work was conducted. We also wish to thank Allison Lewis and Eric Nuschke of Pennsylvania State University for assistance in the field and lab.

Author Contributions: T.C.L., M.E.W., D.W.K. conceived and designed the original experimental treatments, while B.J.R. and H.M.D. conceived and designed the spectral reflectance components. T.C.L., M.E.W., D.W.K., K.D.H., and B.J.R. conducted experiments. B.JR., H.M.D., T.C.L., K.D.H., and T.G.B. wrote the manuscript.

Conflicts of Interest: The authors declare no conflict of interest. The founding sponsors had no role in the design of the study; in the collection, analyses, or interpretation of data; in the writing of the manuscript, and in the decision to publish the results.

Abbreviations

The following abbreviations are used in this manuscript:

DGGE	Denaturing gradient gel electrophoresis
GFP	Green fluorescent protein
HSI	Hyperspectral imaging
PCHIP	Piecewise cubic hermite interpolating polynomial
PICRC	Palau International Coral Reef Center
ROI	Region of interest

References

1. Andréfouét, S.; Payri, C.; Hochberg, E.J.; Hu, C.; Atkinson, M.J.; Muller-Karger, F.E. Use of *in situ* and airborne reflectance for scaling-up spectral discrimination of coral reef macroalgae from species to communities. *Mar. Ecol. Prog. Ser.* **2004**, *283*, 161–177. [CrossRef]
2. Mumby, P.J.; Skirving, W.; Strong, A.E.; Hardy, J.T.; LeDrew, E.F.; Hochberg, E.J.; Stumpf, R.P.; David, L.T. Remote sensing of coral reefs and their physical environment. *Mar. Pollut. Bull.* **2004**, *48*, 219–228. [CrossRef] [PubMed]

3. Goodman, J.; Ustin, S.L. Classification of benthic composition in a coral reef environment using spectral unmixing. *J. Appl. Remote Sens.* **2007**, *1*. [CrossRef]
4. Scopélitis, J.; Andréfouët, S.; Phinn, S.; Chabanet, P.; Naim, O.; Tourrand, C.; Done, T. Changes of coral communities over 35 years: Integrating *in situ* and remote-sensing data on Saint-Leu Reef (la Réunion, Indian Ocean). *Estuar. Coast. Shelf Sci.* **2009**, *84*, 342–352. [CrossRef]
5. Hochberg, E. Spectral reflectance of coral reef bottom-types worldwide and implications for coral reef remote sensing. *Remote Sens. Environ.* **2003**, *85*, 159–173. [CrossRef]
6. Freudenthal, H.D. *Symbiodinium* gen. nov. and *Symbiodinium microadriaticum* sp. nov., a Zooxanthella: Taxonomy, Life Cycle, and Morphology. *J. Protozool.* **1962**, *9*, 45–52. [CrossRef]
7. LaJeunesse, T. Diversity and community structure of symbiotic dinoflagellates from Caribbean coral reefs. *Mar. Biol.* **2002**, *141*, 387–400.
8. LaJeunesse, T.C.; Pettay, D.T.; Sampayo, E.M.; Phongsuwan, N.; Brown, B.; Obura, D.O.; Hoegh-Guldberg, O.; Fitt, W.K. Long-standing environmental conditions, geographic isolation and host-symbiont specificity influence the relative ecological dominance and genetic diversification of coral endosymbionts in the genus Symbiodinium. *J. Biogeogr.* **2010**, *37*, 785–800. [CrossRef]
9. Thornhill, D.J.; Lewis, A.M.; Wham, D.C.; LaJeunesse, T.C. Host-specialist lineages dominate the adaptive radidation of reef coral endosymbionts. *Evolution* **2014**, *68*, 352–367. [CrossRef] [PubMed]
10. LaJeunesse, T.C.; Loh, W.K.; Van Woesik, R.; Hoegh-Guldberg, O.; Schmidt, G.W.; Fitt, W.K. Low symbiont diversity in southern Great Barrier Reef corals, relative to those of the Caribbean. *Limnol. Oceanogr.* **2003**, *48*, 2046–2054. [CrossRef]
11. Tonk, L.; Sampayo, E.M.; LaJeunesse, T.C.; Schrameyer, V.; Hoegh-Guldberg, O. *Symbiodinium* (Dinophyceae) diversity in reef-invertebrates along an offshore to inshore reef gradient near Lizard Island, Great Barrier Reef. *J. Phycol.* **2014**, *50*, 552–563. [CrossRef]
12. Torres-Pérez, J.L.; Guild, L.S.; Armstrong, R.A. Hyperspectral distinction of two Caribbean shallow-water corals based on their pigments and corresponding reflectance. *Remote Sens.* **2012**, *4*, 3813–3832. [CrossRef]
13. Kemp, D.W.; Hernandez-Pech, X.; Iglesias-Prieto, R.; Fitt, W.K.; Schmidt, G.W. Community dynamics and physiology of *Symbiodinium* spp. before, during, and after a coral bleaching event. *Limnol. Oceanogr.* **2014**, *59*, 788–797. [CrossRef]
14. LaJeunesse, T.C.; Smith, R.T.; Finney, J.; Oxenford, H. Outbreak and persistence of opportunistic symbiotic dinoflagellates during the 2005 Caribbean mass coral "bleaching"event. *Proc. R. Soc. B Biol. Sci.* **2009**, *276*, 4139–4148. [CrossRef] [PubMed]
15. LaJeunesse, T.C.; Wham, D.C.; Pettay, D.T.; Parkinson, J.E.; Keshavmurthy, S.; Chen, C.A. Ecologically differentiated stress-tolerant endosymbionts in the dinoflagellate genus *Symbiodinium* (Dinophyceae) Clade D are different species. *Phycologia* **2014**, *53*, 305–319. [CrossRef]
16. Pettay, D.T.; Wham, D.C.; Smith, R.T.; Iglesias-Prieto, R.; LaJeunesse, T.C. Microbial invasion of the Caribbean by an Indo-Pacific coral zooxanthella. *Proc. Natl. Acad. Sci. USA* **2015**, *112*, 7513–7518. [CrossRef] [PubMed]
17. Ragni, M.; Ruth, A.L.; Hennige, S.J.; Suggett, D.J.; Warner, M.E.; Geider, R.J. PSII photoinhibition and photorepair in Symbiodinium (Pyrrhophyta) differs between thermally tolerant and sensitive phylotypes. *Mar. Ecol. Prog. Ser.* **2010**, *406*, 57–70. [CrossRef]
18. Robison, J.D.; Warner, M.E. Differential impacts of photoacclimation and thermal stress on the photobiology of four different phylotypes of *Symbiodinium* (Pyrrhophyta). *J. Phycol.* **2006**, *42*, 568–579. [CrossRef]
19. Steinke, M.; Brading, P.; Kerrison, P.; Warner, M.E.; Suggett, D.J. Concentrations of dimethylsulfoniopropionate and dimethyl sulfide are strain-specific in symbiotic dinoflagellates (*Symbiodinium* sp., Dinophyceae). *J. Phycol.* **2011**, *47*, 775–783. [CrossRef]
20. Berkelmans, R.; van Oppen, M.J. The role of zooxanthellae in the thermal tolerance of corals: A "nugget of hope" for coral reefs in an era of climate change. *Proc. R. Soc. B Biol. Sci.* **2006**, *273*, 2305–2312. [CrossRef] [PubMed]
21. Grottoli, A.G.; Warner, M.E.; Levas, S.J.; Aschaffenburg, M.D.; Schoepf, V.; McGinley, M.; Baumann, J.; Matsui, Y. The cumulative impact of annual coral bleaching can turn some coral species winners into losers. *Glob. Chang. Biol.* **2014**, *20*, 3823–3833. [CrossRef] [PubMed]
22. Silverstein, R.N.; Cunning, R.; Baker, A.C. Change in algal symbiont communities after bleaching, not prior heat exposure, increases heat tolerance of reef corals. *Glob. Change Biol.* **2015**, *21*, 236–249. [CrossRef] [PubMed]

23. Enríquez, S.; Méndez, E.R.; Prieto, R.I. Multiple scattering on coral skeletons enhances light absorption by symbiotic algae. *Limnol. Oceanogr.* **2005**, *50*, 1025–1032. [CrossRef]
24. Hedley, J.D.; Mumby, P.J. Biological and remote sensing perspectives of pigmentation in coral reef organisms. *Adv. Mar. Biol.* **2002**, *43*, 277–317. [PubMed]
25. Holden, H.; LeDrew, E. Spectral discrimination of healthy and non-healthy corals based on cluster analysis, principal components analysis, and derivative spectroscopy. *Remote Sens. Environ.* **1998**, *65*, 217–224. [CrossRef]
26. Joyce, K.E.; Phinn, S.R. Hyperspectral analysis of chlorophyll content and photosynthetic capacity of coral reef substrates. *Limnol. Oceanogr.* **2003**, *48*, 489–496. [CrossRef]
27. Ralph, P.J.; Larkum, A.W.D.; Kühl, M. Photobiology of endolithic microorganisms in living coral skeletons: 1. Pigmentation, spectral reflectance and variable chlorophyll fluorescence analysis of endoliths in the massive corals Cyphastrea serailia, Porites lutea and Goniastrea australensis. *Mar. Biol.* **2007**, *152*, 395–404. [CrossRef]
28. Rodríguez-Román, A.; Hernández-Pech, X.; E Thome, P.; Enríquez, S.; Iglesias-Prieto, R. Photosynthesis and light utilization in the Caribbean coral Montastraea faveolata recovering from a bleaching event. *Limnol. Oceanogr.* **2006**, *51*, 2702–2710. [CrossRef]
29. Clark, C.D.; Mumby, P.J.; Chisholm, J.R.M.; Jaubert, J.; Andréfouét, S. Spectral discrimination of coral mortality states following a severe bleaching event. *Int. J. Remote Sens.* **2000**, *21*, 2321–2327. [CrossRef]
30. Hochberg, E.J.; Atkinson, M.J. Spectral discrimination of coral reef benthic communities. *Coral Reefs* **2000**, *19*, 164–171. [CrossRef]
31. Myers, M.R.; Hardy, J.T.; Mazel, C.H.; Dustan, P. Optical spectra and pigmentation of Caribbean reef corals and macroalgae. *Coral Reefs* **1999**, *18*, 179–186. [CrossRef]
32. Caras, T.; Karnieli, A. Ground-level spectroscopy analyses and classification of coral reefs using a hyperspectral camera. *Coral Reefs* **2013**, *32*, 825–834. [CrossRef]
33. Caras, T.; Karnieli, A. Ground-level classification of a coral reef using a hyperspectral camera. *Remote Sens.* **2015**, *7*, 7521–7544. [CrossRef]
34. Leiper, I.; Phinn, S.; Dekker, A.G. Spectral reflectance of coral reef benthos and substrate assemblages on Heron Reef, Australia. *Int. J. Remote Sens.* **2012**, *33*, 3946–3965. [CrossRef]
35. Lucas, M.; Goodman, J. Linking coral reef remote sensing and field ecology: It's a matter of scale. *J. Mar. Sci. Eng.* **2014**, *3*, 1–20. [CrossRef]
36. Anderson, D.A.; Armstrong, R.A.; Weil, E. Hyperspectral sensing of disease stress in the Caribbean reef-building coral, Orbicella faveolata—Perspectives for the field of coral disease monitoring. *PLoS ONE* **2013**, *8*, e81478. [CrossRef] [PubMed]
37. Hochberg, E.J.; Apprill, A.M.; Atkinson, M.J.; Bidigare, R.R. Bio-optical modeling of photosynthetic pigments in corals. *Coral Reefs* **2006**, *25*, 99–109. [CrossRef]
38. Dierssen, H.M.; Chlus, A.; Russell, B. Hyperspectral discrimination of floating mats of seagrass wrack and the macroalgae sargassum in coastal waters of Greater Florida Bay using airborne remote sensing. *Remote Sens. Environ.* **2015**, *167*, 247–258. [CrossRef]
39. Mahlein, A.K.; Steiner, U.; Hillnhütter, C.; Dehne, H.W.; Oerke, E.C. Hyperspectral imaging for small-scale analysis of symptoms caused by different sugar beet diseases. *Plant Methods* **2012**, *8*. [CrossRef] [PubMed]
40. Nansen, C.; Ribeiro, L.P.; Dadour, I.; Roberts, J.D. Detection of temporal changes in insect body reflectance in response to killing agents. *PLoS ONE* **2015**, *10*, e0124866. [CrossRef] [PubMed]
41. Rascher, U.; Nichol, C.J.; Small, C.; Hendricks, L. Monitoring spatio-temporal dynamics of photosynthesis with a portable hyperspectral imaging system. *Photogramm. Eng. Remote Sens.* **2007**, *73*, 45–56. [CrossRef]
42. Römer, C.; Wahabzada, M.; Ballvora, A.; Pinto, F.; Rossini, M.; Panigada, C.; Behmann, J.; Léon, J.; Thurau, C.; Bauckhage, C.; *et al.* Early drought stress detection in cereals: Simplex volume maximisation for hyperspectral image analysis. *Funct. Plant Biol.* **2012**, *39*, 878–890. [CrossRef]
43. Russell, B.J.; Dierssen, H.M. Use of hyperspectral imagery to assess cryptic color matching in sargassum associated crabs. *PLoS ONE* **2015**, *10*, e0136260. [CrossRef] [PubMed]
44. Behrendt, L.; Larkum, A.W.; Norman, A.; Qvortrup, K.; Chen, M.; Ralph, P.; Sørensen, S.J.; Trampe, E.; Kühl, M. Endolithic chlorophyll d-containing phototrophs. *ISME J.* **2011**, *5*, 1072–1076. [CrossRef] [PubMed]
45. Kühl, M.; Polerecky, L. Functional and structural imaging of phototrophic microbial communities and symbioses. *Aquat. Microb. Ecol.* **2008**, *53*, 99–118. [CrossRef]

46. Mehrubeoglu, M.; Smith, D.K.; Smith, S.W.; Strychar, K.B.; McLauchlan, L. Investigating coral hyperspectral properties across coral species and coral state using hyperspectral imaging. *Proc. SPIE* **2013**. [CrossRef]
47. Johnsen, G.; Volent, Z.; Dierssen, H.; Pettersen, R.; Ardelan, M.V.; Søreide, F.; Fearns, P.; Ludvigsen, M.; Moline, M. Underwater hyperspectral imagery to create biogeochemical maps of seafloor properties. In *Subsea Optics and Imaging*; Elsevier: Amsterdam, The Netherlands, 2013; pp. 508–540.
48. Dierssen, H.M. Overview of hyperspectral remote sensing for mapping marine benthic habitats from airborne and underwater sensors. *Proc. SPIE* **2013**. [CrossRef]
49. Chennu, A.; Färber, P.; Volkenborn, N.; Al-Najjar, M.A.A.; Janssen, F.; de Beer, D.; Polerecky, L. Hyperspectral imaging of the microscale distribution and dynamics of microphytobenthos in intertidal sediments: Hyperspectral imaging of MPB biofilms. *Limnol. Oceanogr. Methods* **2013**, *11*, 511–528. [CrossRef]
50. Golbuu, Y.; Victor, S.; Penland, L.; Idip, D.; Emaurois, C.; Okaji, K.; Yukihira, H.; Iwase, A.; van Woesik, R. Palau's coral reefs show differential habitat recovery following the 1998-bleaching event. *Coral Reefs* **2007**, *26*, 319–332. [CrossRef]
51. Van Woesik, R.; Houk, P.; Isechal, A.L.; Idechong, J.W.; Victor, S.; Golbuu, Y. Climate-change refugia in the sheltered bays of Palau: Analogs of future reefs. *Ecol. Evol.* **2012**, *2*, 2474–2484. [CrossRef] [PubMed]
52. Golbuu, Y.; Bauman, A.; Kuartei, J.; Victor, S. The state of coral reef ecosystems of Palau. In *The State of Coral Reef Ecosystems of the United States and Pacific Freely Associated States*; National Oceanic and Atmospheric Administration, National Ocean Service, National Centers for Coastal Ocean Science: Silver Spring, MD, USA, 2005; pp. 488–507.
53. Barkley, H.C.; Cohen, A.L.; Golbuu, Y.; Starczak, V.R.; DeCarlo, T.M.; Shamberger, K.E.F. Changes in coral reef communities across a natural gradient in seawater pH. *Sci. Adv.* **2015**. [CrossRef] [PubMed]
54. Szmant, A.M.; Gassman, N.J. The effects of prolonged "bleaching" on the tissue biomass and reproduction of the reef coral Montastrea annularis. *Coral Reefs* **1990**, *8*, 217–224. [CrossRef]
55. Fitt, W.K.; McFarland, F.K.; Warner, M.E.; Chilcoat, G.C. Seasonal patterns of tissue biomass and densities of symbiotic dinoflagellates in reef corals and relation to coral bleaching. *Limnol. Oceanogr.* **2000**, *45*, 677–685. [CrossRef]
56. Suggett, D.J.; Prášil, O.; Borowitzka, M.A. *Chlorophyll a Fluorescence in Aquatic Sciences: Methods and Applications*; Springer: Dordrecht, The Netherlands, 2010.
57. Marsh, J.A. Primary productivity of reef-building calcareous red algae. *Ecology* **1970**, *51*, 255–263. [CrossRef]
58. Zhang, H.; Voss, K.J. Bi-directional reflectance of dry and submerged Labsphere Spectralon plaque. *Appl. Opt.* **2006**, *45*, 7924–7927.
59. Hochberg, E.J.; Atkinson, M.J.; Apprill, A.; Andréfouét, S. Spectral reflectance of coral. *Coral Reefs* **2004**, *23*, 84–95. [CrossRef]
60. Torres-Pérez, J.L.; Guild, L.S.; Armstrong, R.A.; Corredor, J.; Zuluaga-Montero, A.; Polanco, R. Relative pigment composition and remote sensing reflectance of Caribbean shallow-water corals. *PLoS ONE* **2015**, *10*, e0143709. [CrossRef] [PubMed]
61. Mazel, C.H. Coral fluorescence characteristics: Excitation/emmission spectra, fluorescence efficiences, and contribution to apparent reflectance. *Proc. SPIE* **1997**. [CrossRef]
62. Mazel, C.H.; Fuchs, E. Contribution of fluorescence to the spectral signature and perceived color of corals. *Limnol. Oceanogr.* **2003**, *48*, 390–401. [CrossRef]
63. Salih, A.; Larkum, A.W.; Cox, G.; Kühl, M.; Hoegh-Guldberg, O. Fluorescent pigments in corals are photoprotective. *Nature* **2000**, *408*, 850–853. [CrossRef] [PubMed]
64. Bou-Abdallah, F.; Chasteen, N.D.; Lesser, M.P. Quenching of superoxide radicals by green fluorescent protein. *Biochim. Biophys. Acta* **2006**, *1760*, 1690–1695. [CrossRef] [PubMed]
65. Mazel, C.H.; Strand, M.P.; Lesser, M.P.; Crosby, M.P.; Coles, B.; Nevis, A.J. High-resolution determination of coral reef bottom cover from multispectral fluorescence laser line scan imagery. *Limnol. Oceanogr.* **2003**, *48*, 522–534. [CrossRef]
66. Iglesias-Prieto, R.; Trench, R.K. Acclimation and adaptation to irradiance in symbiotic dinoflagellates. I. Responses of the photosynthetic unit to changes in photon flux density. *Mar. Ecol. Prog. Ser.* **1994**, *113*, 163–175. [CrossRef]
67. Iglesias-Prieto, R.; Beltran, V.H.; LaJeunesse, T.C.; Reyes-Bonilla, H.; Thome, P.E. Different algal symbionts explain the vertical distribution of dominant reef corals in the eastern Pacific. *Proc. R. Soc. Lond. B Biol. Sci.* **2004**, *271*, 1757–1763. [CrossRef] [PubMed]

68. Nakamura, T.; van Woesik, R.; Yamasaki, H. Photoinhibition of photosynthesis is reduced by water flow in the reef-building coral Acropora digitifera. *Mar. Ecol. Prog. Ser.* **2005**, *301*, 109–118. [CrossRef]
69. Takahashi, S.; Nakamura, T.; Sakamizu, M.; van Woesik, R.; Yamasaki, H. Repair machinery of symbiotic photosynthesis as the primary target of heat stress for reef-building corals. *Plant Cell Physiol.* **2004**, *45*, 251–255. [CrossRef] [PubMed]
70. Warner, M.E.; Fitt, W.K.; Schmidt, G.W. The effects of elevated temperature on the photosynthetic efficiency of zooxanthellae in hospite from four different species of reef coral: A novel approach. *Plant Cell Environ.* **1996**, *19*, 291–299. [CrossRef]
71. Reichstetter, M.; Fearns, P.; Weeks, S.; McKinna, L.; Roelfsema, C.; Furnas, M. Bottom reflectance in ocean color satellite remote sensing for coral reef environments. *Remote Sens.* **2015**, *7*, 16756–16777. [CrossRef]
72. Garcia, R.; Hedley, J.; Tin, H.; Fearns, P. A method to analyze the potential of optical remote sensing for benthic habitat mapping. *Remote Sens.* **2015**, *7*, 13157–13189. [CrossRef]

Appendix: Supplementary Material, Chapter 2

This material appeared with publication of Chapter 2

Russell, BJ; Dierssen, HM. (2015) Use of hyperspectral imagery to assess cryptic color matching in *Sargassum* associated crabs. *PLOS ONE* doi:10.1371/journal.pone.0136260

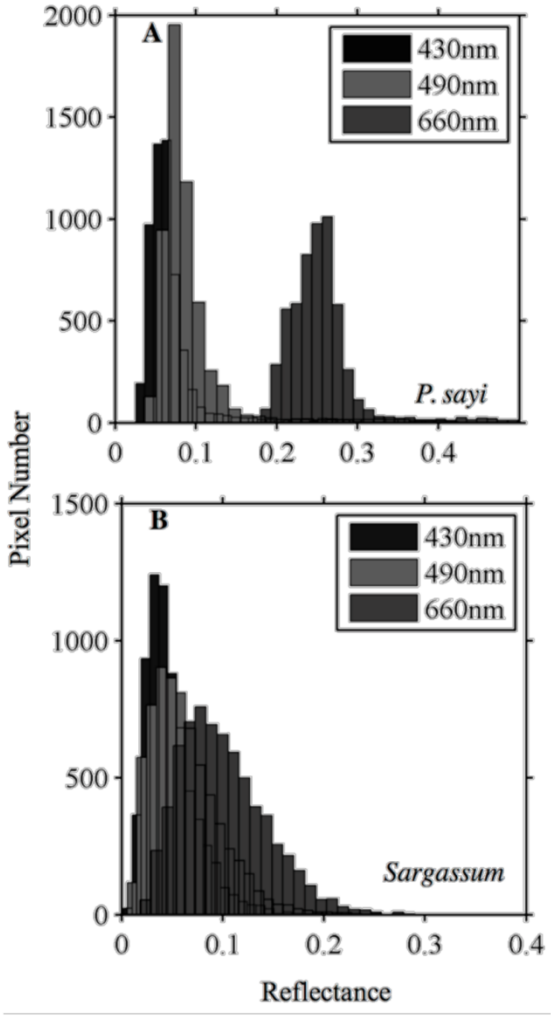

Fig S1. Distribution of *R*(λ) values. Histograms of reflectance values at selected wavelengths corresponding to the visual sensitivities of fish and a region of close spectral matching (430 nm), a region of crab visual sensitivity [67] (490 nm), and high *R*(λ) discrepancy (660 nm) for an individual **A**) *P. sayi* and **B**) its associated *Sargassum* sample. Reflectance for an individual image was generally normally distributed, indicating the suitability of using mean reflectance spectra for chromatic modeling.

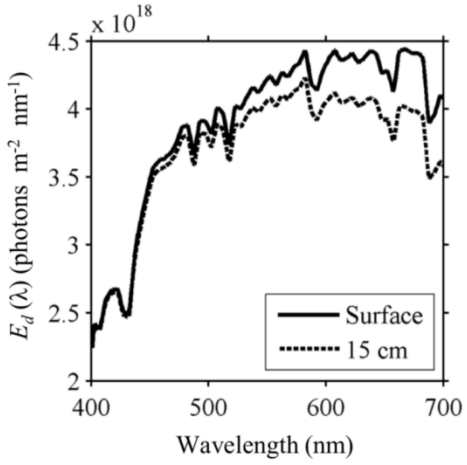

Fig S2. Illumination as downwelling irradiance $E_d(\lambda)$ at the surface (solid line) and at 15cm depth (dashed line). Irradiances are very similar in blue and green (400–550 nm) wavelengths, but diverge at longer wavelengths due to preferential attenuation and transmission across the air-sea interface.

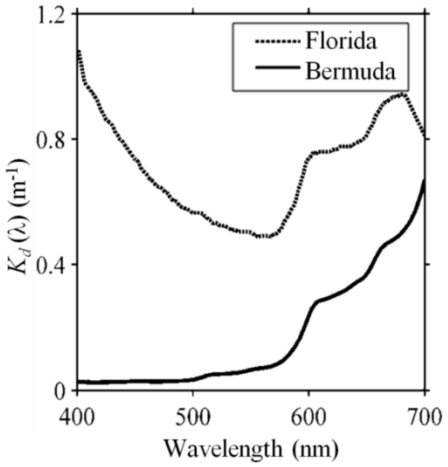

Fig S3. Diffuse attenuation (K_d) used in predator visual models for Bermuda (solid line) and Florida (dashed line) water types. Attenuation for Bermuda waters is low and characteristic of clear oceanic waters, with attenuation increasing exponentially in the red wavelengths. Florida waters attenuate much more strongly, particularly in the blue, due to the presence of colored dissolved organic matter (CDOM) and sediments.

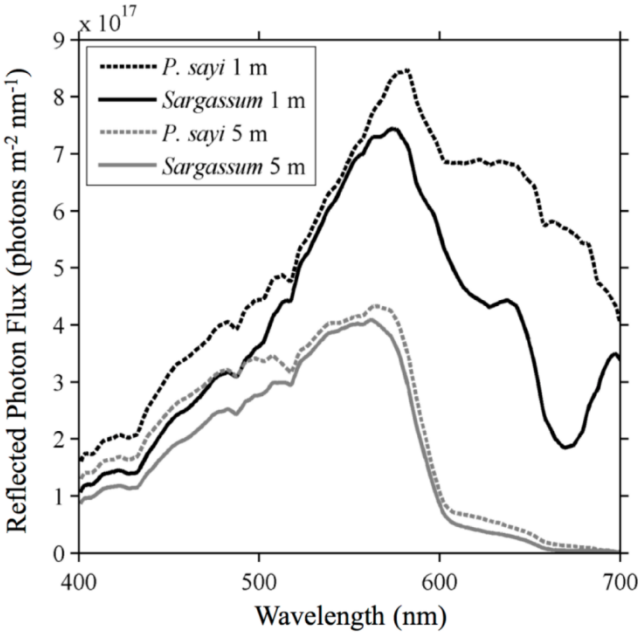

Fig S4. Impact of water column on target signal ($R(\lambda)*I(\lambda)$) for a sample *P.sayi* and associated *Sargassum* in Bermuda water type. Attenuation with distance decreased the difference between reflected light from crab and algae that is available to the observer, modeled here for the avian predator at 1 and 5 m depth. This is particularly true in the highly absorbed red wavelengths, where the spectral signatures of both animal and background converge.